AN *IN VIVO* STUDY TO DETERMINE THE EFFECTS OF OCHRATOXIN A AND *SUTHERLANDIA FRUTESCENS* IN MALE WISTAR RATS

BY

RAVESHNI DURGIAH

BSc., B.Biol.Sc (Hons), (UKZN)

Submitted in partial fulfilment of the requirements for the degree of M.Med.Sci

in the Discipline of Medical Biochemistry, Faculty of Health Science

University of KwaZulu-Natal

2009

ABSTRACT

Ochratoxin A (OTA), a nephrotoxic mycotoxin, is a contaminant of several agricultural food products consumed by animals and humans. Apart from renal toxicity, in particular renal tumours, OTA may also result in teratogenicity, neurotoxicity and immunotoxicity. *Sutherlandia frutescens*, an indigenous medicinal plant, has shown significant potential in strengthening the immune system and in cancer treatment, with minimal side effects. The objective of this study was to determine the effects of OTA in male Wistar rats and ascertain if these effects may be reduced by *S. frutescens*.

Rats were treated by intraperitoneal injection (i.p) with either a control (EtOH:dH_2O;30:70), *S. frutescens* (1.0mg/kg body weight), OTA (0.5mg/kg body weight) or a combination of OTA and *S. frutescens* for a period of 1 or 7 days (n=4). Genotoxicity and metabolic activity in peripheral blood mononuclear cells (PBMCs) were quantified using single cell gel electrophoresis (SCGE) and the methylthiazol tetrazolium (MTT) assay, respectively. Lymphocyte apoptosis and mitochondrial depolarisation were measured by flow cytometry. Fluorescence microscopy was utilised to determine renal tissue apoptosis (Hoechst staining) and OTA localisation using immunohistochemistry (IHC). SDS-PAGE and Western blot were utilised to determine protein expression in kidney tissue and serum.

Ochratoxin A significantly reduced PBMC viability (14%) after 7 days, compared with Day 1 ($p<0.001$). Lymphocyte mitochondrial depolarisation was 56.5% and 66.2% in the OTA-only and combination groups, respectively after 7 days ($p<0.001$). Ochratoxin A produced an increase in DNA damage compared to the control ($p<0.01$). The renal tissue displayed typical signs of apoptosis such as chromatin condensation. Ochratoxin A was immunolocalised within the glomerulus. The protein analysis showed a decreased expression in the kidney mitochondrial protein fraction. Ochratoxin A preferentially bound to serum albumin and a 120kDa protein in the OTA-only and co-treatment groups after the 1-and 7-day regimes. Protein band intensities significantly decreased after the 7-day co-treatment ($p<0.01$).

The data highlights that OTA toxicity is mediated by mitochondrial dysfunction. Furthermore, OTA disruptions in immune function may play a role in renal damage.

DECLARATION

This study represents the original work by the author and has not been submitted in any form to another University. The use of work by others has been duly acknowledged in the text.

The research described in this study was carried out in the Discipline of Medical Biochemistry, Faculty of Health Sciences, University of KwaZulu-Natal, Durban, under the supervision of Prof. A.A. Chuturgoon.

R. Durgiah

ACKNOWLEDGEMENTS

I owe my deepest gratitude to the following people:

My Parents, who have always encouraged and supported me in all my endeavours. Your love and the values you have instilled in me have enabled me to persevere and realise many of my goals.

Prof. A.A. Chuturgoon, for his invaluable guidance, constructive criticism and practical lessons taught, which I will always remember.

Leshern Karamchand, Devan Moodley and Kristina Naidoo, for their assistance, support and for sharing their laboratory expertise with me. I sincerely appreciate it.

My Sisters, for their unwavering belief in me. I am truly blessed to have the both of you.

Treshan Pillay, for his patience and thoughtful gestures. You have motivated and given me strength, and the rare qualities you possess inspire me every day.

ABBREVIATIONS

°C	Degrees Celsius
µg	Microgram
µl	Microlitre
µm	Micrometre
$\Delta\psi m$	Mitochondrial Inner Transmembrane Potential
ADC	Analogue to Digital Converter
ADP	Adenosine Diphosphate
AIDS	Acquired Immune Deficiency Syndrome
AIF	Apoptosis Inducing Factor
ANOVA	Analysis of Variance
Annexin-V-FITC	Annexin-V-Fluorescein Isothiocyanate
ANT	Adenine Nucleotide Transporter
Apaf-1	Apoptotic Protease-Inducing Factor-1
APS	Ammonium Persulphate
Asp	Aspartate
ATP	Adenosine Triphosphate
BCA	Bicinchoninic Acid
BEN	Balkan Endemic Nephropathy
BSA	Bovine Serum Albumin
Ca^{2+}	Calcium ion
CARD	Caspase Recruitment Domain
Caspase	Cysteine-dependent aspartate-specific protease
CHO	Chinese Hamster Ovary
CD4	Cluster of Differentiation 4
CD95	Cluster of Differentiation 95
cFLIP	FLICE Inhibitory Protein
cm	Centimetre
CO_2	Carbon Dioxide
Cu^{2+}	Copper ions
$Cu(II)SO_4$	Copper Sulphate

***CYP*450**	Cytochrome P450
***CYP*2C9**	Cytochrome P450 2C9
Cys	Cysteine
DD	Death Domain
DED	Death Effector Domain
dH_2O	De-ionised Water
DISC	Death-Inducing Signalling Complex
DMSO	Dimethyl Sulphoxide
DNA	Deoxyribonucleic Acid
DNase	Deoxyribonuclease
DTT	Dithiothreitol
EDTA	Ethylenediaminetetraacetic Acid
eF1A-1	Elongation Factor 1-Alpha-1
ER	Endoplasmic Reticulum
ERK1/2	Extracellular Signal Regulated Kinases1 and 2
EtBr	Ethidium Bromide
EtOH	Ethanol
FADD	Fas-associated Death Domain
$FADH_2$	Flavin Adenine Dinucleotide
Fe^{3+}	Iron (III)
FACS	Fluorescence Activated Cell Sorting
FL	Fluorescence
FSC	Forward Light Scatter
GABA	Gamma (γ)-Aminobutyric Acid
GTP	Guanosine Triphosphate
HCO_3^-	Bicarbonate
HIV	Human Immunodeficiency Virus
hr	Hour
HRP	Horse Radish Peroxidase
HSA	Human Serum Albumin
IAP	Inhibitor of Apoptosis Protein
IARC	International Agency for Research on Cancer

IHC	Immunohistochemistry
IHKE	Human Renal Proximal-derived Cells
IM	Inner Mitochondrial Membrane
iNOS	Inducible Nitric Oxide Synthase
i.p	Intraperitoneal
i.v	Intravenous
JNK	Jun N-terminal Kinase
K^+	Potassium ions
KCl	Potassium Chloride
kDa	KiloDalton
kg	Kilogram
K_2EDTA	Dipotassium Ethylenediaminetetraacetic Acid
KH_2PO_4	Potassium Dihydrogen Phosphate
L-ARG	L-Arginine
L-CAV	L-Canavanine
LLC-PK1	Porcine derived Renal Epithelial Cells
LMPA	Low Melting Point Agarose
M	Molar
mA	Milliampere
MAPK	Mitogen Activated Kinase
MDCK-C7	Madin-Darby Canine Kidney Cells
mg	Milligram
min	Minutes
ml	Millilitre
mm	Millimetre
mM	Millimolar
MTT	Methylthiazol Tetrazolium
Mw	Molecular Weight Marker
Na^+	Sodium ions
NA_2EDTA	Disodium Ethylenediaminetetraacetic Acid
NaCl	Sodium Chloride
NADH	Nicotinamide Adenine Dinucleotide (reduced)

NADPH	Nicotinamide Adenine Dinucleotide Phosphate (reduced)
NaOH	Sodium Hydroxide
NK	Natural Killer
nm	Nanometre
NO	Nitric Oxide
OAT	Organic Anion Transporter
OK	Opossum Kidney
OM	Outer Mitochondrial Membrane
OTA	Ochratoxin A
OTA-a	Ochratoxin A-alpha
OTA^-	Ochratoxin A-monoanion
OTA^{2-}	Ochratoxin A-dianion
pAH	p-Aminohippurate
PAH	Phenylalanine Hydroxylase
PARP	Poly (ADP-ribose) Polymerase
PBMC	Peripheral Blood Mononuclear Cells
PBS	Phosphate Buffered Saline
PBST	Phosphate Buffered Saline and Triton X-100
PCD	Programmed Cell Death
Phe	Phenylalanine
PI	Propidium Iodide
PKC	Protein Kinase C
PMT	Photomultiplier Tube
PS	Phosphatidylserine
PT	Permeability Transition
PTPC	Permeability Transition Pore Complex
PVDF	Polyvinylidene Fluoride
RBC	Red Blood Cell
Rf	Relative Mobility
RNA	Ribonucleic Acid
ROS	Reactive Oxygen Species
rpm	Revolutions Per Minute

RT	Room Temperature
SCGE	Single Cell Gel Electrophoresis
SDS	Sodium Dodecyl Sulphate
SDS-PAGE	Sodium Dodecyl Sulphate-Polyacrylamide Gel Electrophoresis
SEM	Standard Error of Mean
SKPT	Rat Kidney Proximal Tubule Cells
Smac/DIABLO	Second mitochondria-derived activator of caspase/direct IAP-binding protein with low pI
SSC	Side Light Scatter
tBid	Truncated Bid
TCA	Tricarboxylic Acid
TEMED	Tetramethylenediamine
TNFR1	Tumour Necrosis Factor Receptor 1
TRADD	TNF-Receptor Death Domain
TRAIL	Tumour Related Apoptosis Inducing Ligand
tRNA	Transfer Ribonucleic Acid
TTBS	Tween-Tris Buffered Saline
UV	Ultraviolet
V	Volts
VDAC	Voltage-Dependent Anion Channel

LIST OF FIGURES

LIST OF TABLES

TABLE OF CONTENTS

CHAPTER 1

INTRODUCTION

Diseases of the kidney and urinary tract together account for approximately 830 000 deaths annually, ranking them 12th among the causes of deaths worldwide (Disease Control Priorities Project, 2008). Furthermore, approximately 2 to 3% of medical admissions in Africa are due to renal-related complaints and it is believed that kidney disease is more prevalent and severe in Africa than in Western countries. The kidneys receive 25% of cardiac output and are therefore susceptible to toxicity and disease.

The kidneys become vulnerable to injury due to the high metabolic activity of renal tubular cells. Also, glomerular filtrate concentration and active cell transport may result in renal tubular cells being exposed to higher concentrations of toxicants than are the cells of other organs. Subsequent disruptions could ultimately result in renal injury or failure. These disruptions may often be the result of dietary mycotoxins. Mycotoxins are toxins produced by various moulds that commonly infect agricultural commodities. When the humidity and temperature conditions are sufficient, there is fungal proliferation and thus an increase in mycotoxin production. There is a growing global concern regarding the impact of mycotoxins on the environment and the resultant economic losses.

Ochratoxin A (OTA), a mycotoxin produced by the fungi *Aspergillus* and *Penicillium* species, is found in several agricultural food products owing to their often improper storage. The presence of OTA in food products such as coffee, wine, beer, grape juice, meat and meat products is possible because of its chemical stability during industrial processing (Al-Anati and Petzinger, 2006). The kidney is the target organ of OTA toxicity and chronic exposure results in the formation of renal tumours. Apart from renal toxicity, OTA also promotes teratogenicity, immunotoxicity and even neurotoxicity. The International Agency for Research on Cancer (IARC) has classified OTA as a group 2B carcinogen, possibly carcinogenic to humans (IARC, 1993). The proposed mechanisms by which OTA disrupts cell homeostasis include DNA damage, protein synthesis inhibition, apoptosis and oxidative stress (Ringot *et al.*, 2006; Marin-Kuan *et al.*, 2008). Mitochondria are significant in the

induction of apoptosis since mitochondria receive signals to induce apoptosis. It is believed that mitochondria may play a significant role in the early toxicity of OTA (Aleo *et al.*, 1991). Furthermore, OTA toxicity may also exaggerate the effects of other diseases.

Complementary medicine is a rapidly growing field and is gaining exposure in modern healthcare. It is believed that 80% of Africans rely on herbal medication and traditional healthcare for the treatment of various ailments (Ojewole, 2008). Medicinal plants are often thought to be safer than conventional medication, having minimal side effects. The medicinal plant *Sutherlandia frutescens*, also commonly known as 'cancer bush', is known for its many diverse uses; it is used, for example, in the treatment of cancer, diabetes, influenza, tuberculosis and anxiety (van Wyk and Albrecht, 2008). Some of the active ingredients found in this plant include L-canavanine, γ-aminobutyric acid (GABA), D-pinitol, L-arginine, flavonoids and triterpenoid saponins. The leaves of the plant are used in the production of the commercial tablets.

Sutherlandia frutescens is currently being used in South Africa for the treatment of HIV/AIDS. The active ingredients in this plant may have positive effects on the immune system of patients. A safety study, conducted by the Medical Research Council of South Africa, showed that *S. frutescens,* at the recommended dose (9mg/kg) and higher, was non-toxic and safe (Seier *et al.*, 2002). The minimal side effects of *S. frutescens* treatment make this plant safe to use and it is also relatively affordable. It is important to realise that individuals with a lower income are often unable to access the necessary treatment. If treatment is unavailable, then these individuals are at a higher risk of suffering from disease. Considering that *S. frutescens* is cost-effective and has various uses, this medicinal plant was used in the present study to determine any cyto-protection against OTA toxicity.

Ochratoxin A poses a serious threat to human and animal health as it is present in many agricultural food products. The eradication of OTA is difficult owing to its chemical and heat stability. Attention needs, therefore, to be focussed on minimising OTA-induced toxicity. Appropriate biochemical assays may prove to be beneficial in disease reduction.

The following aims were investigated in male Wistar rats:

- To determine the effect of OTA immunotoxicity, by evaluating metabolic activity and apoptosis in peripheral blood mononuclear cells;
- To identify the genotoxic potential of OTA;
- To investigate the biochemical and morphological features of OTA-associated renal toxicity;
- To ascertain the cyto-protective properties of *S. frutescens* against OTA toxicity.

CHAPTER 2

LITERATURE REVIEW

Ochratoxin A (OTA), a mycotoxin, is a secondary metabolite of the fungal species *Aspergillus* and *Penicillium* (Köller *et al.*, 2006). The most important fungi to produce OTA are *Aspergillus ochraceus* and *Penicillium verrucosum*. Production of OTA occurs as a result of improper storage conditions, such as high moisture, which results in an excessive proliferation of fungi. The chemical structure of OTA is represented by a polyketide-derived dihydroisocoumarin moiety linked through the 12-carboxy group to L-phenylalanine at carbon 9 (Ringot *et al.*, 2006) (Fig. 2.1).

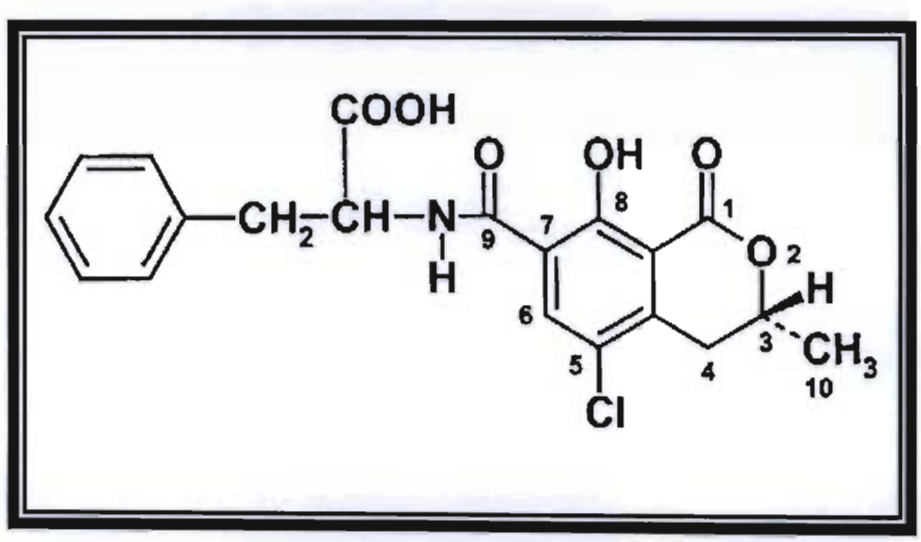

Figure 2.1: Structure of Ochratoxin A (Hassen *et al.*, 2007).

The phenolic group on the dihydroisocoumarin may be involved in the toxicity of OTA. The higher acidity of the phenolic group may be due to the aromatic ring that tightly couples with oxygen and is relatively loose between oxygen and hydrogen. De-protonation of the phenol group of the dihydroisocoumarin forms a phenolate ion and this may be related to either the absorption, elimination or binding of OTA to proteins (Dais *et al.*, 2005). Ochratoxin A is a colourless crystalline compound that fluoresces blue under ultraviolet (UV) light.

Ochratoxin A is commonly found in cereals, beer, wine, coffee, nuts, fruit juice and spices that have not been properly stored (Petzinger and Ziegler, 2000). Humans may be exposed to OTA after ingesting contaminated food or drink. Toxicity may also occur in animals, which may in turn lead to the contamination of meat and milk products.

2.1 MECHANISMS OF TOXICITY

There are certain mechanisms that occur in a cell which make a compound toxic. The initial step is the delivery of the toxin from the site of exposure to the target site. With regard to this, the compound that causes toxicity may be the parent compound, a metabolite or a reactive oxygen or reactive nitrogen species (Ringot *et al.*, 2006). Secondly, the toxic compound may react to a target molecule. This is not, however, always the case, as some xenobiotics may alter the biological environment, leading to a toxic response. Toxicity may also occur if there are changes in cellular signalling. Toxicity can further be induced if the cell's repair mechanisms are disturbed.

Toxicokinetics and toxicodynamics are both important in OTA toxicity. Toxicokinetics refers to the change in concentration of a compound in the organism after a certain period of time (Ringot *et al.*, 2006). Toxicodynamics refers to the interaction of a compound with its biological targets and their subsequent downstream biological effects (Ringot *et al.*, 2006). Another factor that could affect toxicity is bioavailabilty, which is the amount of a particular toxin that reaches the systemic circulation (Marquardt and Frohlich, 1992). The distribution pattern of OTA in pigs, rats, chickens and goats is believed to be in the following descending order: kidney, liver, muscle, fat and/or kidney, muscle, liver and fat (Ringot *et al.*, 2006). After oral administration to mammals, OTA may reach the systemic circulation without any chemical modification, which means that its bioavailability remains high (Marquardt and Frohlich, 1992; Li *et al.*, 1997).

2.2 ROUTE OF TOXIN EXPOSURE

It has been established that when animals are given oral doses of OTA as compared with an intravenous injection (i.v), the half-life of OTA is low (Petzinger and Ziegler, 2000). Intraperitoneal injection (i.p) was chosen for the present study. This serves as a valuable tool in helping to clarify the mechanism of action of mycotoxins (Bondy *et al.*, 1995). Using the i.p route, the toxin is injected into the peritoneal cavity. According to Coria-Avila *et al.* (2007), substances deposited into the peritoneal cavity in rats are absorbed by vessels such as the colic and the intestinal and mesenteric veins, which converge into the anterior mesenteric vein. Blood is subsequently carried to the liver. After being metabolised in the liver, the i.p injected substances are taken to the heart, lungs and, thereafter, into the circulatory system (Coria-Avila *et al.*, 2007). It is believed that despite this long process, the speed of absorption is 25 - 50% the speed of i.v injections. Also, this route eliminates the possible cleavage of the toxin in the digestive tract (Maaroufi *et al.*, 1999).

2.3 BIOTRANSFORMATION OF OCHRATOXIN A

The hydrolysis of OTA results in the formation of a less toxic compound, referred to as OTA-a (O'Brien and Dietrich, 2005). This is formed by the cleavage of the peptide bond by peptidases, such as carboxypeptidase A or acid hydrolysis (Zepnik *et al.*, 2003). It is believed that OTA metabolism is catalysed by cytochrome P450 (*CYP*450) enzymes, which leads to the production of 4-hydroxyochratoxin A (4R-OH-OTA) and 4S-OH-OTA (Marquardt and Frohlich, 1992; O'Brien and Dietrich, 2005; Ringot *et al.*, 2006). These intermediates are less toxic than the parent compound (OTA) and may have a shorter half-life (Li *et al.*, 1997). Simarro Doorten *et al.* (2004) found that *CYP*450-dependent OTA metabolism results in less toxic intermediates than does *CYP*2C9-dependent metabolism. It has also been suggested that OTA quinones may be formed by an iron-porphyrin complex (Gillman *et al.*, 1999).

2.4 EFFECT OF OCHRATOXIN A IN THE BODY

In the body, OTA may accumulate in the liver, blood and kidney (Schwerdt *et al.*, 1996; Maaroufi *et al.*, 1999; Zepnik *et al.*, 2003; Ringot *et al.*, 2006). The toxic properties of OTA include DNA damage, nephrotoxicity, immunotoxicity and carcinogenicity. Ochratoxin A nephrotoxicity may occur as a result of mitochondrial respiration inhibition and lipid peroxidation (Simon *et al.*, 1996). Cell damage by oxidative stress was enhanced when kidney and liver cells were treated with OTA and the production of reactive oxygen species (ROS) in the presence of OTA increased in a time- and dose-dependent manner (Gautier *et al.*, 2001b; Schaaf *et al.*, 2002; Boesch-Saadatmandi *et al.*, 2008). Furthermore, calcium homeostasis, inhibition of protein synthesis and signalling pathways are also disrupted, which can eventually lead to carcinogenesis (Simon *et al.*, 1996; Marin-Kuan *et al.*, 2006). The half-life of OTA in humans exceeds 800 hours (Kamp *et al.*, 2005) and in rats is between 55 and 120 hours (O'Brien and Dietrich, 2005).

Low concentrations of OTA can alter cell homeostasis as it disturbs the cellular pH balance and influences the cellular calcium balance (Schwerdt *et al.*, 2004; Webber *et al.*, 2005). Cellular pH may determine cell proliferation. Also, medium to high doses of OTA may be associated with high incidences of metastasis (Mally and Dekant, 2005).

The pH level of ingested food may also be important for OTA absorption. Both the monoanion (OTA^-) and dianion (OTA^{2-}) forms of OTA are present at physiological pH conditions of the duodenal chyme (Ringot *et al.*, 2006). The fully protonated form is mainly present in acid solutions, such as the upper parts of the gastrointestinal tract (Ringot *et al.*, 2006).

2.5 TARGET ORGAN OF TOXICITY – THE KIDNEY

Several factors determine the susceptibility of a target organ to toxicity. These factors include the pharmacokinetics of the compound, the metabolic fate of the compound and the target organs ability to respond to toxicity (Pfaller and Gstraunthaler, 1998). The kidney is the target organ of OTA toxicity. Typical features associated with OTA-induced renal toxicity are: single cell death, karyomegaly, polyploidy, frequent mitosis and kidney tubular cell degeneration and tubule disorganisation (Maaroufi *et al.*, 1999; Aydin *et al.*, 2003; Schwerdt *et al.*, 2007).

The morphological characteristics and tumours observed in the kidneys of patients diagnosed with Balkan Endemic Nephropathy (BEN) are similar to those of patients exposed to OTA. Moreover, OTA has also been detected in the serum of patients with BEN (O'Brien and Dietrich, 2005). These factors have resulted in the implication of OTA as an underlying factor in BEN (Stoev, 1998; O'Brien and Dietrich, 2005).

2.5.1 Anatomy of the Kidney

The kidneys are bean-shaped organs situated near the middle of the back, just below the rib cage. There are about 30 000 to 34 000 nephrons (functional unit of the kidney) in each adult rat kidney (Madsen and Tisher, 2004). Each nephron consists of three portions: the vascular, glomerular and tubular element (Fig. 2.2).

Structural organisation of the kidney includes the outer cortex, medulla and papilla. While the proximal and distal tubules, glomeruli and peritubular capillaries make up the cortex, the Loop of Henlé and vasa recta make up the medulla. The papilla consists of the terminal portions of the collecting duct and vasa recta (Madsen and Tisher, 2004). The kidney receives about 25% of the cardiac output, making it highly susceptible to toxicity. About 90% of the total renal blood flow is received by cortex, while the medulla and papilla receives 6% and 1%, respectively (De Broe and Roch-Ramel, 1998).

The glomerulus is a complex capillary network that filters blood into an ultrafiltrate. The glomerulus is also the first to receive exposure to a toxicant (Fig. 2.2). There are three barriers that the glomerular filtrate encounters, *viz.*, the capillary endothelium, the capillary basement membrane and the visceral epithelium (podocytes) (Hladky and Rink, 1986; Schnellmann, 2003). Certain permeability-selective and charge-selective properties are present in the glomerulus. The permeability-selective property is directly related to the physicochemical properties of the different cell types within the glomerulus.

Small molecules may freely pass through the glomerulus, while large molecules, however, cannot. Charge-selective properties are related to the anionic coating of the epithelial and endothelial cells and thereby restrict the filtration of anionic molecules (Schnellmann, 2003; Smart and Hodgson, 2008). Toxicants that neutralise or reduce the number of fixed anionic charges will therefore impair the charge or size-selective properties of the glomerulus (Smart and Hodgson, 2008). This results in the excretion of polyanionic and/or high molecular weight proteins.

Next, the ultrafiltrate passes into the tubular portion of the nephron (Fig. 2.2), which begins at the proximal tubule and consists of the proximal convoluted and proximal straight segments. The proximal convoluted tubule plays a major role in the reabsorption of sodium (Na^+), bicarbonate (HCO_3^-), potassium (K^+), calcium (Ca^{2+}), water and organic solutes such as glucose and amino acids. Filtered HCO_3^-, proteins and glucose are reabsorbed in the proximal straight tubule.

From the proximal tubule the filtrate passes into the Loop of Henlé (Fig. 2.2). This portion is critical in concentrating urine. It is permeable to water at the thin descending limb, but after the loop the cells are impermeable to water. This allows for maximum reabsorption of water into the peritubular capillaries. From the Loop of Henlé, tubular fluid moves to the distal tubule and then into the collecting duct.

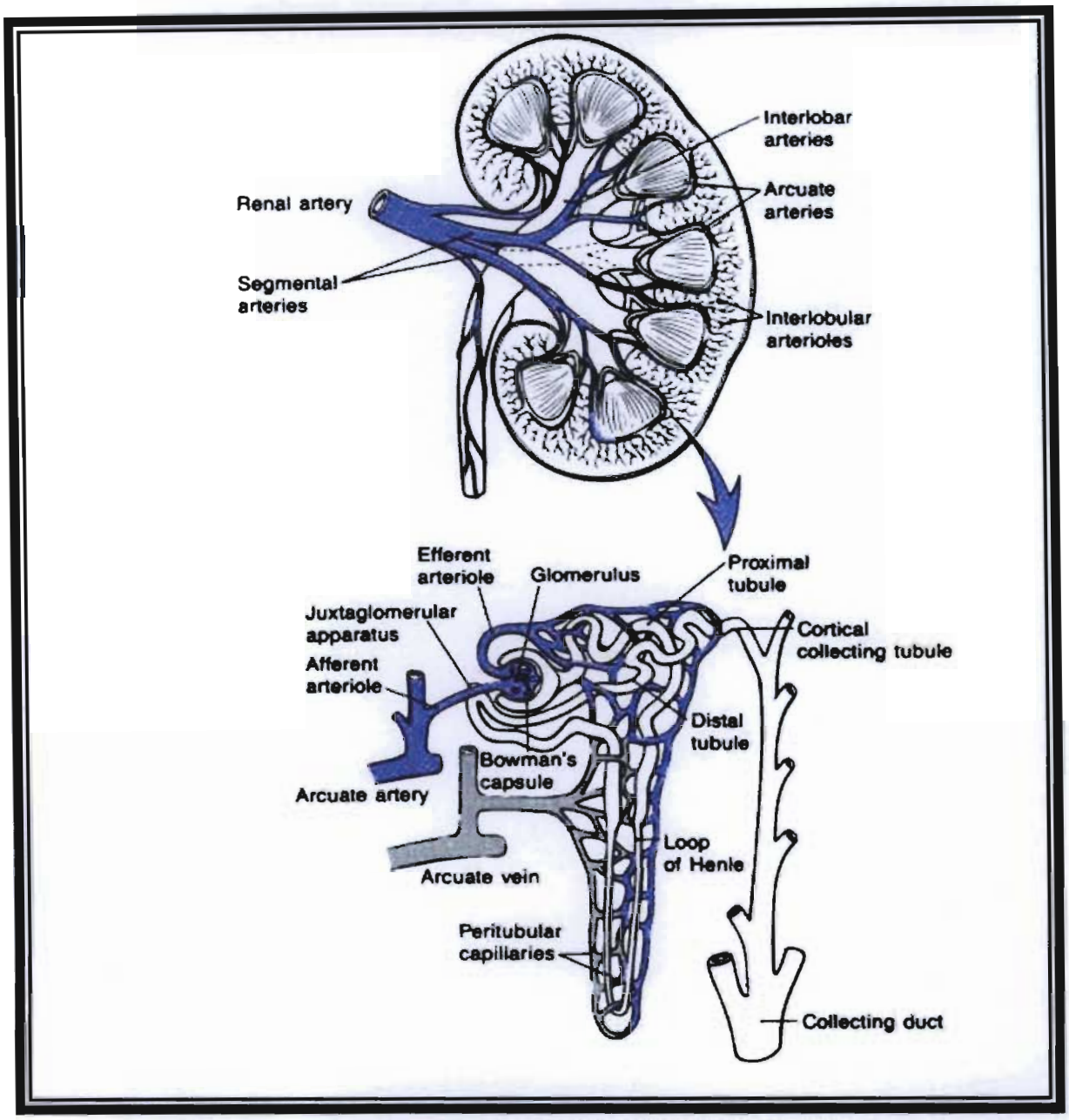

Figure 2.2: Schematic of the kidney showing major blood vessels and the microcirculation of tubular components of each nephron (Schnellman, 2003).

There are significant differences in energy metabolism among the various cell populations that line the nephron. Cells of the proximal convoluted tubule, thick ascending limb, distal convoluted and the collecting tubule are rich in mitochondria (Madsen and Tisher, 2004). These portions thus have a high capacity for oxidative energy production.

2.5.2 Disturbances Produced by Ochratoxin A in the Kidney

The high blood flow rate and the presence of cellular transport systems makes the kidney susceptible to OTA. The effects of OTA may be dose-, time- and, often, species- and age-dependent (Gekle *et al.*, 1995; Mally and Dekant, 2005). Using male Wistar rats as the experimental model, Schwerdt *et al.* (1996) showed that OTA-induced toxicity may change with age. In addition, OTA may be sex-specific, with male rats possibly being more susceptible than female rats (Castegnaro *et al.*, 1998).

Lesions confined to the proximal tubules were observed after OTA treatment (Domijan *et al.*, 2004). Hyaline deposits in the Bowman's capsule and atrophy of the glomerulus were also noted (Ming-Fang Hseih *et al.*, 2004). The increased renal cell proliferation was indicative of OTA carcinogenicity (Mally *et al.*, 2007). Furthermore, it is possible that renal toxicity may be a result of the accumulation of OTA in kidney tissue.

In animal models, such as pig and rat, proximal and distal parts are affected by OTA (Stoev, 1998; Dahlmann *et al.*, 1998). Jung and Endou (1989) have shown that OTA alters only the middle and the terminal portions of the nephron. These authors demonstrated that OTA inhibited ATP synthesis in mitochondria but not in other segments. It was therefore proposed that OTA blocked mitochondrial respiration, and this may have induced the modification of intracellular calcium and subsequently reduced ATP (Simon *et al.*, 1996; Schwerdt *et al.*, 2004). High adherence of OTA to organellar compartments corresponds with the uptake by mitochondria and may result in disturbances in cellular energy metabolism. Furthermore, OTA was responsible for disrupting mitochondrial respiration and oxidative phosphorylation through the impairment of the mitochondrial membrane and the inhibition of electron transfer (Wei *et al.*, 1985). This may subsequently reduce ATP production, which is required by the kidneys for the active reabsorption of water and other substrates.

The disturbance in the calcium electrochemical gradient could also be a determining factor in deciding the fate of a cell, in terms of cell signalling and cell proliferation. This is of importance to the proximal tubule cells, which are rich in mitochondria and have various energy-requiring transport functions. Enzymes in the proximal tubule may also be disrupted

by OTA and may lead to polyuria, with reduced osmolality and morphological changes (Gekle and Silbernagl, 1994; Simon *et al.*, 1996; Ming-Fang Hsieh *et al.*, 2004). Moreover, OTA may decrease the glomerular filtration rate (Gekle and Silbernagl, 1996).

2.6 APOPTOSIS

Apoptosis refers to the controlled energy-dependent death of a cell and is also known as programmed cell death (PCD). The process of apoptosis takes place in a sequential series of steps that result in cells having specific morphological characteristics, such as cell shrinkage, condensation of chromatin and cytoplasm and DNA fragmentation (Hotchkiss and Nicholson, 2006) (Fig. 2.3). In addition, mutations in the proteins that participate in apoptosis can lead to cancer development.

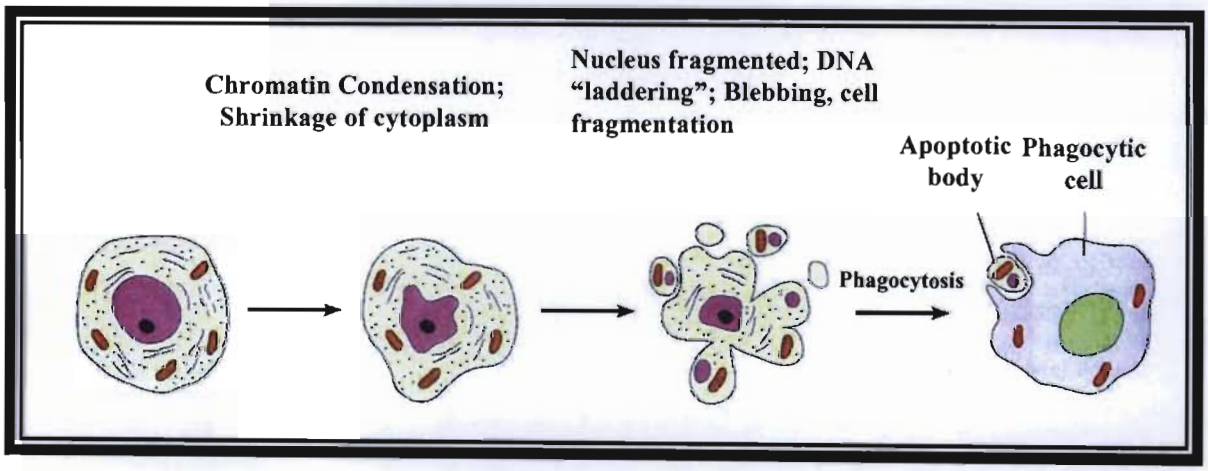

Figure 2.3: Diagrammatic representation of the morphological changes that take place during apoptosis (Becker *et al.*, 2003).

There are several phases that occur during cell death. These include induction, decision and execution/degradation. Induction/initiation is dependent on the nature of the death-inducing signal, i.e., the intrinsic or extrinsic signals (Kroemer *et al.*, 2007) (Fig. 2.4). A pivotal role is played by a group of proteases (caspases) in the regulation of apoptotic cell death.

Caspases (**c**ysteine-dependent **asp**artate-specific prote**ases**) are proteases that catalyse a cysteine (Cys)-mediated hydrolysis of peptide bonds which immediately follow aspartate (Rastogi *et al.*, 2009). Initially, proteases are produced in an inactive form called

pro-caspases (zymogens), which are then cleaved at two aspartate (Asp) sites to create the active enzymes (caspase) in a proteolytic cascade that usually involves other caspases (Desagher and Martinou, 2000; Rastogi *et al.*, 2009) (Fig. 2.4). The active caspases are a hetrotetramer of two large and two small sub-units. Caspases are divided into extrinsic (caspase-2, -8 and -10) and intrinsic (caspase-9) initiator caspases and executioner/effector (caspase-3, -6 and -7) caspases. The initiator caspases contain death domains, such as death effector domains (DED) (pro-caspase-8 and -10) or caspase recruitment domains (CARD) (pro-caspase-9 and -2) (Hengartner, 2000). These death domains facilitate the recruitment of caspases to work together with molecules that direct their activation, in response to intrinsic or extrinsic signals (Rastogi *et al.*, 2009).

2.6.1 The Extrinsic Pathway

The extrinsic pathway is a result of the activation of death receptors (ligand-induced) at cell surface. Death receptors, characterised by cysteine-rich extracellular domains and an intracellular cytoplasmic death domain (DD) sequence, include tumour necrosis factor receptor 1 (TNFR1), CD95/FAS and tumour-related apoptosis inducing ligand (TRAIL) (Kroemer *et al.*, 2007) (Fig. 2.4). When the ligand binds to the specific receptors, it leads to the attachment of adaptor proteins (FADD or TRADD) (Rastogi *et al.*, 2009) (Fig. 2.4). Procaspase-8 then associates with the adaptor proteins, resulting in a death inducing signalling complex (DISC) (Smart and Hodgson, 2008). Thereafter, caspase-8 is activated, which in turn triggers apoptosis. However, caspase-8 activation may be prevented by cellular caspase-8 (FLICE)-like inhibitory protein (cFLIP) (Hotchkiss and Nicholson, 2006; Smart and Hodgson, 2008) (Fig. 2.4).

2.6.2 The Intrinsic Pathway

Intracellular stress damage to DNA and ER induces the intrinsic pathway (Fig. 2.4). This pathway facilitates apoptosis due to an intracellular cascade of events and mitochondrial permeabilisation plays a critical role (Heiskanen *et al.*, 1999; Zamzami *et al.*, 1995; Desagher and Martinou, 2000; Mayer and Oberbauer, 2003; Kroemer *et al.*, 2007). Mitochondrial permeabilisation results from the opening of the permeability transition pore complex (PTPC), which is a transmembrane channel between the outer (OM) and inner mitochondrial

membranes (IM). The PTPC is formed through the interaction of the voltage-dependent-anion channels (VDAC) in the OM and the adenine nucleotide transporter (ANT) in the IM (Desagher and Martinou, 2000). This causes apoptotic effectors – such as cytochrome c, second mitochondria-derived activator of caspase/direct IAP protein with low pI (Smac/Diablo) and apoptosis inducing factor (AIF) – to leak out of the mitochondrial matrix (Kroemer *et al.*, 1997) (Fig. 2.4).

Mitochondrial inner transmembrane potential ($\Delta\psi m$) results from the asymmetric distribution of protons and other ions on both sides of the IM. This results in a chemical and electrical gradient that is essential for oxidative phosphorylation and mitochondrial function (Kroemer *et al.*, 1997). The release of cyochrome c is thus usually followed by a collapse of the $\Delta\psi m$, known as permeability transition (PT) or mitochondrial depolarisation, and is used as one of the determining factors of apoptosis (Heiskanen *et al.*, 1999; Dubmann *et al.*, 2003; Kroemer *et al.*, 2007).

Released cytochrome c binds to a cytoplasmic protein called the apoptotic protease activating factor-1 (Apaf-1) (Hotchkiss and Nicholson, 2006) (Fig. 2.4). Thereafter, procaspase-9 binds to cytochrome c and Apaf-1 to form a complex called the apoptosome (Fig. 2.4). This activates the initiator caspase-9, which cleaves other executioner caspases (-3 and -7), ultimately leading to apoptosis. Also, the activation of caspase-3 (via extrinsic and intrinsic pathways) results in phosphatidylserine externalisation on apoptotic cells, allowing for the early recognition and phagocytosis of apoptotic cells (Smart and Hodgson, 2008).

Caspases are kept under tight control by specific proteins. These proteins belong to the Bcl-2 family, which favour (Bax, Bid, Bik, Bak or Bad) or inhibit (Bcl2 or Bcl-X_L) apoptosis (Petit *et al.*, 1996; Kroemer *et al.*, 1997) (Fig. 2.4). Bax and Bad facilitate apoptosis by binding to VDAC, thus stimulating permeabilisation of the outer mitochondrial membrane (Mayer and Oberbauer, 2003) (Fig. 2.4). This results in the leakage of cytochrome c out of the mitochondria into the cytoplasm.

Crosstalk between the intrinsic and extrinsic pathways also leads to the activation of pro-apoptotic proteins. Caspase-8 can also proteolytically activate Bid, forming truncated Bid

(tBid), and induces membrane permeabilisation (Fig. 2.4). This represents the main link between intrinsic and extrinsic apoptotic pathways (Kroemer *et al.*, 2007). Furthermore, DNA damage may activate caspase-2, which may in turn promote the release of cytochrome c and other pro-apoptotic factors from the mitochondria (Guo *et al.*, 2002).

Bcl-2 and Bcl-X_L are mitochondrial proteins and inhibit apoptosis by blocking the release of cytochrome c from the mitochondria (Mayer and Oberbauer, 2003). However, the over-expression of Bcl-2 may result in tumour formation. In addition to the Bcl-2 anti-apoptotic protein inhibitor of apoptosis proteins (IAPs) XIAP, c-IAP1 and c-AIP2 are expressed in cells, which bind directly to and inhibit caspase-3 and -7 (Kroemer *et al.*, 2007; Rastogi *et al.*, 2009) (Fig. 2.4).

There are various checkpoints present in the mitochondria that control apoptosis. Some of these signals are: cytosolic and organellar concentrations of protons, Ca^{2+}, K^+ and Na^+, metabolites such as ADP/ATP, glutathione, kinases and phosphatases (Kroemer *et al.*, 2007). Exogenous factors, such as certain viral proteins and xenobiotics, play a role in determining apoptosis. Ultimately, a point is reached in which death-inducing signals may predominate over survival signals, thus leading to mitochondrial membrane permeabilisation and cell death.

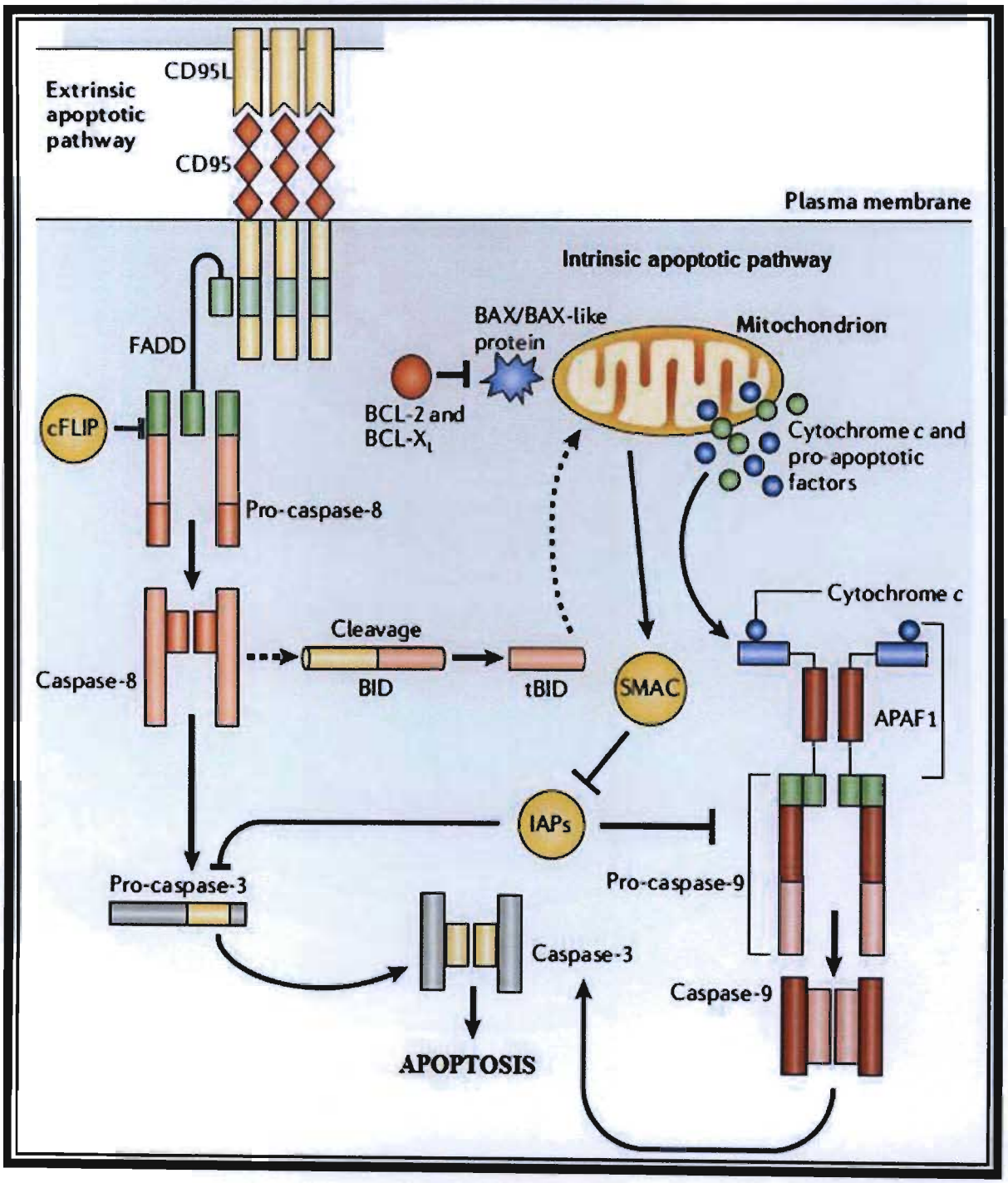

Figure 2.4: An illustration of apoptosis activation by the extrinsic pathway (left) and intrinsic (mitochondrial) pathway (right) and the role of caspases; ← and ⊢ represent activation and inhibition, respectively (Hotchkiss and Nicholson, 2006).

2.6.3 Apoptosis: A Factor in Ochratoxin A Toxicity

Ochratoxin A-induced apoptosis was reported *in vivo* and *in vitro* (Petrik *et al.*, 2003;Atroshi *et al.*, 2000; Gekle *et al.*, 2000; Domijan *et al.*, 2004; Kamp *et al.*, 2005). Features associated with apoptosis, such as DNA fragmentation, caspase-3 activity and chromatin condensation, were observed after OTA treatment (Seegers *et al.*, 1994a; Seegers *et al.*, 1994b; Schwerdt *et al.*, 2004). Additionally, apoptosis was demonstrated in kidney tissue after OTA treatment (Domijan *et al.*, 2004; Petrik *et al.*, 2003). A study on male Wistar rats showed that OTA increased the number of cells undergoing apoptosis in tubular epithelial cells (Petrik *et al.*, 2003).

It was noted in a study by Schwerdt *et al.* (2004) that the mitochondrial membrane potential was decreased in MDCK-C7 cells incubated with OTA, suggesting a role in OTA-induced apoptosis. A loss of mitochondrial potential could result in cellular energetic failure, Ca^{2+} overloading, generation of ROS, loss of osmotic regulation, and cell death. Ochratoxin A also caused disruptions in the pro- and anti-apoptotic proteins of the Bcl family (Assaf *et al.*, 2004). Furthermore, OTA produced oxidative stress (Omar *et al.*, 1990; Petrik *et al.*, 2003; Boesch-Saadatmandi *et al.*, 2008), a trigger of apoptosis.

Moreover, the pH of the cell influences OTA's effect on apoptotic induction. It is believed that a slightly basic pH may reduce the activation of caspase-3 and DNA ladder formation; however, the opposite is observed with an acidic pH (Blank and Wolffram, 2004; Schwerdt *et al.*, 2004). In addition, OTA also increased apoptosis in immune cells (Seegers *et al.*, 1994b; Assaf *et al.*, 2004).

2.7 IMMUNOTOXICITY

The immune system comprises several tissues and white blood cells which play a crucial role in defending the body against infectious agents (Smart and Hodgson, 2008). Immunotoxicity usually occurs when xenobiotic compounds produce unfavourable effects in the immune system. The immunotoxic effects of OTA have been studied in different experimental animals, particularly in rodents (Muller *et al.*, 1999; Assaf *et al.*, 2004; Alvarez *et al.*, 2004; Al-Anati and Petzinger, 2006; Odhav *et al.*, 2008). In mice, OTA produced a decreased

immune response after i.p injection (Prior and Sisodia, 1982). In this particular study the antibody response was decreased over a period of time, and this reduced the ability of the animal to respond to an immunological challenge.

Ochratoxin A may also be associated with the inhibition of DNA synthesis in resting and activated T-lymphoctyes. It has been postulated that OTA induces aberrations on X chromosomes of a similar type to those previously detected in lymphocytes from BEN patients (Stoev, 1998).

The depletion of lymphoid cells and the suppression of antibody response was observed in rats after the oral administration of OTA. A decrease in T-cell response, natural killer (NK) cell activity and bacteriolytic capability of macrophages were also noted (Luster *et al.*, 1987; Stoev, 1998; Alvarez *et al.*, 2004). Furthermore, low concentrations of OTA decreased both NK and cytotoxic T-cell activities *in vitro* (Alvarez-Erviti *et al.*, 2005). Studies on pigs also revealed the immunotoxic potential of OTA (Muller *et al.*, 1999) where the production of ROS increased in whole blood and reduced lymphocyte levels.

Odhav *et al.* (2008) showed that OTA caused morphological changes in human lymphocytes and neutrophils. The featured morphological changes included cell membrane disruption, damage to cytoplasmic organelles and loss of nuclear integrity. These changes affected the immune response by increasing the susceptibility to various infections. A study by Assaf *et al.* (2004) showed a decrease in mitochondrial membrane potential in OTA-treated human peripheral blood mononuclear cells (PBMCs). Ochratoxin A-induced immunotoxicity could occur as a result of protein synthesis inhibition and cell death, and may in turn cause a decrease in the number of immune-competent cells (Assaf *et al.*, 2004; Al-Anati and Petzinger, 2006).

2.8 CELL SIGNALLING PATHWAYS

The signalling pathways, such as those regulated by transcription factors or by kinases, may contribute to OTA toxicity. Mitogen-activated protein kinases respond to extracellular signals and transduce signals from the cellular membrane to the nucleus (Schilter *et al.*, 2005).

The MAPK pathway consists of a serial sequence of protein kinases that phosphorylate and regulate the respective downstream kinases, leading to the activation of MAPK. The mitogen-activated protein kinases have been suggested to play an antagonistic role upon OTA exposure (Marin-Kuan *et al.*, 2007). Extracellular signal regulated kinases1 and 2 (ERK1/2) are pro-mitotic, however, p38 and Jun N-terminal kinase (JNK) support apoptosis, fibrosis and inflammation (Gekle *et al.*, 2000; Sauvant *et al.*, 2005). A balance between these two groups may be important determinants of cellular fate, which was also shown using proximal tubular cells (Arany *et al.*, 2004; Barisic *et al.*, 2005). A study by Barisic *et al.* (2005) found a disruption in the balance of pro- and anti-apoptotic signals when cells were exposed to OTA. Furthermore, the activation of ERK1/2 was not strong enough to stimulate cell survival.

2.9 EFFECT OF OCHRATOXIN A ON PROTEINS

Serum albumin is the most abundant protein in plasma. The binding of OTA to albumin results in a mobile reservoir that can slowly be released, thus retarding elimination (Kumagi, 1985; Schwerdt *et al.*, 1999; O'Brien and Dietrich, 2005). A study on albumin-deficient rats showed that OTA was eliminated faster in albumin-deficient rats than normal rats (Kumagi, 1985). The OTA mobile reservoir may contribute to the development of chronic diseases. It is believed that OTA binds to human serum albumin (HSA) as a dianion (OTA^{2-}) at two sites and that the exact amino acid sequences at the binding sites are crucial in determining OTA binding (Il'ichev *et al.*, 2002; Grajewski *et al.*, 2008).

Schwerdt *et al.* (1999) demonstrated that, proteins with molecular masses between 55kDa and 60kDa, 40kDa and 45kDa, and 20kDa and 25kDa exhibited high OTA-binding capacity. These proteins included those from kidney proximal tubule cells of opossum (OK), pig (LLC-PK1), rat (SKPT) and human (IHKE). It was also shown that OTA bound to many proteins of rat organs, particularly proteins with molecular masses of 62kDa, 40kDa and 26kDa.

Ochratoxin A's primary mechanism of toxicity seems to be associated with the enzymes involved in phenylalanine (Phe) metabolism *viz.*, phenyl transferase and phenylalanine hydroxylase (PAH) (Zanic-Grubisic *et al.*, 2000). Furthermore, OTA compromises protein

synthesis by interacting with phenylalanine-handling proteins at the post-transcriptional level, such as phenylalanyl-tRNA-synthetase (Schwerdt *et al.*, 1999; Stoev, 1998; Simon *et al.*, 1996; Marin-Kuan *et al.*, 2006). This alteration may have an effect on the production of tyrosine from phenylalanine.

The organic anion transport (OAT) system in the proximal tubule is vital for the efficient removal of toxic compounds from the kidney, on a blood-to-lumen basis (Russel *et al.*, 2002). This transport system consists of a basolaterally-located organic anion exchanger, which is dependent upon the inward-directed Na^+ gradient in order to drive the uptake of a-ketoglutarate (Groves *et al.*, 1998). a-Ketoglutarate is exchanged for p-amminohippurate (pAH) or any other competitive organic anion, subsequently resulting in the excretion of xenobiotics (Smart and Hodgson, 2008). It has been suggested that OTA may result in the impairment of organic anion secretion (Sauvant *et al.*, 1998). Gekle and Silbernagl (1994) found a reduced amount of renal secretion and clearance of pAH after a 6-day *in vivo* exposure to rats. An impairment of the OAT system may also be one of the reasons behind OTA's long half-life. Indirect toxic effects could also result from the organic anion transport disruption.

The acute and chronic toxicity by OTA is related directly or indirectly to the inhibition of transport carrier proteins located in the inner mitochondria (Horvath *et al.*, 2002), which may lead to the inhibition of mitochondrial respiration. Furthermore, OTA-induced oxidative stress may disrupt protein function and impair its ability to carry out essential functions in the cell (Domijan *et al.*, 2005).

In a study by Marin-Kuan *et al.* (2006), elongation factor 1-alpha-1 (*eF1A-1*) was down regulated in OTA-treated samples. Elongation factor 1-alpha-1 promotes GTP-binding of aminoacyl-tRNA to the A-site of the ribosomes during biosynthesis. Therefore, if *eF1A-1* is inhibited, protein biosynthesis cannot take place. The same authors have also found that prostaglandin F2 receptor negative regulator and eukaryotic translation initiation factor 4E binding protein 1 are up regulated upon OTA exposure. Both these proteins are involved in the negative regulation of protein synthesis.

2.10 POSSIBLE GENOTOXIC EFFECTS OF OCHRATOXIN A

Genotoxicity refers to the alteration of genetic material, which can be caused by chemical compounds. These compounds can be described as genotoxins and can cause genetic mutations and tumours. If there is minor damage, the cell uses repair processes to return to an 'undamaged' state. An enzyme known as Poly (ADP-ribose) polymerase (PARP) is involved in DNA repair, however, this function is inhibited when it is cleaved by caspase-3, one of the executors of apoptosis (Smart and Hodgson, 2008).

The disruptions in normal cell cycle induced by OTA may constitute the underlying mechanisms of its carcinogenic and nephropathy-inducing activities (O'Brien *et al.*, 2001; Kamp *et al.*, 2005). Kamp *et al.* (2005) observed a decrease in S-phase (synthesis) cells, while the G0 (Resting)/G1 (Gap 1) cells increased. The decrease in the S-phase population was suggested to occur as a result of the inhibition of DNA replication. It is believed that DNA damage induced by OTA can begin at concentration levels which are not yet cytotoxic.

Ochratoxin A treatment resulted in DNA strand breaks in the kidneys, livers and spleens of mice or rats when given either a single dose or by chronic administration *in vivo* (Creppy *et al.*, 1985; Kane *et al.*, 1986; Zeljezic *et al.*, 2006). In addition, OTA induced X-trisomy in cultured human lymphocytes (Manolova *et al.*, 1990). Recently, genotoxic effects such as DNA strand breaks, sister chromatid exchanges, chromosomal aberrations and induction of micronuclei were detected in mammalian systems in response to OTA (Mally and Dekant, 2005; Kamp *et al.*, 2005).

Ochratoxin A-induced DNA damage may occur by DNA-reactive genotoxic mechanisms or DNA non-reactive (epigenetic) genotoxic mechanisms. The direct interaction of a compound with DNA is referred to as the DNA reactive mechanism. During the biotransformation of OTA reactive intermediates may be formed which may bind to DNA and increase tumour formation. Gillman *et al.* (1998) hypothesised that DNA damage may occur due to the photoactivation of OTA. The photoactivation of OTA may lead to the production of a reactive quinone derivative responsible for OTA's DNA adduction properties. Studies conducted *in vivo* (mice and rats) showed DNA adducts after OTA treatment

(Obrecht-Pflumio *et al.*, 1996; Castegnaro *et al.*, 1998). However, it is believed that DNA adducts could be formed by secondary effects *in vivo* (Obrecht-Pflumio and Dirheimer, 2000). The DNA non-reactive mechanism is therefore becoming prominent (Gautier *et al.*, 2001a; Marin-Kuan *et al.*, 2008). This implies that DNA damage may occur through the generation of ROS or cytotoxicity (Zepnik *et al.*, 2001; Kamp *et al.*, 2005; Arbillaga *et al.*, 2007a). It was also evident from previous studies (Schlatter *et al.*, 1996; Gautier *et al.*, 2001a) that although DNA damage occurred, DNA adduct formation was not observed or it was below the level of detection.

2.11 THE MEDICINAL PLANT *SUTHERLANDIA FRUTESCENS*

Sutherlandia frutescens (Fig. 2.5), a flowering bush-type plant, belongs to the Pea family (*Fabaceae*) and is native to South Africa's Western Cape and Karoo region. *Sutherlandia frutescens* has been used in the treatment of cancer, tuberculosis, diabetes, chronic fatigue syndrome, influenza, rheumatoid arthritis, osteoarthritis, reflux oesophagitis, anxiety and clinical depression (Chinkwo, 2005; Mills *et al.*, 2005; Chadwick *et al.*, 2007). Currently, *S. frutescens* is being used in South Africa in the treatment of HIV/AIDS; it helps improve mood and appetite, and is also helpful in increasing CD4 counts and reducing viral loads. Based on primate safety studies, the South African Ministry of Health has concluded that *S. frutescens* is safe to use (Mills *et al.*, 2005; Seier *et al.*, 2002).

Figure 2.5: An illustration of the *Sutherlandia frutescens* plant: A) The medicinal plant showing flowers and leaves; B) Flowers and pods; C) Dried product (leaves) that will be used commercially (van Wyk and Albrecht, 2008).

The leaves of this plant contain L-canavanine (L-CAV), D-pinitol and γ-aminobutyric acid (GABA) (Fig. 2.6). Free amino acids, asparagine, proline and arginine have also been identified in *S. frutescens* (van Wyk and Albrecht, 2008). This medicinal plant also contains phenolic compounds, such as flavonoids and tannins.

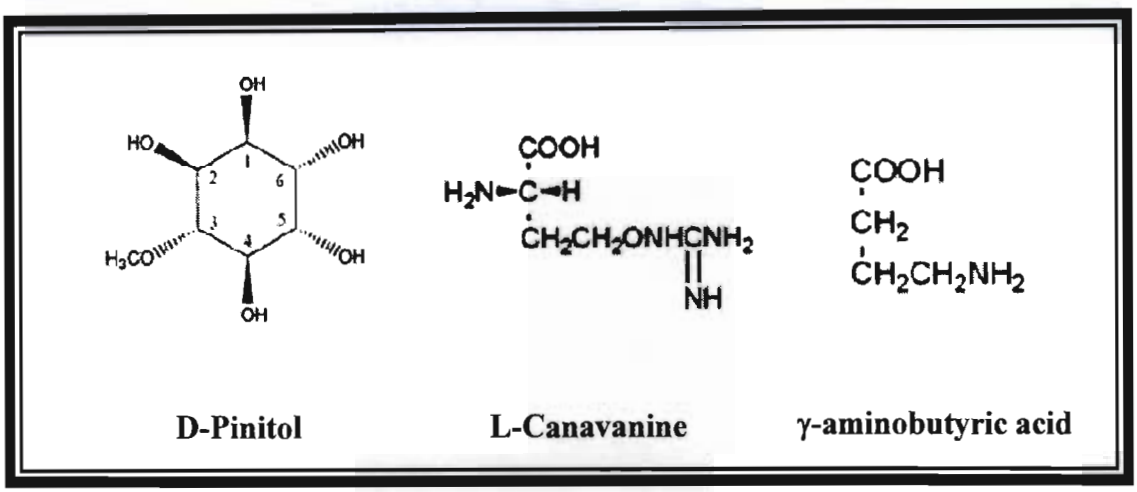

Figure 2.6: Chemical structures of the major compounds found in *Sutherlandia frutescens* (Davis *et al.*, 2000; van Wyk and Albrecht, 2008).

The leaves of *S. frutescens* may serve as a hypoglycaemic agent for the treatment of type-2 diabetes (Chadwick *et al.*, 2007). This may be attributed to the presence of D-pinitol, a type of sugar, which shows potential as a therapeutic agent in the treatment of diabetes (Sia, 2004; van Wyk and Albrecht, 2008). D-Pinitol stands out as it may improve glucose metabolism and thereby increase cellular energy and help reduce fatigue (van Wyk and Albrecht, 2008). In addition, GABA, a weak acid and inhibitory neurotransmitter, may also serve as a possible anti-tumour agent, which may prevent metastasis *in vivo* (Tai *et al.*, 2004).

L-canavanine is an L-arginine (L-ARG) analogue (Fig. 2.7), present in large quantities in the leaves of *S. frutescens*. It is a non-protein amino acid, also known as a secondary or anti-metabolite. As a result, it is not usually used to synthesise cellular proteins but is known to replace L-ARG and produce aberrant canavanyl or non-functional proteins (Akaogi *et al.*, 2006). Subsequently, L-CAV, may affect the tertiary and/or quarternary structure unique to the protein (Bence and Crooks, 2003).

It is suggested that L-CAV competes with L-ARG cellular enzymes such as arginyl tRNA synthetase, inducible nitric oxide synthetase (iNOS) and arginase (Akaogi *et al.*, 2006). L-canavanine is useful in treating many ailments and assists in the breakdown of about 20 amino acids. Each leaf may contain 2.2 – 3mg of L-CAV, which has anti-bacterial, anti-fungal and anti-viral activities (Sia, 2004). Furthermore, L-CAV and its major metabolite canaline may also have anti-tumour properties and are being used as anti-cancer drugs since they tend to induce apoptosis (Tai *et al.*, 2004; Chinkwo, 2005). Protein synthesis, as well as RNA and DNA metabolic pathways, may also be altered by L-CAV (Worthen *et al.*, 1998).

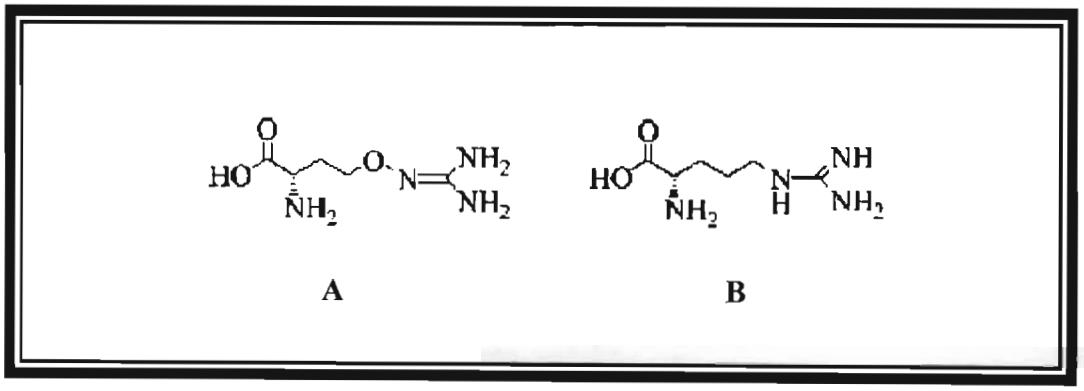

Figure 2.7: Chemical structures of L-canavanine (A) and L-arginine (B) (Bence and Crooks, 2003).

It was also suggested that *S. frutescens* could possibly act as an immunomodulator for the treatment of diseases associated with an overproduction of reactive oxidants (Fernandes *et al.*, 2004). Furthermore, *S. frutescens* was identified as being anti-mutagenic (Reid *et al.*, 2006). Therefore this plant could also have the potential to act as an anti-carcinogenic and chemo-preventative agent.

Since the complete avoidance of OTA in food is difficult, it is imperative to understand the effects of OTA on the body. Studies concerning OTA are important seeing that this toxin is found in a wide variety of food items ingested by both humans and animals. According to the existing literature, OTA produces a number of undesirable cell alterations in the kidneys. Since the kidneys have the important function of eliminating waste from the body, understanding the mechanisms by which OTA induces toxicity is vital. Thus by investigating the mechanisms involved in OTA toxicity the socioeconomic implications that OTA produces may be minimised.

CHAPTER 3

ANIMAL TREATMENT AND SAMPLE STORAGE

3.1 ANIMAL ETHICS

Animal ethics was approved by the University of KwaZulu-Natal Ethics Committee (Faculty of Health Sciences) (Reference number 022/07/Animal). All animal procedures, i.e., injecting, bleeding and animal handling were performed by trained experts in the field of animal handling. These individuals included a registered veterinarian, veterinarian technologist and technicians at the Biomedical Resource Unit (University of KwaZulu-Natal), where the animals were housed.

3.2 ANIMAL TREATMENT

Male Wistar rats (*Rattus novergicus*), weighing between 200 – 300g, were used. The rats were randomly chosen, weighed and then acclimatised for three days prior to treatment. Animals were housed in metabolic cages and were allowed free access to normal food and water. Rats were treated with either vehicle only (EtOH:H_2O; 30:70), *S. frutescens* extract (Phyto Nova Natural Medicines (S.A)), Ochratoxin A (OTA) (Sigma-Aldrich (S.A) or a combination of OTA and *S. frutescens* extract. Ochratoxin A was administered at 0.5mg/kg body weight (Schwerdt *et al.*, 1996; Zeljezic *et al.*, 2006) and *S. frutescens* extract at 1.0mg/kg body weight (Stander *et al.*, 2007) by intraperitoneal (i.p) injection. Both OTA and *S. frutescens* extract were diluted with the vehicle prior to injection (Appendix A). Rats received treatments (vehicle only, *S. frutescens* extract, OTA-only or a combination of OTA and *S. frutescens* extract) for a period of only 1 day (Day 1) or 7 consecutive days (Day 7). Therefore, animals were divided into eight groups, with four rats in each group (Table 3.1).

During the period that the rats were observed under treatment, a drop of tail blood (approximately 20µl) was taken on Day 0, Day 1 and Day 7, for the Comet Assay. The rats were placed in a warm chamber for 1 – 2 minutes. A tube restrainer was used to restrain the

animals, leaving only the tail exposed. The lower part of the tail was swabbed with a disinfectant. Thereafter, a sterile 1 inch, 23 gauge injection needle was used to prick the tail. After the required time periods (1 day and 7 days), each rat was placed in an inhalation chamber that contained anaesthetic halothane. As soon as breathing stopped, animals were removed, exsanguanated, and organs harvested.

Table 3.1: Animal treatment and duration

Group	Animal Treatment	Duration
Group 1	Control (n=4)	1 day
Group 2	*S. frutescens* only (n=4)	1 day
Group 3	OTA only (n=4)	1 day
Group 4	OTA and *S. frutescens* (n=4)	1 day
Group 5	Control (n=4)	7 days
Group 6	*S. frutescens* only (n=4)	7 days
Group 7	OTA only (n=4)	7 days
Group 8	OTA and *S. frutescens* (n=4)	7 days

3.3 BLOOD COLLECTION

On the day of organ harvest, rat blood was collected by cardiac puncture. This method was selected based on its ease and rapidity with minimal contamination. A combined volume of 6ml blood was collected for each rat in two types of blood tubes. Heparinised tubes were used for whole blood collection and tubes containing serum gel were used for serum.

3.4 BLOOD SEPARATION

Following blood collection from each rat, bloods were immediately separated in order to obtain peripheral blood mononuclear cells (PBMCs). All handling of blood was carried out under a safety cabinet equipped with a vertical laminar flow.

For better separation, blood was mixed with an equal amount of phosphate buffered saline (PBS) (Merck (S.A). Thereafter, the blood-PBS mixture was layered onto an equal volume of Histopaque-1077 (Sigma-Aldrich (S.A) (approximately 3ml) and the samples were centrifuged (25 min, 2 500rpm, room temperature (RT)). Histopaque-1077, adjusted to a density of 1.077±0.001g/ml, is a mixture of polysucrose and sodium diatriozoate and helps in the recovery of viable mononuclear cells from small volumes of blood.

After centrifugation, three distinct layers were obtained: plasma, PBMCs (buffy coat) and red blood cells (RBCs) (Fig. 3.1).

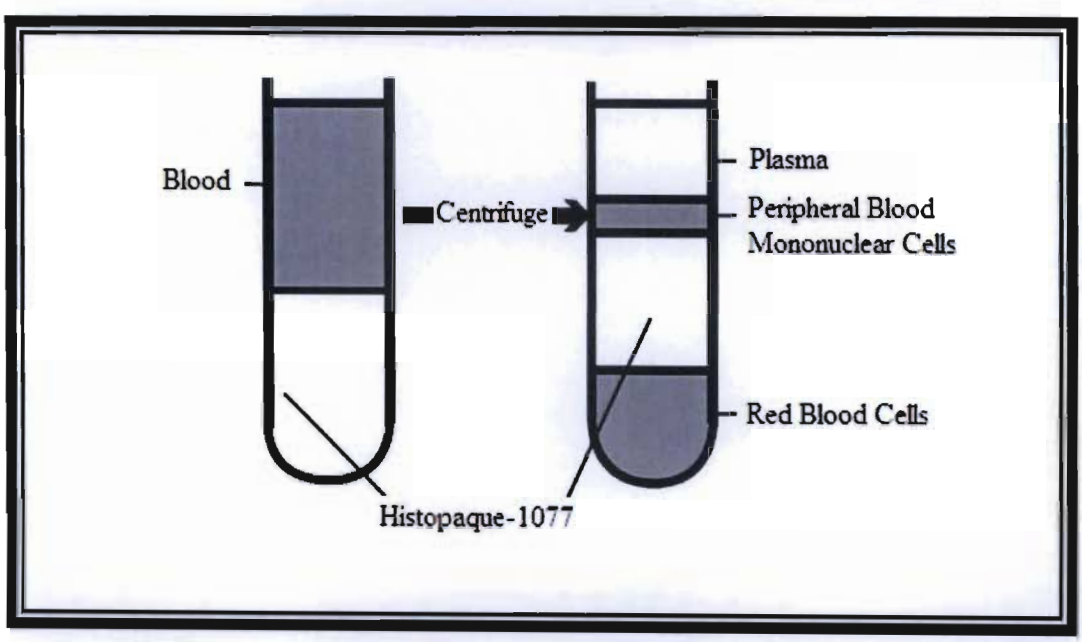

Figure 3.1: Separation of peripheral blood mononuclear cells from whole blood using Histopaque-1077. Three distinct layers are formed: plasma, mononuclear cells and red blood cells (Sigma-Aldrich, 2003).

The top layer (plasma) was carefully removed and aliquoted into cryovials, and stored (-80°C) for future use. Care was taken not to touch the buffy coat layer, as removal of this layer reduces the number of PBMCs obtained. Next, PBMCs were aspirated and transferred into eppendorfs. Isolated PBMCs were then washed with PBS (15 min, 3 500rpm). The supernatant was discarded and the pellet obtained was re-suspended in PBS (700µl).

3.5 CELL COUNTING

Thereafter, PBMCs were counted using a haemocytometer. This device consists of a thickened glass slide that has a small chamber of grids that is cut into the glass. The chamber has a fixed volume and has 9 large squares etched into it. Each large corner square contains 16 smaller squares. The large squares measure 1mm x 1mm and are 0.1mm deep. The cell suspension (10µl) (50µl trypan blue stain, 50µl complete culture media and 50µl PBMCs) was loaded into a clean haemocytometer chamber. Cells within the 4 corner squares (orange squares in Fig. 3.2) were counted with the aid of an inverted microscope, set at 400x magnification.

Trypan blue (Merck (S.A)) was mixed with PBMCs in order to differentiate the viable cells from the dead cells. The dye is taken up by dead cells, but is excluded from live cells. As a result, viable cells appear as bright transluscent structures while dead cells stain blue. When counting cells, only cells touching the top and left borders were counted, while those touching the bottom and right borders were excluded (Fig. 3.2). The count was mathematically converted to number of cells/cm^3 and the cell number was adjusted to 1×10^6 cells/ml. Cell viability was calculated according to the following equations:

Cells per ml= Average count per square x *dilution factor x* 10^4

Total cells = (Cells per ml x *(original volume of fluid from which cell sample was taken))*

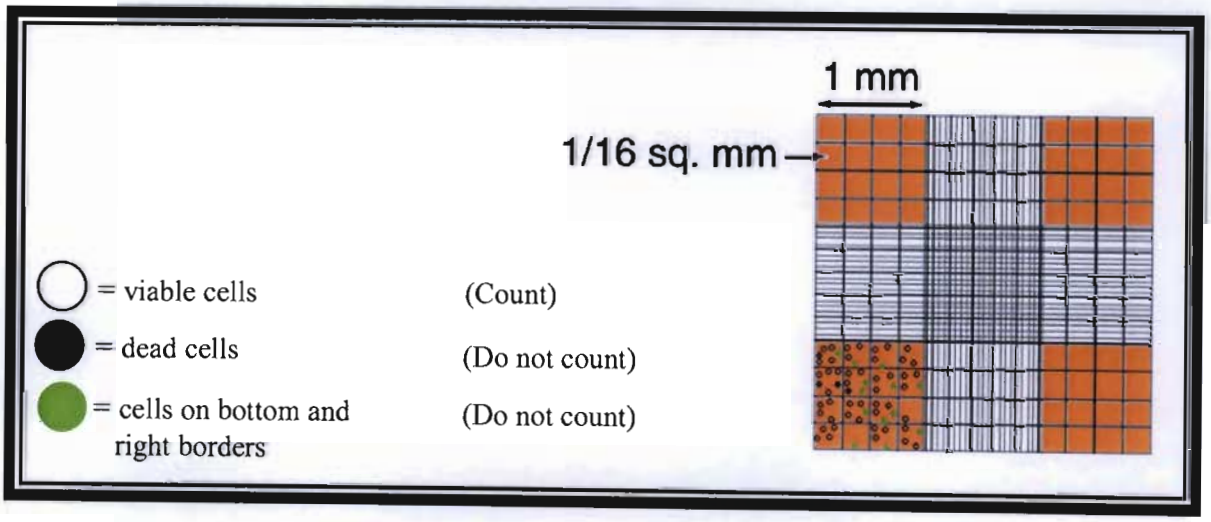

Figure 3.2: Illustration of the cell counting procedure.

Peripheral blood mononuclear cells (PBMCs) were then used to assay for apoptosis and cell viability using flow cytometry and the methylthiazol tetrazolium (MTT) assay, respectively.

3.6 CRYOPRESERVATION

Cryopreservation serves as an excellent way to sustain cells and provides a renewable source that could be used in the future. Therefore, an aliquot of PBMCs were cryopreserved for future use. The PBMCs were mixed with (1.5ml) cryosolution (90% foetal calf serum (Gibco) and 10% dimethyl sulphoxide (DMSO)). Freezing can result in the formation of ice-crystals and changes in the concentration of electrolytes and pH (Wilson and Walker, 2005). Dimethyl sulphoxide (DMSO) (Merck (S.A)) was therefore used as a cryoprotectant as it lowers the freezing point and prevents ice-crystal formation inside the cell. The addition of foetal calf serum ensured that the cells also had a good supply of nutrients. The cryosolution was added to the PBMCs in a drop-wise manner. Cryosolution and PBMCs were thoroughly mixed, and was then placed in a nalgene cooler. The nalgene cooler allowed the temperature to decrease by -1°C/min and required the addition of 100% isopropanol (Merck (S.A)) and mechanical freezing (-80°C).

3.7 ORGAN STORAGE

After the organs were harvested, the organs of interest, the kidneys, were initially bisected and then further cut into smaller pieces. A portion of this tissue was placed into labelled vials according to each treatment and immediately snap-frozen in liquid nitrogen at the Biomedical Resource Unit. This tissue was stored (-80°C) and then later used for protein analysis.

The rat kidneys were also used for histological analysis. Therefore, a fraction of the kidney tissue collected on the day of harvest (as described above) was immediately immersed in Finefix solution (Apollo Scientific). This was done to preserve the tissue in a life-like manner, to prevent tissue autolysis and to protect it from the processing that follows thereafter. Tissue may dry if it is not fixed directly after harvest, which may lead to artefact formation, nuclear shrinkage and cellular organelles may be damaged. The tissue was placed in Finefix solution for approximately 12 hours before processing.

CHAPTER 4

METABOLIC ACTIVITY OF PERIPHERAL BLOOD MONONUCLEAR CELLS FROM OCHRATOXIN A TREATED MALE WISTAR RATS

4.1 INTRODUCTION

When cells are treated with a cytotoxic compound they may undergo either apoptosis or necrosis. Cytotoxicity does not however identify the specific cell death mechanism. A cell cannot survive without a source of energy and chemical building blocks. This energy is obtained from metabolism.

Metabolism refers to the chemical processes that take place in a cell. Harvesting of energy is one of the endpoints of metabolism. The mitochondrion is often referred to as the 'energy powerhouse'; this is because most ATP generation occurs in the mitochondria. The tricarboxylic acid (TCA) cycle (central oxidative pathway in respiration) and electron transport occur within the matrix of the mitochondria. Most of the energy released by oxidations in the TCA cycle is trapped in the electrons carried by NADH and $FADH_2$. These electrons then enter the electron transport chain in order to drive the synthesis of ATP. Due to cellular damage, the energy required for metabolic cell functions and growth can be reduced.

Cellular metabolic activity can be measured by the use of tetrazolium salts. Tetrazolium salts are used extensively in cell proliferation and cytotoxicity assays, enzyme assays, histochemical procedures and bacteriologic screening (Berridge *et al.*, 1996). A distinct chromogenic product (formazan) is formed in each of the above-mentioned procedures (Berridge *et al.*, 1996).

The methylthiazol tetrazolium (MTT) assay is a quantitative colorimetric method, based on the reductive cleavage of the water-soluble monotetrazolium salt MTT (3-[4,5-dimethylthiazol-2-yl]-2,5-diphenyltetrazolium bromide), a pale yellow substrate which yields a purple formazan product (Mosmann, 1983). Since formazan is insoluble, it is solubilised

using an appropriate solvent, and thereafter the absorbance of the solution can be determined using a spectrophotometer. Formazan is directly correlated with metabolically viable cells. Therefore, an increase in the number of viable cells results in an increased absorption of the solution (Bernhard *et al.*, 2003). The MTT assay thus measures the cell proliferation rate and viability, based on metabolic activity (Bernhard *et al.*, 2003).

Only viable (metabolically active) cells can convert MTT to formazan, therefore, MTT is actively transported into viable cells where the tetrazolium ring is cleaved. One mechanism for the reduction of MTT to formazan occurs via the succinate-tetrazolium reductase system (mitochondrial respiratory chain) (Bernhard *et al.*, 2003). It was shown that MTT reduction is also dependent upon the amount of reduced nicotinamide dinucleotides NADH and NADPH (Berridge and Tan, 1993). The MTT assay is sensitive, quick, requires a reduced number of cells, and allows a large number of samples to be processed simultaneously.

Cytotoxic agents may reduce the cells' ability to cleave MTT to formazan. Ochratoxin A is widely known to be cytotoxic to cells. Subsequently, cell viability and metabolic activity were determined in PBMCs of rats treated with OTA. Furthermore, the cyto-protective effects of *S. frutescens* on PBMCs from OTA treated rats were also examined.

4.2 MATERIALS AND METHODS

4.2.1 Materials

MTT salt was purchased from Calbiochem (S.A.); Dimethyl sulphoxide (DMSO) and PBS tablets were obtained from Merck (S.A.); 96 well microtiter plates were purchased from the Scientific Group (S.A.). All other chemicals were purchased from Merck (S.A.).

4.2.2 Methods

4.2.2.1 Methylthiazol Tetrazolium Assay

Peripheral blood mononuclear cells (PBMCs) were isolated by differential centrifugation, as discussed in Chapter 3.

A 50µl PBMC aliquot (1×10^6 cells/ml) from each treatment was added to a 96 well microtiter plate. Methylthiazol tetrazolium (5mg/ml) salt solution (in PBS, pH 7.4) (10µl) was then added to each well containing PBMCs. These steps were performed in a safety cabinet equipped with a vertical laminar flow hood, to ensure that the cell suspension was protected from any foreign particles that may affect the experiment.

Cells were then incubated (1 hr, 37°C), to allow for the reaction to take place. Thereafter, cells were centrifuged (10 min, 2 000rpm, RT). After centrifugation, the supernatant was discarded and DMSO (200µl) was added to each well. Dimethyl sulphoxide is a polar aprotic solvent (cannot donate hydrogen) and dissolves both polar and non-polar compounds. Therefore, DMSO solubilises the formazan (insoluble) product formed. Cells were re-incubated (30 min, 37°C). Thereafter, the optical density was measured spectrophotometrically at a wavelength of 590nm, with a reference wavelength of 655nm, using a Quant ELISA plate reader (Analytical Diagnostic products (S.A.)).

The assay was performed in triplicate and mean cell viability was calculated by comparing the absorbance of each treatment to that of the control:

$$Cell\ Viability\ (\%) = \left(\frac{Mean\ absorbance\ of\ treatment\ cells}{Mean\ absorbance of\ control\ cells}\right)\times 100$$

4.2.3 Statistical Analysis

Statistical significance was determined using One-Way Analysis of Variance (ANOVA) and the Tukey-Kramer Multiple comparisons test on GraphPad Instat v3.06 (GraphPad Software, San Diego, CA). A probability value (p) of less than 0.05 ($p<0.05$) was considered statistically significant.

4.3 RESULTS

In order to determine statistical significance, treatments were initially compared with the control for the same durations. Thereafter, comparisons were made between the Day 1 and Day 7 regimes. The PBMC viability of the rat control groups (Group 1 and Group 5) was 100% (Fig. 4.1).

Statistical analysis showed that there were significant increases in PBMC viability after the *S. frutescens* (Group 2), OTA-only (Group 3) and combination (OTA and *S. frutescens*) (Group 4) Day 1 treatments when compared to the control ($p<0.001$) (Fig. 4.1). While treatment with *S. frutescens*-only (Day 1) resulted in a 168.8% viability, the OTA-only and combination treatments both produced PBMC viabilities of 208% after 1 day (Fig. 4.1). No significant difference in viability was observed between the OTA-only and combination treated rat PBMCs (Day 1). However, rats treated with a combination of OTA and *S. frutescens* exhibited a significantly higher (1.23-fold) PBMC viability after Day 1 than did the rats treated only with *S. frutescens* ($p<0.001$) (Fig. 4.1).

Following a 7-day treatment, the OTA-only treated rat group (Group 7) showed a significant decrease (7.14-fold) in PBMC viability (14%) compared to the control (Day 7) ($p<0.001$) (Fig. 4.1). The PBMC viability of the combination-treated rat group (73%) (Group 8) was 1.37-fold lower compared to the control ($p<0.05$) (Fig. 4.1). No significant difference was observed between the PBMC viabilities of the *S. frutescens* (Group 6) (106%) and control rat groups. In addition, PBMCs from the combination-treated rats (7 days) showed a significantly higher (5.21-fold) PBMC viability than did those treated with OTA alone ($p<0.001$). The results also show a significantly lower (1.45-fold) PBMC viability in the combination group when compared to the *S. frutescens*-only treated rats, after 7 days ($p<0.01$) (Fig. 4.1).

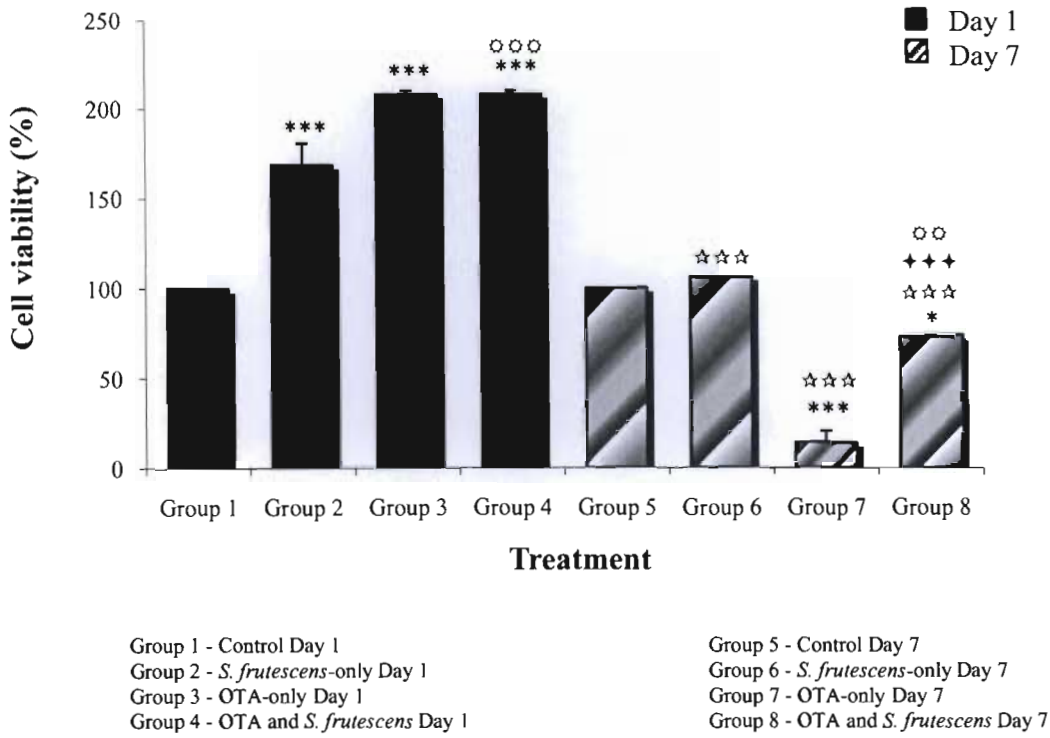

Figure 4.1: Measurement of peripheral blood mononuclear cell viability by the MTT assay. Data represent the mean ±SEM (n=4). Comparisons were made with controls and between Day 1 and Day 7 treatments. * represents comparison with control *p<0.05 ***p<0.001. ☆ represents comparison between Day 1 and Day 7 treatments ☆☆☆p<0.001. ✦ represents the comparison between OTA-only and the co-treatment ✦✦✦p<0.001. ○ represents comparison between *S. frutescens*-only and the combination group ○○p<0.01 ○○○p<0.001.

In order to determine the effect of treatment duration on toxicity, comparisons in PBMC viability were made between the Day 1 and Day 7 treatments. The viability of PBMCs from the *S. frutescens* treated rats after 7 days was 106% (Fig. 4.1); this was significantly lower (1.59-fold) than the Day 1 treatment (168.8%) (p<0.001). After a period of 7 days, the PBMC viability of the OTA-only treatment was 14% and this was 14.85-fold lower than the Day 1 regime (p<0.001) (Fig. 4.1). Furthermore, there was a significant decrease (2.85-fold) in PBMC viability when rats were treated with a combination of OTA and *S. frutescens* for 7 days (73%), compared to the Day 1 treatment (208%) (p<0.001) (Fig. 4.1).

4.4 DISCUSSION

The reduction of tetrazolium salts in the MTT assay is dependent upon metabolic activity, which in turn determines cell viability. An increase in viability means that the cells are metabolically active. Peripheral blood mononuclear cell viability of the *S. frutescens*-only treatment group was higher than the control after 1 day. D-Pinitol is known to have anti-diabetic effects; it acts like insulin and promotes glucose transport and glycogen synthesis, and therefore increases energy production (van Wyk and Albrecht, 2008). Subsequently, an increase in PBMC viability after the Day 1 *S. frutescens*-only treatment may have been due to the D-Pinitol activity, and thus the MTT activity in these cells was high. However, the PBMC viability of the *S. frutescens*-only treated rats significantly decreased after 7 days when compared with the Day 1 *S. frutescens* treatment. Thus, it is possible that with repeated doses, *S. frutescens* may be more effective. A high PBMC viability was maintained after 7 days at 106%, which suggests cells were still metabolically active.

An increase in rat PBMC viability after the Day 1 OTA-only and combination treatment indicates that metabolic activity in these cells was high. Furthermore, it is possible that OTA may affect cellular signalling and regulation, creating a mitogenic effect, which may result in an increase in glucose utilisation and therefore, the increased metabolic activity. In addition, the increase in cell viability after the Day 1 treatment could be a possible stress-response mechanism. It is also known that a degree of toxicity may induce cell regeneration and proliferation, which may increase the risk of various genetic errors and subsequently lead to cell transformation and tumour development (Schilter *et al.*, 2005).

A decrease in PBMC viability of the OTA-only treated rats after 7 days suggests that the time period in which the toxin was in the body may have had converse effects. As previously mentioned, the presence of OTA in the body for an extended period of time could result in cell death (Schwerdt *et al.*, 2007). It is believed that mitogen-activated kinases (MAPKs) may play an antagonistic role upon OTA exposure (Marin-Kuan *et al.*, 2007; Marin-Kuan *et al.*, 2008). Insulin is the main hormone responsible for glucose uptake in cells and its functions are dependent on MAPK signalling. If OTA causes disruptions in MAPKs, it is possible that the insulin function may be hampered and that the glucose uptake into cells will be decreased.

NADH production in the cell will thus be reduced, resulting in a decrease in dehydrogenases, which subsequently decreases cell viability. It is possible that this may have occurred after the 7-day OTA-only treatment. This alteration of insulin function may lead to diabetes and, if not treated, ultimately lead to severe kidney disease.

Immune cells such as lymphocytes can utilise glutamine, in addition to glucose, at high rates and glutamine is required for both lymphocyte proliferation and cytokine production (Mates *et al.*, 2002; Newsholme *et al.*, 2003). The immediate product of glutamine metabolism is L-glutamate (Newsholme *et al.*, 2003). The conversion of glutamine to glutamate ultimately results in α-ketoglutarate, an intermediate of the TCA cycle, through transamination. Initially, the amino group of glutamine is hydrolysed, thus yielding glutamate and ammonium. Glutamate is then further metabolised to α-ketoglutarate. Thus, if there is a decrease in the conversion of glutamate to α-ketoglutarate, subsequent steps in the TCA cycle will be minimised. This leads to a reduction in the production of NADH and therefore the reduction of formazan production. This would alter the TCA cycle and energy production would therefore be decreased leading to a lower cell viability, which was noticed in the OTA-only treated rats on Day 7. α-Ketoglutarate is important in the TCA cycle and is therefore linked to ATP production.

Although α-ketoglutarate is produced by mitochondria in the kidney, blood concentrations are also important. ATP is vital to the kidney because of the active transport that takes place. Furthermore, α-ketoglutarate is known to be important in the movement of xenobiotics or drugs from the blood into the kidney, where it is excreted (Smart and Hodgson, 2008). However, when the level of α-ketoglutarate in kidney cells decreases, the α-ketoglutarate produced in the blood will be transported into the kidney cells. Any changes in α-ketoglutarate in the lymphocytes therefore affects the kidneys. As has been shown in other studies, OTA may be responsible for altering mitochondrial function (Aleo *et al.*, 1991; Bouaziz *et al.*, 2008), and this in turn may be the result of disruptions in the glutamine metabolism.

In order to maintain high rates of glutaminolysis (despite the plasma level of glutamine), the flux through the glutaminolytic pathway is controlled (Newsholme *et al.*, 1985). Therefore,

factors such as: glutamine transport across the cell and mitochondrial membranes; glutaminase and oxoglutarate dehydrogenase; and changes in intracellular Ca^{2+}, may play a pivotal role in controlling glutaminolysis (Newsholme *et al.*, 1985). It is owing to the loss of control of these factors that glutaminolysis may have decreased, thus altering the conversion of glutamine to α-ketoglutarate.

It is also believed that white blood cells and immune cells migrate to OTA-damaged organs (such as the kidney and liver), and this reduces the number of immune cells in the bloodstream (Al-Anati and Petzinger, 2006). The disruption of cell proliferation, interference with cell surface receptors, signalling pathways or metabolic activities may be responsible for alterations in the immune response. A decreased number of immune cells in the bloodstream results in sensitivity to infections due to the suppression of humoral and cell-mediated immune response. The results of the present study show that OTA is not only cytotoxic, but it is also highly immunotoxic, as has been shown in other studies (Alvarez *et al.*, 2004; Alvarez-Erviti *et al.*, 2005).

Sutherlandia frutescens is believed to have anti-proliferative effects (Tai *et al.*, 2004; Reid *et al.*, 2006 and van Wyk and Albrecht, 2008). An analysis of the Day 1 combination treatment, however, showed that PBMC viability was significantly higher than that of the control. It should also be noted that there was no significant difference between the co-treatment and OTA-only group after Day 1. It is possible that the anti-proliferative effects of *S. frutescens* may not have been effective after the Day 1 treatment. Instead, OTA and *S. frutescens* together continued to increase PBMC viability.

The PBMC viability of the 7-day combination regime (Group 8) was significantly lower than that of the Day 1 treatment ($p<0.001$) (Fig. 4.1). It has been suggested that for *S. frutescens* to be effective in *vivo*, its active ingredients must be absorbed and presented to the targets at concentrations that can actually exert an effect (Tai *et al.*, 2004). Therefore, the repeated injection of doses of *S. frutescens* into rats could ensure the effectiveness of this medicinal plant. While the OTA-only treatment (Day 7) resulted in an extremely low cell viability, treatment with the combination of OTA and *S. frutescens* significantly increased cell viability after 7 days compared to the control (Fig. 4.1). Considering that D-pinitol may have

insulin-like effects, it is possible that D-pinitol may have counteracted any disruption in insulin function which OTA may have caused. It is evident that only after a period of 7 days did the plant's properties become effective in assisting in the maintenance of cell viability. The results thus point to *S. frutescens* protective role towards immune cells.

Anti-proliferative effects of *S. frutescens* have been studied using various cancer cell lines (Tai *et al.*, 2004; Stander *et al.*, 2007). Active compounds in *S. frutescens* are believed to produce these anti-proliferative effects. The diverse biological activities of L-CAV have led to the evaluation of its potential as an anti-cancer agent (Worthen *et al.*, 1998). L-canavanine has been shown to bring about anti-proliferative effects *in vivo*. Being an L-ARG analogue, L-CAV can replace L-ARG. L-canavanine is less basic and slightly longer than L-ARG, and it exists in an amino rather than an imino tautomeric form (Bence and Crooks, 2003). The incorporation of L-CAV can therefore affect the quarternary structure of proteins and can lead to changes in growth.

It is believed that the anti-proliferative effects of L-CAV are the result of its conversion to the arginase metabolite, L-canaline, which can disrupt biochemical pathways involving L-ornithine and polyamines (Bence *et al.*, 2002). Both L-ornithine and polyamines influence cell growth. L-ornithine may increase the levels of growth-promoting hormones, such as insulin and growth hormone, and if cellular polyamine synthesis is stopped, then cell growth is inhibited. It is now also believed that the major triterpenoids of *S. frutescens* are closely related in structure to cycloartane-type triterpenoids, which have proven cancer chemopreventive activities (van Wyk and Albrecht, 2008). Subsequently, these antiproliferative effects may have resulted in the decreased PBMC viability noticed after the 7 day (Group 7) *S. frutescens* and combination regime, as compared with Day 1 (Group 3) regimes (Fig. 4.1).

Furthermore, GABA is a weak acid and disrupts mitochondrial polarity. When mitochondria are fully polarised, they will produce more ATP. GABA, however, decreases mitochondrial membrane polarity and ATP production, thus reducing cell viability. This may therefore have resulted in a reduced source of energy and subsequently a reduced PBMC viability, shown at Day 7 in the OTA and *S. frutescens* combination treatment (Group 8) and also in the

S. frutescens-only group (Group 6) (Fig. 4.1). Together with this, OTA also causes disruptions in mitochondrial oxidative phosphorylation through the succinate-dependent electron transfer activities (Wei *et al.*, 1985). This may also be a reason behind the reduced PBMC viability noticed after the OTA-only and combination treatments.

4.5 CONCLUSION

Peripheral blood mononuclear cell viability, when rats were treated with OTA alone or with the combination of OTA and *S. frutescens* for 1 day, was significantly higher than the control. Drastic changes were observed after the 7-day treatment with OTA alone, which caused the PBMC viability to decrease. These results confirm the immunotoxic potential of OTA. In addition, the results indicate the possible (immuno) protective role of *S. frutescens*. Ochratoxin A exerted its toxic effects on PBMCs in a time-dependent fashion.

CHAPTER 5

GENOTOXIC EFFECTS OF OCHRATOXIN A ON RAT PERIPHERAL BLOOD MONONUCLEAR CELLS

5.1 INTRODUCTION

Genotoxicity is the field of toxicology that assesses the effect of chemicals or xenobiotics on DNA and/or RNA of living organisms (Smart and Hodgson, 2008). The nucleus is the site where genotoxic agents exert their toxicities. Eukaryotic chromosomes contain DNA (50-100cm in length) and have to be condensed 10^5 fold to fit within a nucleus of 5-10μm (Mckelvey-Martin *et al.*, 1993). However, the occurrence of DNA damage is possible. DNA damage can include single and double strand breaks in the DNA backbone, cross-links between DNA and DNA bases and proteins, as well as chemical additions to DNA base pairs (adducts) (Smart and Hodgson, 2008). Chemicals can also intercalate between base pairs. In normal living cells high molecular weight chromosomal DNA is contained within the nucleus, but there is no DNA in the cytoplasm. In apoptotic cells, deoxyribonuclease (DNase) activation leads to low molecular weight fragments in the cytoplasm and the nucleus. The amount of high molecular weight uncleaved DNA declines in the nucleus because of the action of endonucleases.

Single cell gel electrophoresis (SCGE) is a technique used for the detection of DNA damage. Originally developed and referred to as the Comet Assay (Ostling and Johanson, 1984), this method used neutral conditions and only permitted the detection of double strand DNA breaks (Rojas *et al.*, 1999). This method was subsequently modified by Singh *et al.* (1988) in order to incorporate alkaline conditions. This ensures the detection of DNA double strand breaks and alkali labile sites, DNA-DNA/DNA-protein cross-linking, as well as single strand breaks associated with incompletely repaired excision in individual cells. The assay can be used with a variety of cell types and also has a wide variety of applications, such as genotoxicity and DNA repair studies, clinical applications and human and environmental monitoring (Rojas *et al.*, 1999).

DNA damage is determined by examining the individual comets that form after electrophoresis. Briefly, cells, mixed with low-melting-point agarose (LMPA), are sandwiched between two layers of LMPA on a microscope slide. Cells are then placed in a lysis solution (a highly aqueous salt solution and detergent). The salt disrupts proteins and the bonding pattern within the cell, whilst the detergent (Triton X-100) dissolves cellular membranes. Incubating samples in lysing solution ensures that only the DNA of the cell remains. Prior to electrophoresis, DNA unwinding is achieved by placing cell laden slides in an electrophoretic buffer (pH 13), and DNA starts to unwind from sites of strand breakage (Rojas *et al.*, 1999; Tice *et al.*, 2000). DNA that is damaged loses its compact structure and moves into the agarose matrix in an electric field. The negatively charged loose DNA moves towards the anode forming a comet-shaped image. The head of the comet represents the undamaged DNA, while the tail represents the damaged DNA. Comet tails are the result of the migration of relaxed DNA loops to a limited distance and the length of these loops determines the length of the comet tail (Zeljezic *et al.*, 2006).

The DNA can be viewed through the use of ethidium bromide (EtBr) staining (an intercalating dye). After excitation, red fluorescence is produced and individual cells may be examined. Fluorescence intensity and length is related to the number of DNA strand breaks induced by the test agent (McKelvey-Martin *et al.*, 1993). The parameter most commonly used to quantify DNA damage is the length of DNA migration (tail length) in micrometres (μm) (Rojas *et al.*, 1999). Migration length is directly related to fragment size and is expected to be proportional to the extent of DNA damage (Tice *et al.*, 2000); therefore, longer tail lengths mean greater DNA damage.

An advantage of using SCGE is that detection of DNA damage can be made at the level of the single cell and that only a small number of cells is required. Furthermore, almost any eukaryotic cell population can be used and the assay is able to evaluate DNA damage in non-proliferating cells (Rojas *et al.*, 1999). This assay is sensitive, simple, cost-effective and data can be obtained within a few hours of sampling.

The aim of the work reported in this chapter was to assess the immuno-genotoxicity of OTA in male Wistar rats using SCGE. In addition, PBMCs from rats treated with *S. frutescens* and in combination with OTA were examined for genotoxicity.

5.2 MATERIALS AND METHODS

5.2.1 Materials

Low melting point agarose (LMPA) was purchased from Whitehead Scientific (S.A.); Sodium chloride (NaCl), Ethylenediaminetetraacetic acid (EDTA), Tris, Dimethyl sulphoxide (DMSO), Sodium hydroxide (NaOH), Disodium ethylenediaminetetraacetic acid (Na_2EDTA), Triton X-100 and Ethidium bromide (EtBr) were obtained from Merck (S.A.); Slides and Coverslips were purchased from Shalom Laboratories (S.A.). All other reagents were obtained from Merck (S.A.).

5.2.2 Methods

Initially, 1% LMPA (400µl) (Appendix B1) was dispensed onto a glass slide. This was immediately covered with a coverslip and allowed to set (10 min, 4°C), thereby forming a layer of agarose over the slide. After removing the coverslips, a mixture of rat whole blood (20µl) and 0.5% LMPA (180µl) (Appendix B1) was added over the first layer, then allowed to set (20 min, 4°C). A final layer of 0.5% LMPA (200µl) was added over the second layer. The third layer was allowed to solidify for ±20 min. The above steps were crucial since the agarose layer had to be fixed onto the slide in order for it to withstand the steps that followed. Subsequent to the removal of the coverslips, slides were placed in freshly prepared cold lysing solution (Appendix B2) (1 hr).

Thereafter, slides were equilibrated (20 min) in the electrophoresis buffer (pH 13) (Appendix B3) to allow the DNA to unwind prior to electrophoresis. Following equilibration, the samples were electrophoresed (35 min, 300mA (25V)) to allow for the migration of DNA.

After electrophoresis, the agarose-layered slides were washed with 0.4M Tris (pH 7.4) (Appendix B4) (3 washes for 5 min each). The washing procedure removes excess electrophoresis buffer and neutralises the gel. The slides were handled carefully in order to prevent any agitation of the agarose layers. Good drainage is important, as excess electrophoresis buffer could interfere with the EtBr staining and minimises background intensity on the slides.

Finally, gels were stained with 40µl EtBr (20µg/ml). Images were viewed using an Olympus IXSI microscope. The Comet tail lengths in 50 randomly selected cells for each treatment were measured using the Analysis LS Research software. These steps were carried out under minimal light conditions.

5.2.3 Statistical Analysis

Statistical analysis was performed using GraphPad Instat v3.06 (GraphPad Software, San Diego, CA). Comparisons between treatments were made using One-Way Analysis of Variance (ANOVA). Significant differences were determined using Tukey-Kramer Multiple comparison tests. A probability value (p) of less than 0.05 ($p<0.05$) was considered statistically significant.

5.3 RESULTS AND DISCUSSION

One of the hallmarks of the advanced stages of apoptosis is DNA fragmentation. Since the measurement of a comet tail length is related to DNA fragmentation (single strand breaks), the tail lengths can be used as a measure of apoptosis.

Cells undergoing apoptosis and necrosis can be distinguished from one another based on the characteristics of the comets produced. Apoptotic cells can be recognised by a small comet head and a long fan-like tail and most of the DNA migrates out of the nucleus. This sets it apart from healthy cells where most of the DNA remains intact within the nucleus. Necrotic cells (double stranded DNA breaks), however, are characterised by a non-dense, large comet head and a shorter, narrow tail.

The analysis of the SCGE photomicrographs shows that the pre-treatment groups (Day 0) produced no DNA damage (Fig. 5.1a-d). In the control group, cells retained a dense nuclear stain and showed minimal comet length variations between Day 0 to Day 7 (Fig. 5.1a-i). The control group treatments contained ethanol, which had minimal effects on rat PBMC DNA damage.

A gradual duration-dependent increase in comet tail length was noticed in the *S. frutescens* rat group (Fig. 5.1 and Fig. 5.2). The longest tail length was produced by *S. frutescens*-only at Day 7 (Fig. 5.1j) and the tail length was significantly longer when compared with the control for the same period ($P<0.001$). The presence of long tail lengths are strong indicators of apoptosis in the immune cells.

Previous studies on cultured cells showed that *S. frutescens* possessed apoptotic inducing abilities (Tai *et al.*, 2004; Chinkwo, 2005). The study by Chinkwo (2005) demonstrated that *S. frutescens* produced similar DNA fragmentation patterns as compared to known inducers of apoptosis, such as ceramide. Ceramide can indirectly activate caspases which leads to induction and increased caspase-3 activity that results in the activation of endonucleases and DNA fragmentation (Selzner *et al.*, 2001). Thus, *S. frutescens* seems to have a similar action on DNA fragmentation and apoptosis.

Sutherlandia frutescens is widely known for its use as an anti-tumour agent and the compounds present in *S. frutescens* are believed to work together to perform this function. Among the plant's active ingredients, L-CAV is believed to be a potent anti-tumour agent. A study by Hare (1969) showed that L-CAV can induce alterations in the nuclear architecture of mammalian cells. These alterations were characterised by the formation of irregular aggregates of nucleoplasmic contents attached to the nuclear membrane. The authors proposed that L-CAV was able to induce such an effect as a result of the formation of canavanyl protein-DNA aggregates.

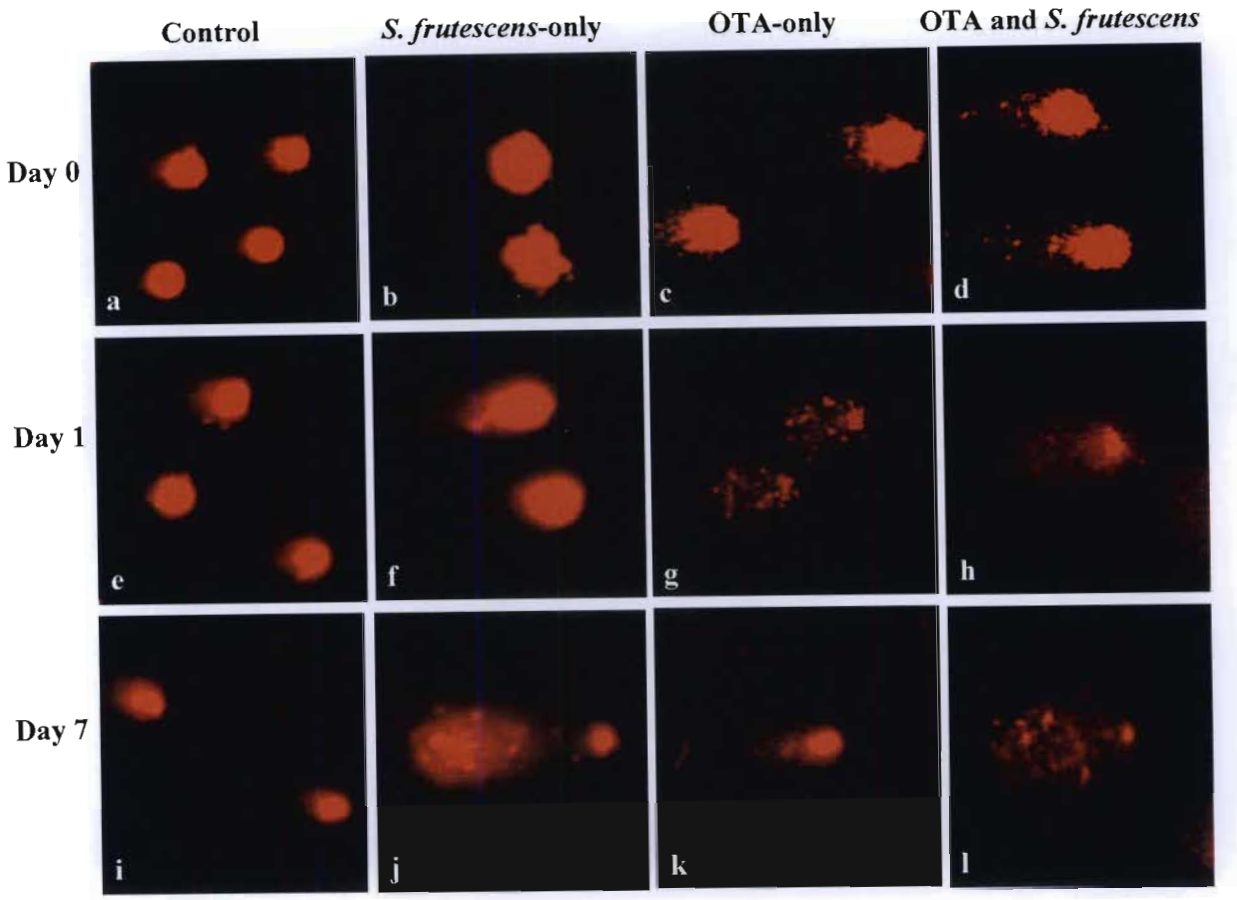

Figure 5.1: Photomicrographs showing comet formation on Days 0, 1 and 7.

The persisting presence of L-CAV may result in cell death (Akaogi *et al.*, 2006). A study using human Jurkat cells, conducted by Jang *et al.* (2002), showed that L-CAV increased the sub-G1 phase, which represents apoptotic cells, in a dose dependent manner. The authors concluded that L-CAV-induced apoptotic DNA fragmentation accompanied the activation of caspase-3.

Furthermore, it is believed that L-CAV competes with L-ARG cellular enzymes, such as iNOS and arginase (Akaogi *et al.*, 2006). Subsequently, L-CAV may disrupt biochemical pathways involving L-ornithine since arginase facilitates the hydrolysis of L-ARG to L-ornithine, which is a precursor of polyamines (Bence *et al.*, 2002). It is known that polyamines (organic cations of low molecular weight) promote cell growth and that if polyamine synthesis is inhibited then cell growth is stopped. As a result of their polybasic character, polyamines adhere strongly to nucleic acids, thereby stabilising DNA by

neutralising the negative charges of the phosphate groups and decreasing the repulsion between the strands of DNA (Yerlikaya, 2004). Studies have shown that polyamine-depleted cells undergo changes in chromatin and DNA structure (Berger *et al.*, 2007). Furthermore, histone acetylases and deacetylases, which influence histone function, are regulated by gene promoters and inhibitors, which, in turn, are controlled by polyamines (Criss, 2003). Thus polyamines play a vital role in the maintenance of genome integrity, and disruptions in polyamine homeostasis may result in decreased polyamines, which may severely affect DNA structure and integrity. Thus, L-CAV may alter DNA integrity as a result of its inhibitory effect on arginases and subsequent effects on L-ornithine and polyamine synthesis.

In addition, GABA may also act as an anti-tumour agent, which may prevent metastasis *in vivo* (Tai *et al.*, 2004). Also, the triterpenoids present in the leaves of *S. frutescens* may possess apoptotic-inducing abilities (Kikuchi *et al.*, 2007; van Wyk and Albrecht, 2008).

Observation of the OTA-treated rat PBMCs revealed that the comet tail lengths increased after 1 day and was significantly longer than that of the control (1 day) ($p<0.01$). However, a slight decrease in tail lengths was noted after the 7-day OTA treatment (Fig. 5.1i-l and 5.2). Also, tail lengths of the OTA and *S. frutescens* combination group at Day 7 were significantly shorter than that of the *S. frutescens*-only group for the same period ($p<0.001$).

The co-treatment with *S. frutescens* after 7 days resulted in a slight increase in DNA damage, however not significant. Shorter tail lengths were produced by the Day 1 co-treatment compared with the OTA treatment for the same duration. It is possible that *S. frutescens* may have delayed the onset of OTA-induced DNA damage (Fig. 5.2).

Ochratoxin A demonstrated the capacity to induce DNA damage in target as well as non-target organs, such as the kidney, liver, spleen and peripheral lymphocytes (Mally *et al.*, 2005; Kamp *et al.*, 2005). It is evident from this, as well as from a previous study (Mally *et al.*, 2005), that OTA may induce DNA damage in immune cells. A study by Seegers *et al.* (1994b) demonstrated that OTA treatment resulted in apoptosis-associated DNA degradation in human lymphocytes.

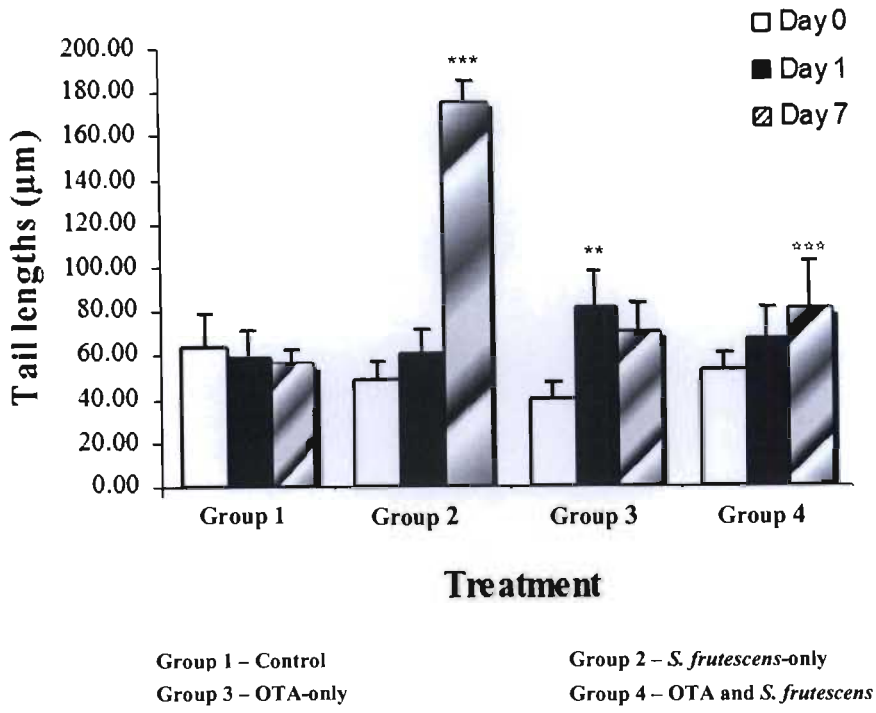

Figure 5.2: A measure of DNA damage by single cell gel electrophoresis in blood taken from male Wistar rats on Days 0, 1 and 7 (n=4). Values represented as mean ±SEM. * indicates comparison with the control for the same periods of time **p<0.01 ***p<0.001. ☆ indicates the comparison between *S. frutescens*-only and combination treatment ☆☆☆p<0.001.

If DNA damage is minor then repair mechanisms become active, however, apoptosis is induced if DNA damage is severe. An unregulated growth of cells may however result if apoptosis is not activated, leading to the formation of tumours that may be cancerous. The decrease in rat PBMC comet tail length at Day 7 may be indicative of an increase in DNA repair mechanisms. It is also possible that fewer viable cells were available (Mally *et al.*, 2005), since many cells may have succumbed to OTA toxicity. It has also been proposed that the biotransformation of OTA may lead to the production of reactive intermediates (Ringot *et al.*, 2006). These intermediates may lead to the formation of DNA adducts, thereby resulting in DNA damage.

Oxidative stress is believed to be one of the factors that induce OTA toxicity. The differences in DNA damage could possibly therefore be attributed to oxidative stress. This response may occur if the antioxidant system is inefficient and therefore reactive intermediates or free

radicals (ROS) are not detoxified. Subsequently, these reactive species can target DNA, resulting in DNA damage. Schaaf *et al.* (2002) and Mally *et al.* (2005) suggested that DNA damage from OTA toxicity could be due to oxidative stress. This oxidative stress may be a result of disruptions in the mitochondrial electron transport chain.

Furthermore, OTA is a known disruptor of mitochondrial function; it was shown that OTA caused DNA damage *in vitro* by forming 8-oxoguanine (an oxidative DNA damage product) (Schaaf *et al.*, 2002; Arbillaga *et al.*, 2007a). It is reasonable to assume that in the present study OTA caused disruptions in mitochondrial function leading to increased oxidative stress. This increased oxidative stress could be responsible for the rat PBMC DNA damage. This has subsequently brought about the debate concerning DNA-reactive and DNA-non-reactive mechanisms for DNA damage due to the presence of OTA (Gautier *et al.*, 2001a; Marin-Kuan *et al.*, 2006; Marin-Kuan *et al.*, 2008). The present study indicates that OTA induces DNA damage in rat immune cells, which was significant after a 1-day treatment.

5.4 CONCLUSION

The control did not show any changes in DNA damage. The comet tail lengths of the *S. frutescens*-only treatment increased with the duration of time. In addition, the longest tail lengths were produced by the *S. frutescens*-only treatment after 7 days. Since SCGE is used as a measure of apoptosis, it is possible that the apoptotic-inducing agents present in *S. frutescens* may have caused the increase in comet tail length observed on Day 7.

The present study indicates that OTA produces a degree of DNA damage in immune cells. After a period of 7 days, however, the tail lengths diminished, which is indicative of a decrease in DNA damage. It was noted that a combination of *S. frutescens* and OTA may delay the onset of DNA damage. The observed changes in DNA damage may be due to apoptosis rather than necrosis as indicated by the shape of the Comet tails.

CHAPTER 6

FLOW CYTOMETRIC ANALYSIS OF APOPTOSIS AND MITOCHONDRIAL MEMBRANE POTENTIAL IN LYMPHOCYTES OF OCHRATOXIN A TREATED MALE WISTAR RATS

6.1 INTRODUCTION

Cell death occurs by two mechanisms, i.e., apoptosis and necrosis. Apoptosis, known as programmed cell death, is a programmed transition from an intact metabolically active state into a number of shrunken apoptotic bodies (Hotchkiss and Nicholson, 2006). In contrast, necrotic death is a passive form of cell death and is characterised by the swelling and rupture of injured cells, resulting in inflammation. Whereas necrosis does not require energy, apoptosis is an ATP requiring process (Rastogi *et al.*, 2009).

Mitochondria are organelles involved in major metabolic pathways, however, cells undergoing apoptosis are characterised by a disruption in mitochondrial physiology. During apoptosis, mitochondrial permeability is altered resulting in the release of cytochrome c from inside the mitochondria to the cytoplasm (Heiskanen *et al.*, 1999). Cytochrome c release is also coupled with the depolarisation of the mitochondrial membrane and caspase activation (Heiskanen *et al.*, 1999; Kroemer *et al.*, 2007).

Apoptosis can be detected through characteristic morphological cell changes. These changes include: exposure of phosphatidylserine on the external side of the cell membrane, fragmentation of DNA, aggregation of chromatin and the creation of apoptotic bodies. Flow cytometry is widely used to detect the morphological changes characteristic of cells undergoing apoptosis.

6.1.1 Flow Cytometry

Flow cytometry is a technique used for making rapid measurements on particles or cells as they flow in a fluid stream one at a time through a laser beam (Ormerod, 2000). Cells are sorted into different populations using fluorescence-activated cell sorting (FACS) (Fig. 6.1). The advantages of flow cytometry are that measurements are made on individual cells and multiple cellular parameters can be measured. It is easier to process body fluids as compared with solid tissues. Blood contains individual cells that can be stained and processed directly on the flow cytometer. Solid tissues, however, are not easy to process, because enzymatic digestion and detergents may be required for the preparation of some tissues and organelles (Ormerod, 2000).

6.1.1.1 Fluidics, Optics and Electronics

A flow cytometer comprises three functional systems, *viz.*, fluidics, optics and electronics (BD Biosciences, 2000). Measurements are made based on a particle's relative size, internal complexity and relative fluorescence intensity (Ormerod, 2000). The fluidic system delivers particles/cells of a fluid stream, singly, to a particular point that is intersected by an illuminating beam. Therefore, flow cytometric tubes containing cells are placed in the centre of an enclosed chamber through which the sample flows into a flowing stream of sheath fluid (BD Biosciences, 2000). Particles are restricted to the centre of the fluid stream by a process referred to as hydrodynamic focussing (BD Biosciences, 2000).

Light from each particle that is passed through the laser beam is captured. Thus an optical system is also incorporated into the flow cytometer and it consists of excitation optics and collection optics (BD Bioscience, 2000). In order to produce specific wavelengths, the light source has to be efficient and intense, as measurements are made based on light as a source of excitation. Thus the (argon) laser beam is used and the illumination source is part of the excitation optics (Ormerod, 2000).

As the cell passes through the laser beam, it scatters light at all angles. Forward scatter (FSC) refers to the emission of light in a forward direction and this is dependent upon particle size, therefore different cell populations can be distinguished from one another (Rahman, 2006).

Side scatter (SSC) describes light that is scattered in a perpendicular direction. This type of light scatter is dependent on the number of organelles inside the cell (Rahman, 2006) and if few organelles are present in the cell, then side scatter is low.

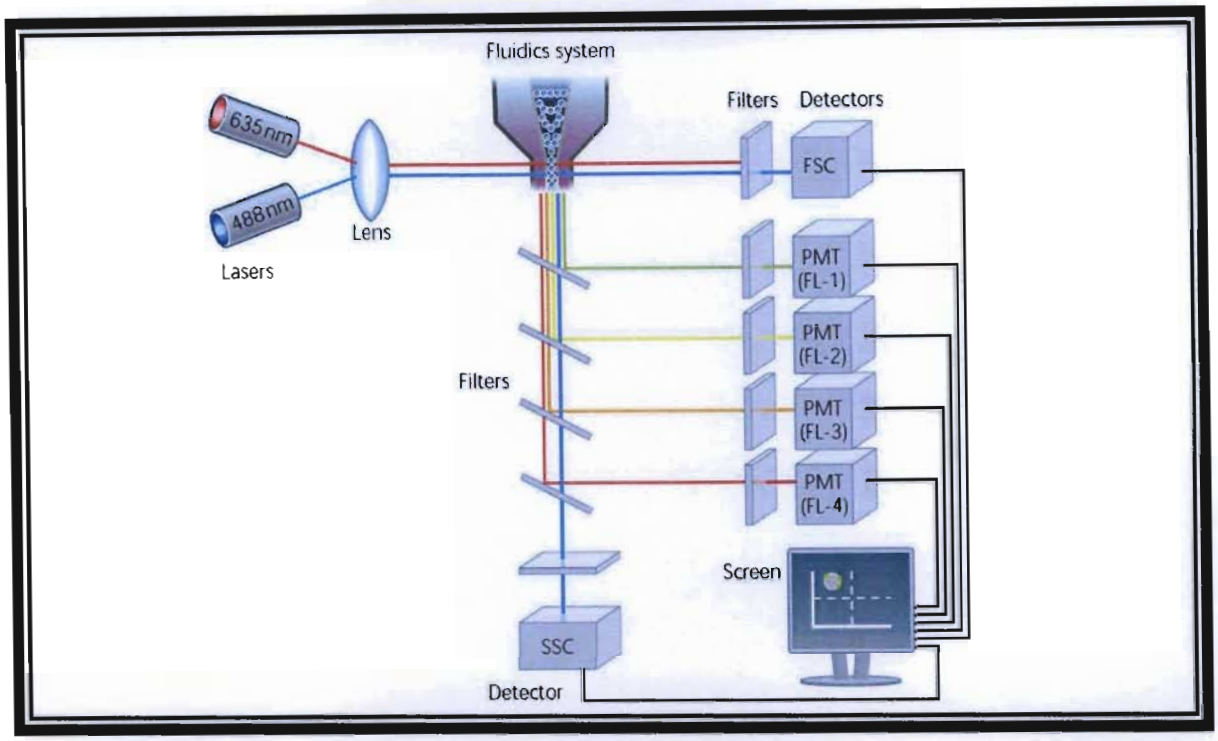

Figure 6.1: Illustration showing flow cytometer instrumentation. Suspensions are passed through the fluidics system and the light scattered by cells is collected by photodetectors. Signals are digitised and passed on to the computer for display and analysis (Rahman, 2006).

The conjugation of fluorescent dyes to ligands and to polyclonal and monoclonal antibodies can be used in determining specific aspects of a cell, such as cell surface and cytoplasmic factors (Ormerod, 2000). Also, the ability of different compounds to fluoresce at different wavelengths enables several parameters to be analysed. The scattered and fluorescent light generated by cells passing through the illuminating beam is collected by photodetectors via dichroic mirrors and optical filters (bandpass and shortpass filters). This makes up the collection optics (BD Bioscience, 2000). Thereafter, fluorescence and side scattered signals are diverted to the photomultiplier tubes (PMT) and forward scattered signals are diverted to the photodiode (Rahman, 2006).

Photodetectors convert photon pulses into electronic signals. The analogue to digital converter (ADC) allows the electrical pulses to be digitised so that data may be displayed on a computer. Electronic and computational processing results in a graphic display which can then be analysed (Ormerod, 2000).

6.1.1.2 Graphical Display

The most common and useful way of display is through frequency histograms and dual parameter plots, also known as dot/scatter plots. The frequency histogram is a direct representation of the number of events occurring for each channel of the ADC. Dot plots are a 2-dimensional representation of the frequency histogram and FSC and SSC parameters for a particular sample are used to obtain the histogram. The FSC and SSC differ between cells and particles, and thus the biochemical, biophysical and molecular properties can be studied (Ormerod, 2000).

6.1.2 Flow Cytometric Detection of Apoptosis and Necrosis

In the early stages of apoptosis, the translocation of negatively charged phosphatidylserine (PS) from the internal to the external cell membrane takes place (Fig. 6.2). This allows for the detection and rapid phagocytosis of the cells.

Annexin V is a protein that binds in a Ca^{2+}-dependent manner to PS (Fig. 6.2) and therefore, serves as an excellent probe to detect apoptotic cells (Ormerod, 2000). Annexin V will not bind to healthy cells. Since necrotic cells also contain PS, apoptotic cells must be differentiated from necrotic cells. This is done by using a vital dye such as propidium iodide (PI) which only stains cells with disrupted cell membranes (Ormerod, 2000), since it is not membrane-permeable. In flow cytometry, Annexin V is conjugated to fluorescein isothiocyanate (FITC) (Vermes *et al.*, 1995), which possesses an excitation wavelength of 488nm and emits light signals at wavelength 518nm. Since the morphology of apoptotic and necrotic cells are different, forward and side scatter properties of the cell can be used to identify apoptotic from necrotic cells.

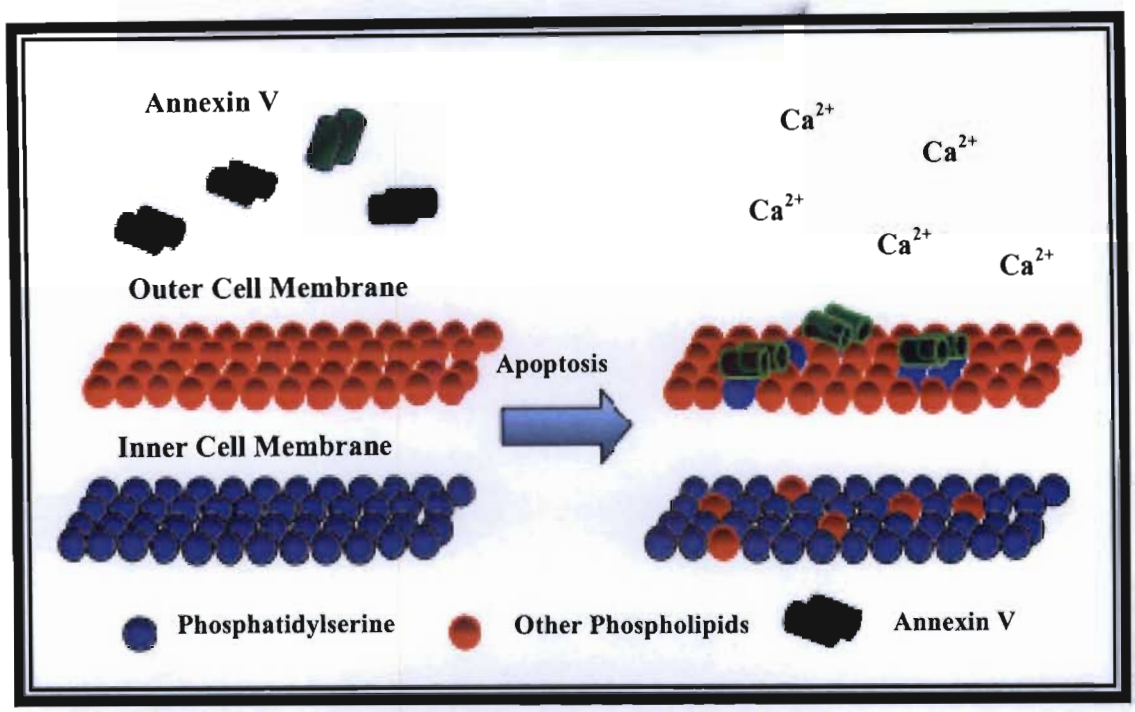

Figure 6.2: Illustration of phosphatidylserine flipping during apoptosis and the subsequent binding of Annexin V to phosphatidylserine (Trevigen, 2007).

6.1.3 Mitochondrial Membrane Depolarisation Detection

A prominent characteristic of apoptosis is the change in mitochondrial membrane potential ($\Delta\Psi m$) (Kroemer *et al.*, 2007). Energy released during oxidation reactions in the mitochondrial respiratory chain is stored as a negative electrochemical gradient across the mitochondrial membrane and the membrane potential is referred to as being polarised. However, during apoptosis there may be a collapse in $\Delta\Psi m$, which results in depolarised mitochondria (Kroemer *et al.*, 1997). Mitochondrial depolarisation is often used as an indicator of apoptosis.

JC-1 (5,5', 6,6'-tetrachloro-1, 1', 3,3'-tetraethylbenzimidazolcarbocyanine iodide) is a membrane-permeable lipophillic cationic fluorochrome that is used to measure $\Delta\Psi m$ (Ormerod, 2000). JC-1 is excited using a wavelength of 488nm. The fluorescence emission spectrum is dependent on its concentration, which in turn is determined by the status of the $\Delta\Psi m$. JC-1 can occur as aggregates or monomers, each with different emission spectra: 527nm and 590nm respectively (BD Biosciences, 2003). While aggregates form at high dye concentration, monomers form at low concentrations. Both exhibit green fluorescence, but

JC-1 aggregates show a red spectral shift (BD Biosciences, 2003). JC-1 selectively enters mitochondria and changes colour from green to red as the membrane potential increases. Thus, in healthy cells, mitochondria are polarised and JC-1 is rapidly taken up, forming JC-1 aggregates and a higher red fluorescence emission (Fluorescence (FL)-2 channel). JC-1 does not accumulate in apoptotic (unhealthy) cells with depolarised mitochondria and it remains in the cytoplasm as monomers (green fluorescence) (BD Biosciences, 2003).

The aim of the study reported in this chapter was to determine the apoptotic potential of OTA and *S. frutescens* on rat lymphocytes.

6.2 MATERIALS AND METHODS

6.2.1 Materials

Annexin-V-FLUOS staining kit was purchased from Roche Diagnostics (Penzberg, Germany); BD^{TM} MitoScreen Kit was obtained from Becton Dickinson, BD Biosciences (San Jose, CA). All other reagents were obtained from Merck (S.A).

6.2.2 Methods

Peripheral blood mononuclear cells (PBMCs) were isolated by differential centrifugation, as discussed in Chapter 3.

6.2.2.1 Flow Cytometric Analysis of Peripheral Blood Mononuclear Cells – Sample Preparation

Initially, an aliquot of (100µl) PBMCs (1×10^6 cells/ml) was transferred to appropriately labelled polystyrene flow cytometric tubes and pelleted by centrifugation (5 min, 200xg). Pellets obtained were re-suspended in the appropriate labelling solution (Annexin-V-FLUOS or JC-1)

6.2.2.2 Staining of Peripheral Blood Mononuclear Cells

6.2.2.2a Annexin V-FLUOS/Propidium Iodide

Annexin-V-FLUOS labelling solution was prepared by diluting the Annexin-V-FLUOS labelling reagent (20µl) and the PI solution incubation buffer (1ml).

The pellet obtained (in 6.2.2.1) was re-suspended in 100µl Annexin-V-FLUOS reagent and incubated in the dark (15 min, RT). The Annexin reagent is light-sensitive, therefore, procedures were carried out under minimal light exposure.

6.2.2.2b Mitochondrial Membrane Potential – JC-1

The pellet (in 6.2.2.1) was re-suspended in freshly prepared JC-1 working solution (500µl). Tubes were vortexed thoroughly to eliminate any cell-to-cell clumping and then incubated in a CO_2 incubator (15 min, 37°C). After the required time period, stained PBMCs were washed with JC-1 MitoScreen wash buffer (2ml) (5 min, 400xg, RT).

6.2.2.3 Instrumentation and Analysis of Samples

Both Annexin-V-FLOUS and JC-1 data were analysed using a FACSCalibur flow cytometer. Prior to analysis, an incubation buffer (500µl) was added to each sample of stained PBMCs. Tubes containing the sample were then gently shaken and placed into the flow cytometer. Analysis of all samples was conducted using an excitation wavelength of 488nm. Subsequently, FL1 (Annexin-V-FITC-PS) and FL3 (propidium iodide-DNA) signals were detected via 515nm and 600nm bandpass filters respectively. Similarly, JC-1 monomers were detected at 527nm and JC-1 aggregates at 590nm.

6.2.2.4 Data Analysis

Data was acquired with CellQuest PRO v4.0.2 software (BD Biosciences) and analysed using FlowJo v7.1 Software (Tree Star, Inc.). Analysis was carried out using scatter/density plots. Initially, the total lymphocyte population was distinguished from the heterogeneous population and debris by using the forward and side scatter parameters of the lymphocyte

profile. Thereafter, lymphocytes were gated on their respective fluorescent probes for the respective assays. Regarding the Annexin stained samples, the lymphocyte population was gated at the 10^2 mark on the FL1 and FL3 channels creating cluster gates, thereby differentiating apoptotic and necrotic PBMCs. Apoptotic PBMCs were Annexin-V-FITC positive (x-axis) but PI negative (y-axis) (bottom right quadrant) and necrotic PBMCs were positive for both Annexin-V-FITC and PI (top right quadrant) (Fig. 6.3 and Fig. 6.4).

Since JC-1 monomers and aggregates show fluorescence in both the FL-1 and FL-2 channels, lymphocytes were gated on these channels and were thus recognised as having polarised or depolarised mitochondria (Fig. 6.5). FL-1 bright and FL-2 bright were indicative of healthy cells, with polarised mitochondria. A decrease in the FL-2 channel, where the FL-1 remains high, is indicative of cells with mitochondrial depolarisation.

6.2.3 Statistical Analysis

Flow cytometric data was analysed on GraphPad Instat v3.06 (GraphPad Software, San Diego, CA). Comparisons between the treatments were made using One-Way Analysis of Variance (ANOVA) and the Tukey-Kramer Multiple comparisons test. A probability value (p) of less than 0.05 ($p<0.05$) was considered statistically significant.

6.3 RESULTS AND DISCUSSION

Cell signalling is responsible for the regulation of apoptosis, such that only those cells destined for cell death will die. Therefore, inconsistencies in apoptosis may be attributed to alterations in cell signalling. The lymphocyte population consists of T cells, B cells and natural killer cells. These cells play an important role in the immune system and in the defence against intruders in the body. If the number of lymphocytes decreases, then the immune function becomes compromised, and this may increase the susceptibility to various infections.

The Annexin-V-FLUOS assay differentiates apoptotic from necrotic cells (Table 6.1). After flow cytometric analysis, it was observed that the 1-day OTA-only treatment resulted in a 2.08-fold increase in apoptotic lymphocytes (15%) when compared to the control (7.2%) ($p<0.01$) (Table 6.1 and Fig. 6.3). There was also a 5-fold increase in necrotic lymphocytes compared to the control (Day 1). Furthermore, the 7-day OTA treatment resulted in a 1.22-fold increase in apoptotic lymphocytes (10.1%), but a decreased (1.64-fold) amount of necrotic lymphocytes, compared to the respective controls (Table 6.1).

Table 6.1: Quantification of apoptotic and necrotic lymphocytes represented by the mean ±SEM (n=4). **p<0.01.

Treatment	Duration	Apoptotic (%)	Necrotic (%)
Control	1 day	7.2±2.15	0.2±0.10
S. frutescens-only		11.7±2.39	0.1±0.05
OTA-only		15±0.49**	1±0.16
OTA and *S. frutescens*		13.2±0.12	1.4±0.22
Control	7 days	8.3±0.75	0.2±0.00
S. frutescens-only		9.7±0.79	0.2±0.05
OTA-only		10.1±0.62	0.1±0.08
OTA and *S. frutescens*		12.7±0.94	0.0±0.01

Petrik *et al.* (2003) demonstrated, in a study on male Wistar rats, that OTA treatment can cause an increase in the number of cells undergoing apoptosis in both distal and epithelial kidney cells. According to Al-Anati and Petzinger (2006), OTA-induced apoptosis is not limited to the urinary tract but is also found in the immune system. In relation to other studies, OTA demonstrated the capacity to increase apoptosis in PBMCs (Seegers *et al.*, 1994b; Schwerdt *et al.*, 1999; Gekle *et al.*, 2000; Assaf *et al.*, 2004). In the study by Assaf *et al.* (2004), PBMCs were isolated from healthy donors and then treated with OTA after PBMC separation. This was different from the present *in vivo* study in which rats were initially treated with OTA. Results of that study showed that apoptosis was induced due to a decrease of Bcl-X_L (anti-apoptotic protein) and a disruption of mitochondrial function.

A comparison between the OTA Day 1 and Day 7 regimes indicated that there was a 1.48-fold decrease in the amount (10.1%) of apoptotic lymphocytes and 9.10-fold decrease in necrotic lymphocytes (0.1%) on Day 7 (Table 6.1, Fig. 6.3 and Fig. 6.4.). Thus, the results suggest that OTA toxicity may be influenced by the duration of time the toxin is in the body. The decrease in apoptotic and necrotic lymphocytes may be due to the fact that this study was conducted *in vivo*, thus, if there were disruptions in biochemical pathways, the body may have reacted to it. Similarly, this could explain the difference in the number of necrotic lymphocytes after 1 day (1%) and 7 days (0.1%). Also, the type of cell death stimulated by OTA may be determined by dose and exposure time (Al-Anati and Petzinger, 2006). The results, however, indicate that OTA-induced apoptosis was higher than necrosis.

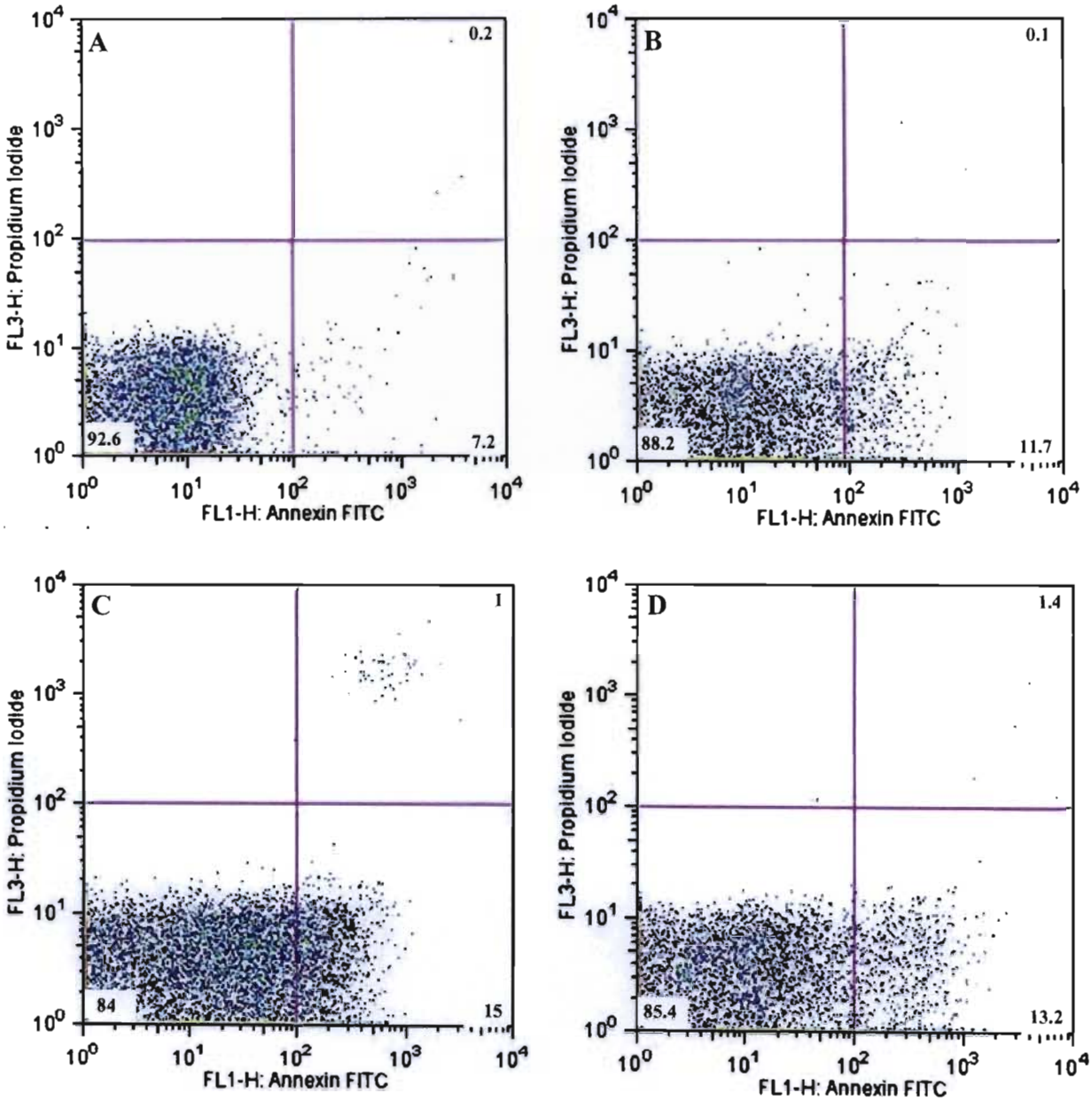

Figure 6.3: Scatter plots showing apoptotic (bottom right quadrant) and necrotic (top right quadrant) rat lymphocytes after Day 1: A) Control; B) *S. frutescens*-only; C) OTA-only; D) OTA and *S. frutescens*.

Flow cytometry showed that the Day 1 *S. frutescens* treatment increased (1.62-fold) the percentage of apoptotic lymphocytes (11.7%) compared to the control (Table 6.1 and Fig. 6.3). In contrast, there was a 2-fold decrease in the amount of necrotic lymphocytes (0.1%) compared to the control (Table 6.1). Chinkwo (2005) confirmed that *S. frutescens* can induce apoptosis in CHO, Caski and Jurkat cells. In that study several morphological features associated with apoptosis were detected, such as PS externalisation, chromatin condensation and DNA fragmentation. In addition, the present study also demonstrated apoptosis-associated DNA fragmentation induced by *S. frutescens* (Chapter 5). Furthermore, gene expression profiles on MCF-7 cells showed that a number of genes required and considered important for apoptosis were expressed after *S. frutescens* treatment (Stander *et al.*, 2007).

The phytocompounds present in *S. frutescens* may contribute to the observed increase in apoptosis (Tai *et al.*, 2004). L-canavanine has been shown to possess apoptotic activity (Jang *et al.*, 2002; Akaogi *et al.*, 2006). In a study by Jang *et al.* (2002), flow cytometric analysis revealed that the sub-G1 phase, which represents apoptotic cells, increased in a dose-dependent manner. Furthermore, L-CAV may also facilitate the shrinkage of tumour growths, in mice and rats (Green *et al.*, 1980; Thomas *et al.*, 1980).

Nitric oxide synthase produces nitric oxide (NO) from L-ARG. Since L-CAV is an L-ARG analogue, L-CAV can replace L-ARG, thereby inhibiting NO synthesis (Akaogi *et al.*, 2006). S-nitrosylation is a biochemical process that involves the reversible coupling of NO to a reactive cysteine thiol, forming molecules referred to as S-nitrosothiols, which modulate protein function (Iyer *et al.*, 2008). Nitric oxide may inhibit apoptosis through S-nitrosylation of various proteins involved in the apoptotic cascade, such as caspase-8, -9 and -3, cFLIP, Bcl-2 and protein kinase C (PKC) (Dash *et al.*, 2007; Iyer *et al.*, 2008). Thus, if L-CAV is substituted in place of L-ARG, NO synthesis will decrease, resulting in S-nitrosylation inhibition and increased apoptosis.

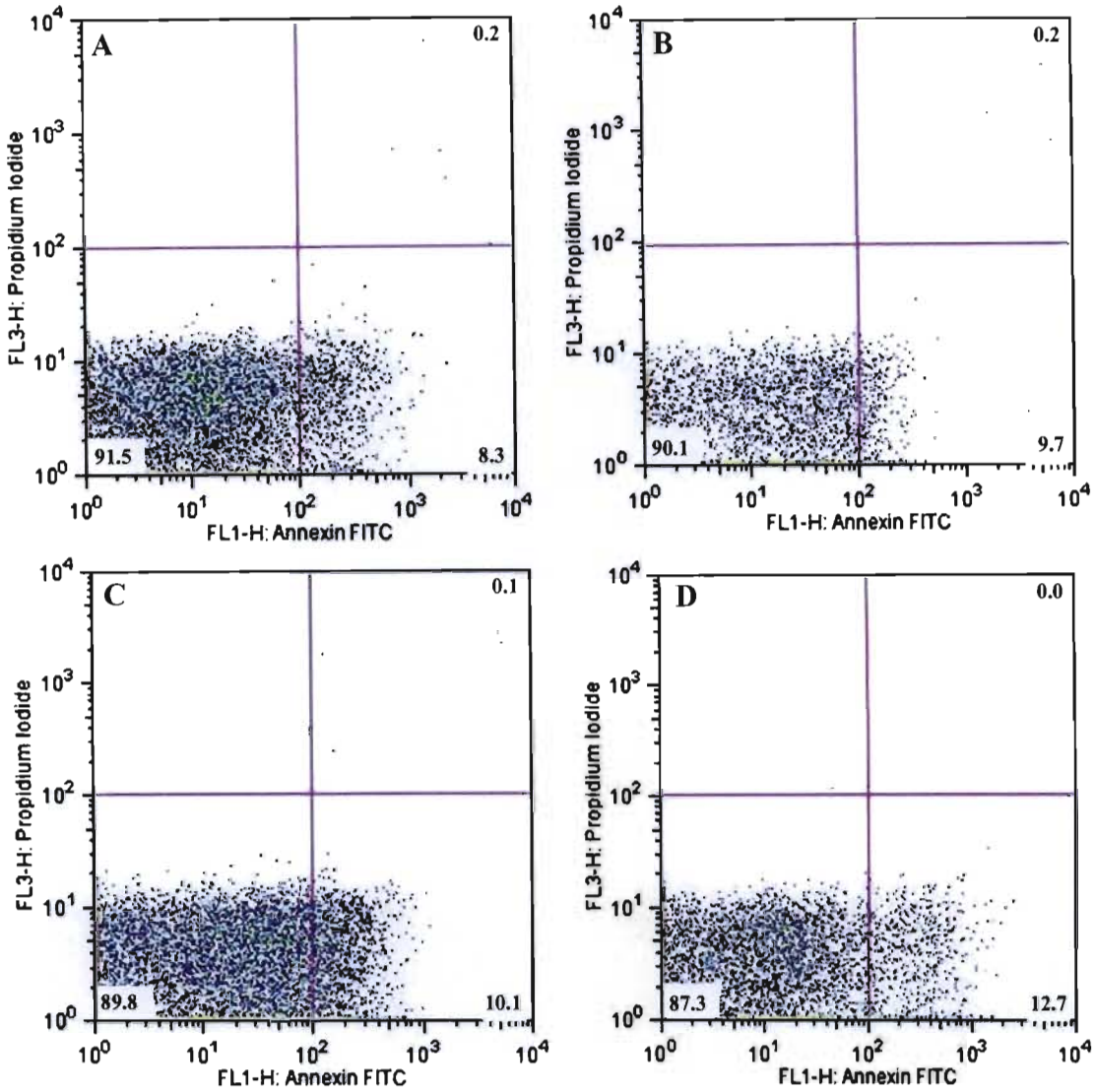

Figure 6.4: Scatter plots showing apoptotic (bottom right quadrant) and necrotic (top right quadrant) rat lymphocytes after Day 7: A) Control; B) *S. frutescens*-only; C) OTA-only; D) OTA and *S. frutescens*.

Furthermore, the major triterpenoids present in *S. frutescens* are structurally related to cycloartane-type triterpenoids which possess proven cancer chemopreventive activity (Kikuchi *et al.*, 2007). Flavonoids, contained in the plant, induced apoptosis in cancer cells (Zhang *et al.*, 2008). Thus it is possible that flavonoids may also be responsible for the apoptotic activity in *S. frutescens*. In light of the above, although L-CAV may be a major inducer of apoptosis, other compounds found in the plant may also play a pivotal role, thus increasing apoptosis.

After the 7-day *S. frutescens* treatment, the Annexin-V-FLUOS assay showed that there was a 1.21-fold decrease in apoptotic lymphocytes (9.7%) but a 2.40-fold increase in necrotic lymphocytes (0.2%), when compared to the 1-day regime (Table 6.1). Necrosis may be induced when there is an excess of ROS or when the antioxidant systems are disturbed (Proskuryakov *et al.*, 2003). Furthermore, L-CAV may result in oxidative stress (Riganti *et al.*, 2003), which may then have resulted in the increase in necrotic lymphocytes noted after the 7-day *S. frutescens* treatment.

Rats were also treated with a combination of *S. frutescens* and OTA. When compared to the respective controls, both Day 1 (13.2%) and Day 7 (12.7%) co-treatments showed an increase in apoptotic lymphocytes (Table 6.1). However, a 1.04-fold decrease in the number (12.7%) of apoptotic lymphocytes was observed after the 7-day combination treatment in comparison to the Day 1 combination group (13.2%).

When compared to the Day 1 OTA-only rat group, the combination treatment (Day 1) showed an antagonistic decrease (1.14-fold) in lymphocyte apoptosis and a 1.40-fold increase in the amount of necrotic lymphocytes (Table 6.1). In contrast, co-treatment after a 7-day period produced a 1.25-fold increase in apoptotic lymphocytes in comparison to the OTA-treated rat lymphocytes, for the same duration. Also, flow cytometry suggests that after the 7-day combination regime necrotic lymphocytes were very few to none (Table 6.1). These results highlight the apoptotic potential of the combination of *S. frutescens* and OTA after an extended period in the body.

The JC-1 assay is used to determine mitochondrial depolarisation, which is an indicator of apoptosis. After analysis of the JC-1 assay (Fig. 6.6), it was evident that, on Day 1, the *S. frutescens* treatment resulted in a significantly higher percentage of lymphocytes (61.6%) with depolarized mitochondria than the control (11.7%) ($p<0.001$). However, after 7 days, *S. frutescens* treatment exhibited a significant decrease (12.2%) in mitochondrial depolarisation compared to the Day 1 *S. frutescens* treatment ($p<0.001$). The high percentage of lymphocytes with depolarised mitochondria may be a result of the apoptosis-inducing ability *S. frutescens*. GABA, a weak acid present in *S. frutescens*, may disrupt the proton gradient of mitochondria and alter mitochondrial polarity. The proton gradient is used to drive the synthesis of ATP. Therefore, GABA may be one of the reasons for the increase in the percentage of cells with depolarised mitochondria. In addition, L-CAV is considered to be a potent anti-cancer agent and may affect mitochondrial function.

On Day 7 there was a significant increase in the number of lymphocytes (56.5%) showing mitochondrial depolarisation in the OTA-only treated rats compared to the control (6.8%) ($p<0.001$) (Fig. 6.6). When compared to the Day 1 OTA rat group, a significant time-dependent (3.71-fold) increase in depolarisation was noted ($p<0.001$). Thus, as suggested by Schwerdt *et al.* (2007), the extended presence of OTA in the body may produce adverse effects.

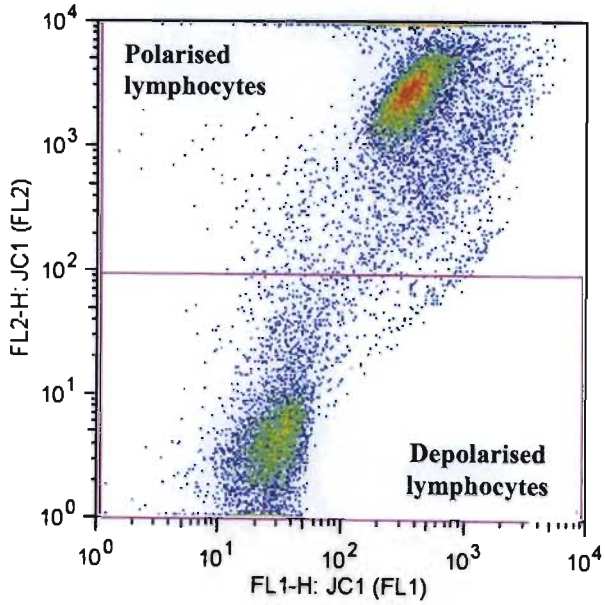

Figure 6.5: An example of a scatter plot of rat lymphocytes stained with JC-1 dye, depicting polarised and depolarised lymphocytes.

It has been proposed that OTA treatment may result in disruptions in mitochondrial function and that this may occur as early events of toxicity (Aleo *et al.*, 1991; Bouaziz *et al.*, 2008). According to Wei *et al.* (1985), OTA is believed to affect mitochondrial respiration and oxidative phosphorylation through the succinate-support electron transfer activities of the mitochondrial respiratory chain. There could subsequently be set-backs in the electron transport chain, resulting in the disruption of mitochondrial function. This may therefore have led to the mitochondrial depolarisation that was observed in the present study. In a study by Assaf *et al.* (2004), OTA treatment of human PBMCs also resulted in a decrease in $\Delta\Psi m$. It was also suggested that acute and chronic toxicity by OTA is either directly or indirectly related to the inhibition of transport carrier proteins located in the inner membrane of mitochondria (Horvath *et al.*, 2002). As a result, this may lead to the inhibition of mitochondrial respiration.

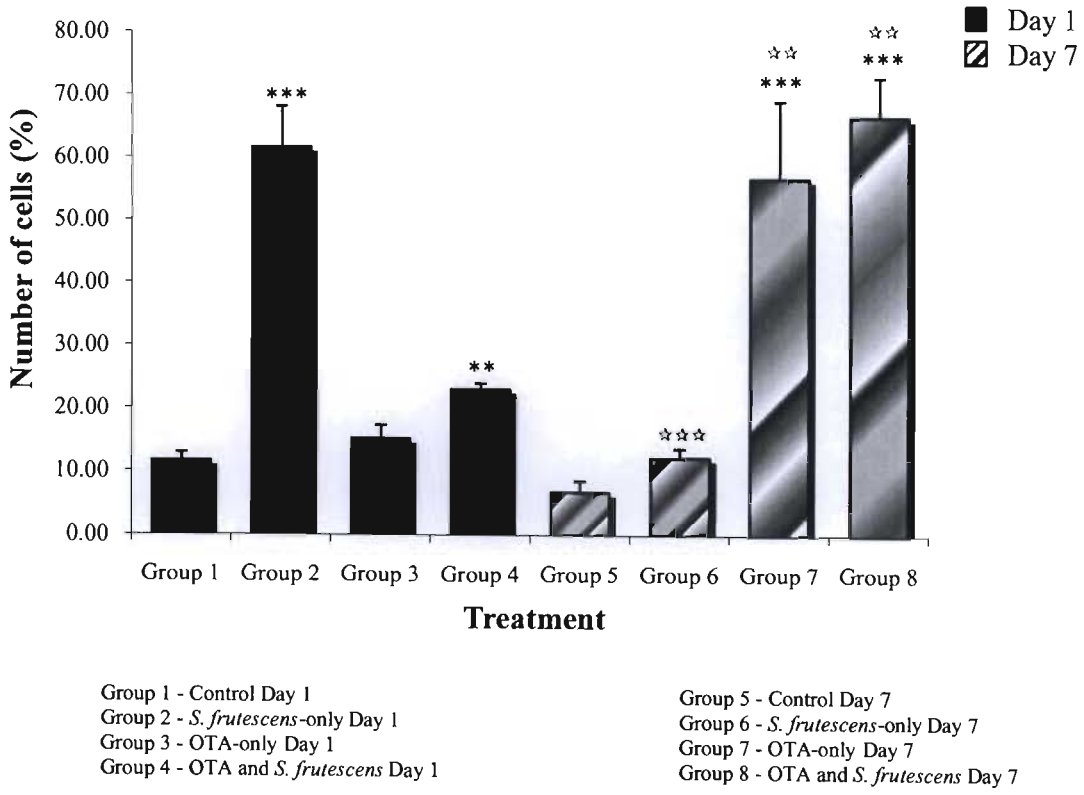

Figure 6.6: Effect on mitochondrial membrane depolarisation after Ochratoxin A and *Sutherlandia frutescens* treatment. Data represent the mean ±SEM (n= 4). * indicates comparison between treatments and control **p<0.01, ***p<0.001. ☆ represents comparison between Day 1 and Day 7 regimes ☆☆p<0.01, ☆☆☆p<0.001.

In addition, it is known that glutamine serves as a major fuel for immune cells, such as lymphocytes (Mates *et al.*, 2002). Glutamine metabolism (glutaminolysis) results in the production of glutamate (Newsholme *et al.*, 2003), which is a crucial substrate for mitochondrial respiration. Glutamate may be transaminated to α-ketoglutarate, an intermediate in the TCA cycle. Since glutamine is an important source of energy in lymphocytes, if glutamine metabolism is disrupted, then the supply of key components such as α-ketoglutarate may decrease. This would alter the TCA cycle and therefore energy production (ATP) would be reduced. It is thus possible that the observed changes in $\Delta\Psi m$ in the present study could be attributed to alterations in glutamine metabolism.

This means that the metabolic activity in cells will decrease and that cell viability will therefore decrease. Alterations in $\Delta\Psi m$ may also lead to an inhibition of ATP synthesis. A comparison can be made with the PBMCs tested in chapter 4 (Fig. 4.1). It was observed that after a 7-day OTA treatment, cell viability significantly decreased. This further points out that OTA produces cellular toxicity by disrupting mitochondrial activity. In addition, a decreased ATP level will alter other ATP-dependent processes, which may mediate immunotoxicity.

The depletion of ATP reserves deprives the endoplasmic and plasma membrane Ca^{2+} pumps of fuel, causing an elevation of Ca^{2+} in the cytoplasm. There would subsequently be an influx of Ca^{2+} into the mitochondria, which would result in a decrease in mitochondrial membrane potential (Cribb *et al.*, 2005) and a decrease in ATP. Thus it is possible that OTA may have caused a disruption in calcium in the cell.

Disruptions in electron transport may result in an increased production of ROS. Opening of the PTPC can be triggered by several factors, one of them being ROS, which causes a sudden permeability of the inner mitochondrial membrane (Skulachev, 1996; Desagher and Martinou, 2000). It is believed that increased ROS in the presence of Ca^{2+} causes cross-linking of mitochondrial protein thiols, which facilitates the opening of the PTPC (Fagian *et al.*, 1990). Thus OTA may have caused an increase in ROS in lymphocytes, which may in turn have triggered mitochondrial depolarisation. Other studies have indicated that OTA may cause oxidative stress (Gautier *et al.*, 2001b; Boesch-Saadatmandi *et al.*, 2008).

The regulation of pro-and anti-apoptotic signals is important since it ensures that only necessary apoptosis takes place (Kroemer *et al.*, 2007). The Bcl-2 family of proteins play a significant role in the permeability of the outer mitochondrial membrane and in the regulation of cell death. In the presence of cell death-promoting proteins (Bax and Bad), cytochrome c is released from the mitochondrion, followed by the depolarisation of mitochondria and, subsequently, apoptosis. In this regard, it is possible that OTA may have caused defects in pro- and anti-apoptotic signals.

A study by Arbillaga *et al.* (2007b) showed that, while there was an up-regulation of genes of the mitochondrial electron transport chain, genes associated with apoptosis were down-regulated. In the context of that study, the observed significant increase in the percentage of lymphocytes with depolarised mitochondria (OTA-only Day 7) (Fig. 6.6) but low apoptosis (Table 6.1) could be related to those factors. Also, looking back at the SCGE results (Chapter 5), it was observed that on Day 7 no significant difference was obtained between comet tail lengths of the OTA-treated rat group and the control (Fig. 5.2), which may indicate a lack of apoptosis.

After 1 day, the combination of *S. frutescens* and OTA resulted in a higher percentage (23%) of lymphocyte mitochondrial depolarisation when compared to the control ($p<0.01$). Interestingly, a 7-day combination regime (Fig. 6.6), produced a 9.71-fold increase in lymphocyte mitochondrial depolarisation (66.2%), which was significantly different from the control over the same duration ($p<0.001$). Incidentally, a significant time-dependent increase (2.88-fold) in lymphocyte depolarisation was also noted after co-treatment ($p<0.01$). Thus the co-treatment may have resulted in a synergistic effect on lymphocyte mitochondrial depolarisation. This may have occurred since both OTA and *S. frutescens* disrupt mitochondrial function.

Disruptions of the $\Delta\psi m$ occur before cells exhibit DNA fragmentation or before the exposure of PS on the outer membrane leaflet (Kroemer *et al.*, 1997). It is possible for this reason that, significant results were acquired from the JC-1 assay, but not from the Annexin-V-FLUOS assay. Al-Anati and Petzinger (2006) have indicated that OTA-mediated immunotoxicity may occur by non-specific cell destruction, such as an interference with the cell's energy

supply. In accordance with this and other studies (Wei *et al.*, 1985; Petrik, *et al.*, 2003; Bouaziz *et al.*, 2008), the present data points to the strong effect of OTA on mitochondrial function, which may in turn induce immunotoxicity. The immune system may respond earlier to OTA than it does to other organs. Altered immune function may result in an increased incidence of disease or cancer, which may be linked to the various effects produced by OTA, since endogenous defence mechanisms will be impaired.

6.4 CONCLUSION

The Annexin-V-FLUOS assay revealed that the number of apoptotic lymphocytes was significantly higher in the Day 1 OTA-only treated rat group, compared to the control for the same duration. When considering other treatments, however, no significant differences in lymphocyte apoptosis were observed. Results acquired from the JC-1 assay showed that the percentage of lymphocyte mitochondrial depolarisation significantly increased in the *S. frutescens* rat group after 1 day and in the OTA-only and co-treatment rat groups after 7 days. Furthermore, OTA and *S. frutescens* together resulted in a synergistic increase in lymphocyte mitochondrial depolarisation.

CHAPTER 7

EXAMINATION OF RAT KIDNEYS BY FLUORESCENCE MICROSCOPY

7.1 INTRODUCTION

The examination of tissue by microscopy is important for assessing the toxicity of chemicals. By delving into the structure of the cell, the morphological features associated with cytotoxicity can be further understood. There are several morphological alterations that can occur during and after cellular damage. These can be viewed by use of special optical techniques, such as phase-contrast microscopy, differential interference contrast microscopy and fluorescence microscopy (Becker *et al.*, 2003).

7.1.1 Fluorescence Microscopy

In the fluorescence microscope, light coming from a mercury lamp passes through a specific excitation filter that removes all wavelengths, except those wavelengths absorbed by the dye (Herman, 1998). In response to light absorption, the dye fluoresces by releasing longer wavelengths. The wavelength of fluorescence needs to be removed from that of the exciting light in order to allow adequate separation of the two wavelengths (Ormerod, 2000). Therefore, the fluorescent light leaving the specimen passes through a second filter, called the barrier filter (Herman, 1998), which eliminates all wavelengths except the fluorescent light. Contrast is attained after passage of light through the barrier filter, and therefore the specimen stained by a fluorescent dye is visualised against a dark background (Herman, 1998; Wilson and Walker, 2005). Certain biological molecules, such as chlorophyll, may emit fluorescence naturally; this is called autofluorescence (Herman, 1998). Other molecules in cells require fluorescent probes to detect various aspects of that cell. Fluorescence is a sensitive method of detection. Fluorochromes can also be used to label other probes, such as antibodies, so that the localisation of particular antigens can be achieved.

7.1.2 Hoechst Stain

Hoechst stains are part of a family of fluorescent stains that is used to identify DNA (Ormerod, 2000). It is membrane permeant and binds specifically to the adenine-thymine base pairs in double-stranded DNA. Since the dye is bound to DNA, it is therefore used to visualise nuclei. The dye emits blue/green fluorescent light at an emission spectrum of around 461nm, at the nuclear area. During apoptosis the nucleus of the cell is made up of highly condensed chromatin. After viewing slides by fluorescence microscopy, the distinct morphological changes of the nucleus chromatin can be observed (Willingham, 1999). Furthermore, the nuclei of apoptotic cells may develop a horseshoe shaped appearance when stained or may appear as complete, intensely fluorescent spherical beads.

7.1.3 Immunohistochemistry

The detection of antigens in tissue sections is referred to as immunohistochemistry (IHC). An antigen is any foreign molecule that is recognised by an antibody. In this study, immunohistochemistry was used for the quantification of the toxicant (OTA) in kidney tissue. There are two types of methods that can be used for detection, i.e., direct and indirect methods (Ramos-Vara, 2005) (Fig. 7.1).

The direct methods use a primary antibody that is directly tagged to a fluorochrome. In contrast, the technique used in indirect methods involves an initial incubation with an unlabelled primary antibody, which recognises and then binds to the antigen of interest. This is followed by a subsequent incubation with a fluorescent or enzyme-labelled secondary antibody, which is then visualised by light microscopy (Ramos-Vara, 2005). The utilisation of a secondary antibody which is conjugated to a fluorochrome makes the detection of the antigen-primary antibody-secondary antibody complex easier. The indirect technique is more commonly used and has several advantages, such as greater sensitivity and that stronger signals are obtained (Wilson and Walker, 2005). Therefore, the indirect method was applied to the present study.

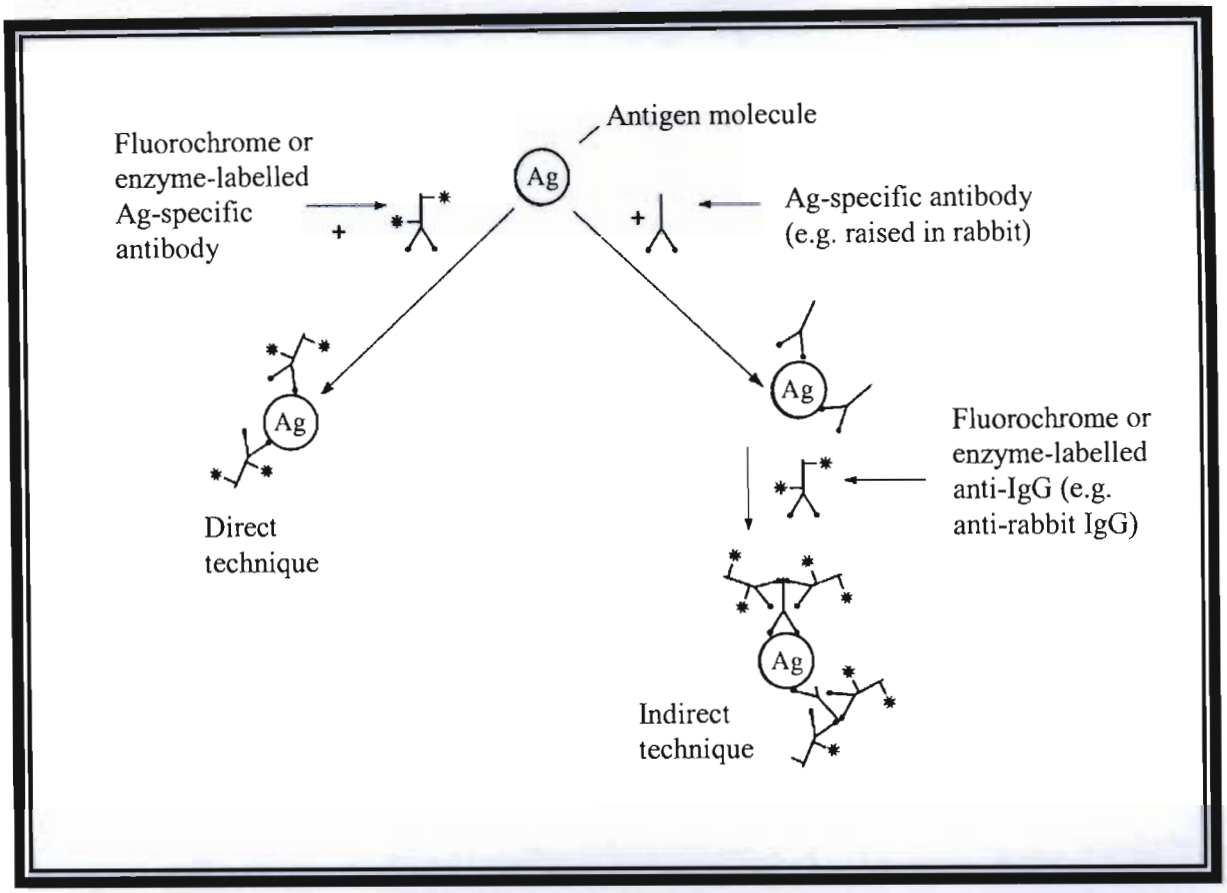

Figure 7.1: Diagrammatic representation of direct and indirect immunohistochemical methods (Wilson and Walker, 2005).

Usually, an antigen retrieval step is carried out before antigen detection, since some antigenic sites might have become masked during tissue fixation. Antigen retrieval serves to break the methylene bridges (formed by fixation) and cross-link proteins, which makes the primary antibody inaccessible to the antigen (Ramos-Vara, 2005). There are two methods of antigen retrieval: enzymatic or heat-mediated. Enzymatic antigen retrieval is much more gentle than heat-mediated, however, it does takes longer and may sometimes damage the morphology of the section (Ramos-Vara, 2005).

The aim of the study reported in this section was to identify the morphological aspects associated with apoptosis (chromatin condensation) and to immunolocalise OTA in kidney sections of male Wistar rats. In addition, kidneys from rats treated with *S. frutescens* were examined for possible cyto-protective effects.

7.2 MATERIALS AND METHODS

7.2.1 Materials

Finefix solution was purchased from Milestone (Italy); Ethanol, Xylene, Paraffin wax, Tri-sodium citrate (dehydrate) and PBS tablets were purchased from Merck (S.A); Poly-L-lysine, Fluorescent-labelled secondary antibody and DPX mountant were purchased from Capital Laboratory Supplies (S.A.); Hoechst 33342 and Bovine Serum Albumin (BSA) were purchased from Roche Diagnostics (S.A.); Anti-OTA was purchased from Abcam; Triton X-100 was acquired from Biorad (S.A.); and slides and coverslips were acquired from Shalom Laboratories (S.A.). All other reagents and chemicals were obtained from Merck (S.A).

7.2.2 Methods

7.2.2.1 Specimen Preparation

After immersion in Finefix solution (Chapter 3), samples were removed from the solution and then dehydrated through a series of increased alcohol concentration: 50% ethanol, 70%, 90% and two changes in 100% ethanol (1 hr each). The time period for specimen dehydration varies with size, thus large specimens were dehydrated for a longer period of time. When the kidneys were immersed in these solutions, gentle agitation was required to allow equal dehydration on all sides. The kidney tissue was then placed in a 1:1 solution of xylene and ethanol, followed by a clearing step in 100% xylene. Ethanol steps were followed with xylene to remove alcohol from tissue sections. Xylene is toxic and all steps that required xylene usage were carried out in a fume hood.

Finally, paraffin wax was heated in a water bath from a solid state to a liquid state. There were two changes in the paraffin wax, which allows infiltration into tissue. Paraffin wax (liquid at 60°C) is used since it serves as a good medium, one that provides excellent morphological detail and resolution. After infiltration, tissue was placed in moulds and covered with paraffin wax. The wax-containing moulds were set at room temperature.

Thereafter, paraffin blocks were sectioned at 3μm using a microtome. Sections were placed in a water bath (50°C) in order to remove any wrinkles or creases that may have formed on the section. Sections were picked up on poly-L-lysine coated slides. This type of coated slide is used since it allows the section to adhere onto the slide. Once the sections were picked up on the slides, slides were dried on a hot plate (60°C) to remove any water that may have been trapped underneath the section.

7.2.2.2 Preparation Before Staining

Before any staining procedure was performed, sections were de-paraffinised and rehydrated. Incomplete removal of paraffin could result in poor staining of the section. Therefore, sections were rinsed in two changes of 100% xylene. Sections were also re-hydrated by rinsing in two changes each of 100% xylene and 100% ethanol (1:1) and one rinse in 95% and 70% ethanol (5 min each). The xylene steps were followed by ethanol to remove xylene from tissue sections. Subsequently, sections were washed with dH_2O. To prevent the sections from drying out, sections were placed in dH_2O water until ready to be used.

7.2.2.3 Hoechst Staining

Tissue sections were initially washed in PBS (pH 7) and then stained with a 1mg/ml solution of Hoechst 33342 and incubated (15 min) in the dark. Following this, the slides were once again washed with PBS and sections were then dehydrated. Dehydration was carried out by dipping slides in increasing concentrations of ethanol (50%, 70%, 90% and 100%) and then rinsing in xylene. Xylene can be toxic, therefore, steps involving xylene were carried out under a fume hood. Sections were then mounted with DPX mountant; the coverslip was placed over the section and then viewed with an Olympus IXSI inverted research microscope which is equipped with the Olympus DP12 microscope digital camera system. Slides were viewed using filter 2, with excitation and barrier wavelengths of 330nm-385nm and 420nm.

7.2.2.4 Immunohistochemistry

7.2.2.4a Heat-Mediated Antigen Retrieval

The antigen retrieval solution, sodium citrate buffer pH 6 (Appendix C1), was allowed to boil and, at this point, slides were placed in the antigen solution, and then placed into the microwave (15 min). Citrate-based solutions enhance the staining intensity of the antibody. Sufficient solution was used so that the slides were completely covered, which in turn allows evaporation to occur during boiling. Slides were then removed from this solution and washed twice with PBS and 0.025% Triton X-100 (PBST) solution (5 min each).

7.2.2.4b Antibody Optimisation

After antigen retrieval, sections were covered with a blocking solution, 2% BSA (Appendix C2) (2 hrs, RT). Slides were then drained for a few seconds on tissue paper and carefully wiped around the sections. Care was taken to avoid drying of sections, since this may cause non-specific antibody binding and high background staining. Tissue sections were placed in a humidified container containing wet tissue paper, which was placed at the bottom of the container. Thereafter, the primary antibody Anti-OTA (100µl) was added to cover the section. Four dilutions were used, 1:50, 1:100, 1:200, 1:500 (Appendix C4), to determine optimal antibody concentration. Sections were incubated overnight with the primary antibody (4°C). Overnight incubation ensured maximum binding of the antibody.

The following day, sections were rinsed twice using PBST solution (5 min each) with gentle agitation. A fluorescent-labelled secondary antibody (1:500) (Appendix C5) was then applied over the section (1 hr, RT). After 1 hr the slides were rinsed in PBST (3 rinses 5 min each). Slides were then coverslipped and viewed. A primary antibody dilution of 1:100 was chosen.

7.2.2.4c Antibody Incubation and Image Analysis

The same procedure (as in 7.2.2.4b) was carried out for all of the kidney sections, using a primary antibody dilution of 1:100. Images were viewed using an Olympus IXSI microscope.

7.3 RESULTS AND DISCUSSION

Apoptosis results in chromatin condensation. The Hoechst stain, a DNA intercalator, helps to detect and identify chromatin condensation. Analysis of Hoechst-stained images revealed kidney tissue with intense fluorescence in the glomerular region in all of the samples (Fig. 7.2 and Fig. 7.3).

The control (Fig. 7.2) differed from other groups in that no fluorescence was observed outside of the glomerulus. On Day 1, a number of fluorescent nuclei were seen in the glomerular region. However, after 7 days, fluorescent staining decreased. It is known that cells may undergo proliferation in response to stress. Thus, the intense staining of the nuclei in the glomerular area may be indicative of mitosis. This can be deduced, since the morphological aspects of mitosis and apoptosis, such as chromatin condensation and dissolution of nuclear membranes, are similar. The decreased nuclear fluorescent staining at Day 7 may be due to mitosis. It is possible that after 7 days the rats may have adapted to the control treatment conditions.

The rat kidneys that were treated by *S. frutescens* alone (Fig. 7.2) showed nuclear fluorescence that was more intense than that of the control. This staining pattern (Fig. 7.2) depicts nuclei with condensed chromatin. *Sutherlandia frutescens* is a known inducer of apoptosis. L-canavanine (present in *S. frutescens*) has the ability to induce apoptosis. Furthermore, *S. frutescens* causes cell death in cultured cells, which was previously shown by morphological aberrations, phosphatidylserine externalisation, chromatin condensation and nuclear fragmentation (Chinkwo, 2005). Condensation of nuclei with the breakdown of chromatin is characteristic of apoptosis.

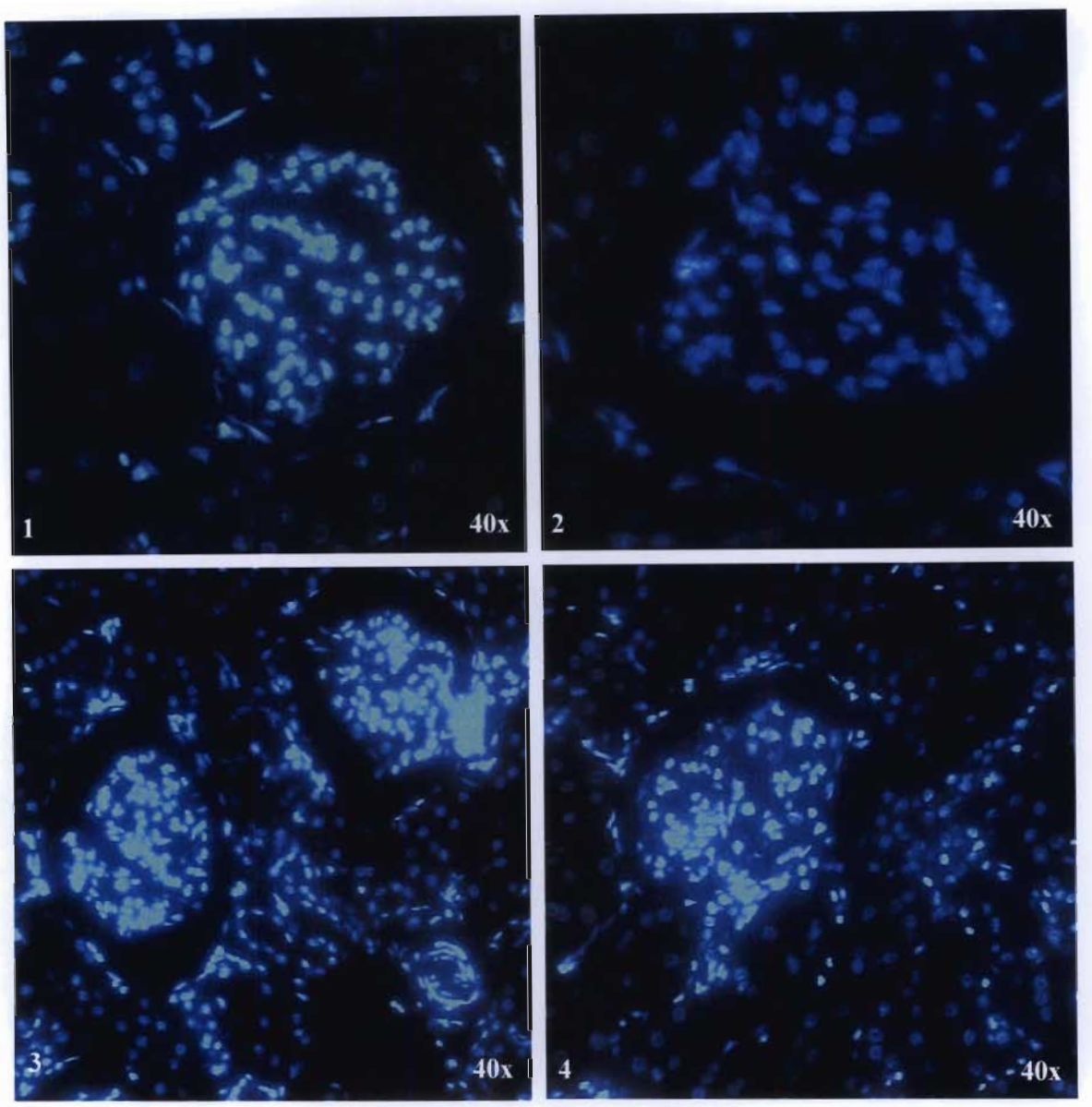

Figure 7.2: Kidney sections stained with Hoechst 33342: 1) Control Day 1 (40x); 2) Control Day 7 (40x); 3) *S. frutescens*-only Day 1 (40x); 4) *S. frutescens*-only Day 7 (40x).

Fluorescence intensity was higher in the OTA-only treatment groups on Day 7 compared with Day 1 (Fig. 7.3). There were numerous condensed nuclei in the glomeruli of the Day 7 OTA-only treated kidney sections. Kidney sections from the co-treatment rat group showed that fluorescent staining was higher after the 7-day treatment. The staining pattern in the combination groups (Days 1 and 7) did not differ significantly from the OTA-only treatments. The images of the kidney sections suggest that OTA may induce renal cell injury (Fig. 7.3).

Renal cell injury was previously noted by Domijan *et al.* (2004) and Schwerdt *et al.* (2007). In acute toxicity studies, OTA-induced cell death was reported *in vivo* in rat renal tubules and in mice embryos and livers (Petrik *et al.*, 2003). Petrik *et al.* (2003) found that OTA induced apoptosis in both proximal and distal tubule cells in the kidneys of male Wistar rats (treated for 10 – 60 days), whilst the present study showed apoptosis to occur only in the glomerular area (treated for 1 and 7 days). Although these images are strongly suggestive of apoptotic processes, the PBMC assays for apoptosis was not significant (Chapter 6).

It is also known that after a toxic insult some cells suffer injury and may undergo programmed cell death. In the case of OTA, the glomerulus may be the site where cellular damage is initiated. Cells present in the glomeruli, such as glomerular visceral epithelial cells (podocytes), maintain the structure and function of the glomerular basement membrane. These cells aid the filtration process by providing a permeability barrier. Thus, persistent glomerular apoptosis may decrease the filtration capacity. And also, defects in the glomerular wall structure can thus lead to proteinuria (Ming-Fang Hseih *et al.*, 2004). Furthermore, apoptosis in glomerular cells is the cause of many glomerular diseases and could be one of the reasons behind OTA-induced renal toxicity.

The kidney is a prime organ in which intense oxidative processes can take place and this may lead to the production of ROS. In addition to glomerular cells, polymorphonuclear leukocytes and monocytes are potential sources of ROS within the glomerulus. Furthermore, OTA may induce oxidative damage through the production of ROS or lipid peroxidation (Schaaf *et al.*, 2002; Petrik *et al.*, 2003). Reactive oxygen species are common initiators of apoptosis, which may account for the intense staining pattern (Fig. 7.3). The glomerulus is the first site of

exposure to toxins in the kidney. Considering that apoptosis was detected in the glomerulus, it is possible that OTA renal toxicity may begin with injury to the glomerular area.

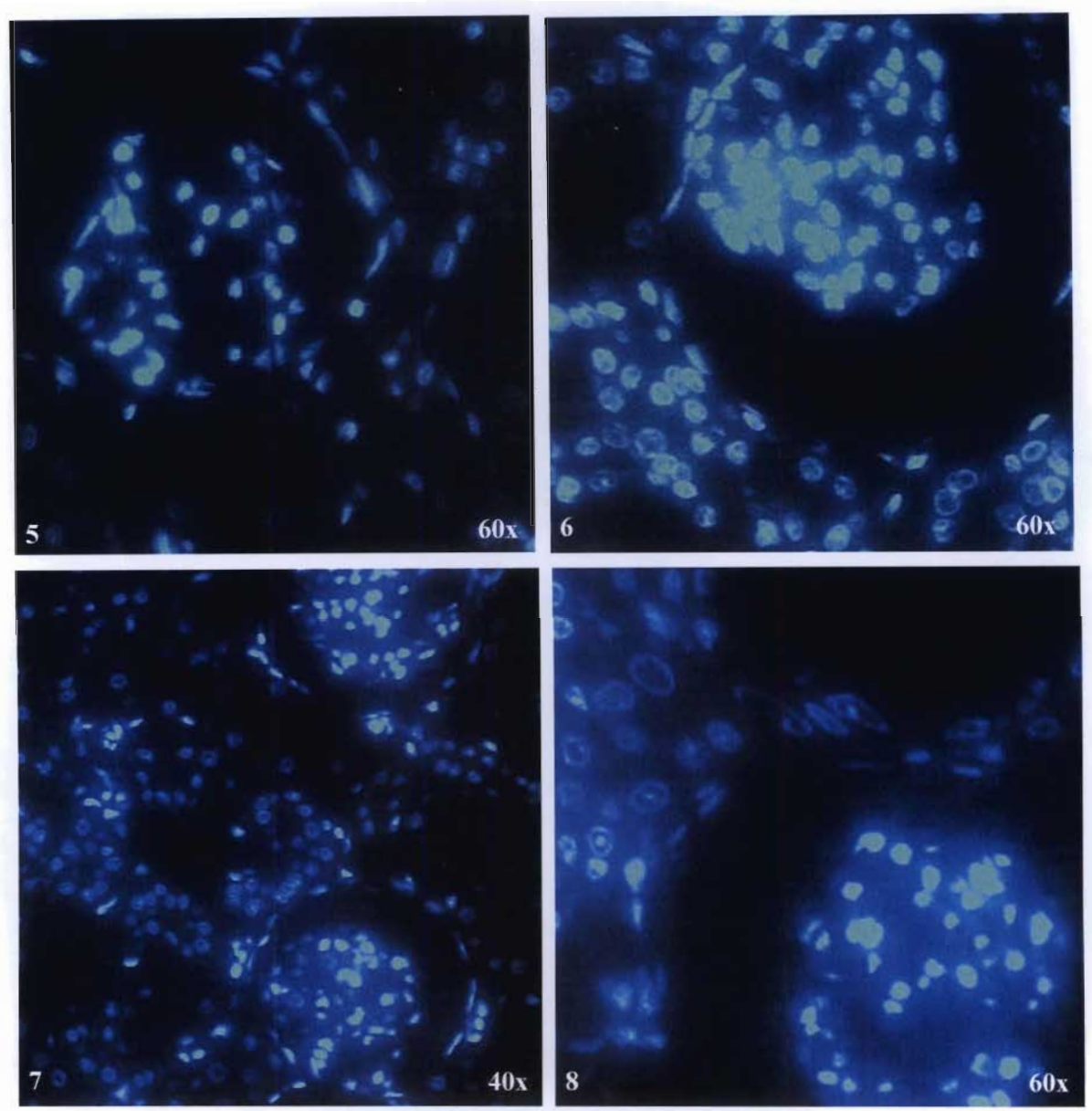

Figure 7.3: Photomicrographs illustrating kidney sections stained with Hoechst 33342: 5) OTA-only Day 1 (20x); 6) OTA-only Day 7 (40x); 7) OTA and *S. frutescens* Day 1 (20x); 8) OTA and *S. frutescens* Day 7 (20x).

The distribution of an antigen in tissues provides an accurate indication of cytotoxicity. In this case, anti-OTA was used to identify the location and distribution of OTA in the kidneys (Fig. 7.4 and Fig. 7.5).

From the immunostained images, intense fluorescence was observed in the glomerulus of both OTA and co-treated rats at Days 1 and 7 respectively (Fig. 7.5). The glomerulus was the only site at which OTA was detected. This could be due to the increased binding of OTA to albumin. Glomerular filtration does not permit movement of albumin into the ultrafiltrate. Blood passes through the glomerulus and in this area albumin is restricted from passing into the proximal tubule; it exits the glomerulus via the efferent arteriole and rejoins the main bloodstream via the renal vein. If a large portion of the OTA that enters the body is bound to albumin, then it should be difficult for the toxin to be filtered by the glomerulus. Albumin binding may delay OTA elimination by preventing the transfer from blood to the renal cells. Hence, OTA was immunolocalised in the glomerular area only, due to the high levels of albumin.

The glomerulus is the first site in the kidney to be exposed to a toxicant, thus OTA was present in this region. The glomerulus provides a barrier against the transglomerular passage of macromolecules, and thus only small molecules are freely filtered. The filtration of anionic molecules tends to be restricted as compared with that of neutral or cationic molecules of the same size (Schnellmann, 2003). Toxicants that neutralise or reduce the number of fixed anionic charges in the glomerulus will impair the charge or size selective properties in that region (Smart and Hodgson, 2008). This results in the excretion of polyanionic and/or high molecular weight proteins. Subsequently, this may be a reason for the presence of OTA in the glomerular cells.

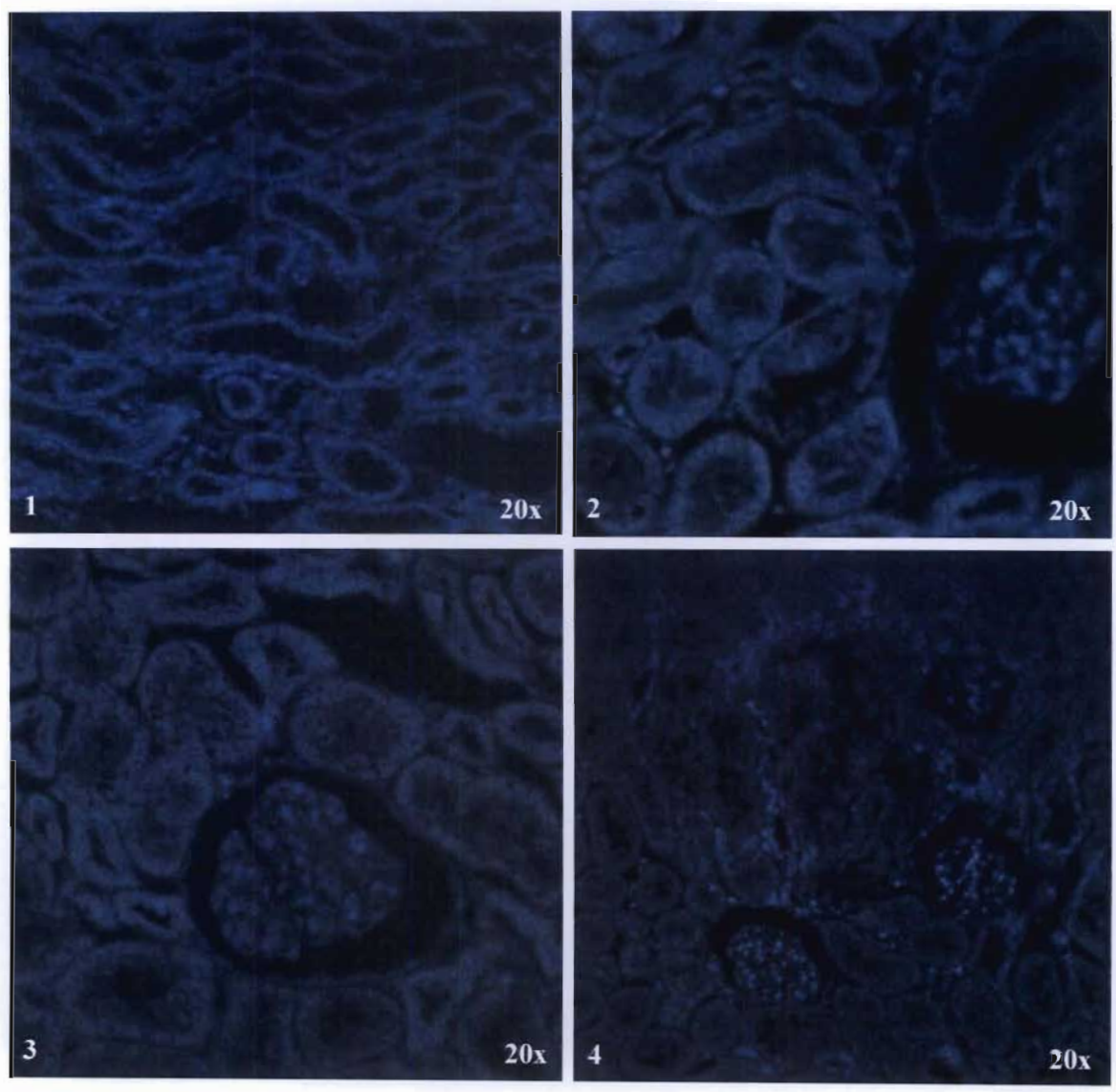

Figure 7.4: Illustration of kidney sections incubated with Anti-OTA: 1) Control Day 1 (20x); 2) Control Day 7 (20x); 3) *S. frutescens*-only Day 1 (20x); 4) *S. frutescens*-only Day **7** (20x).

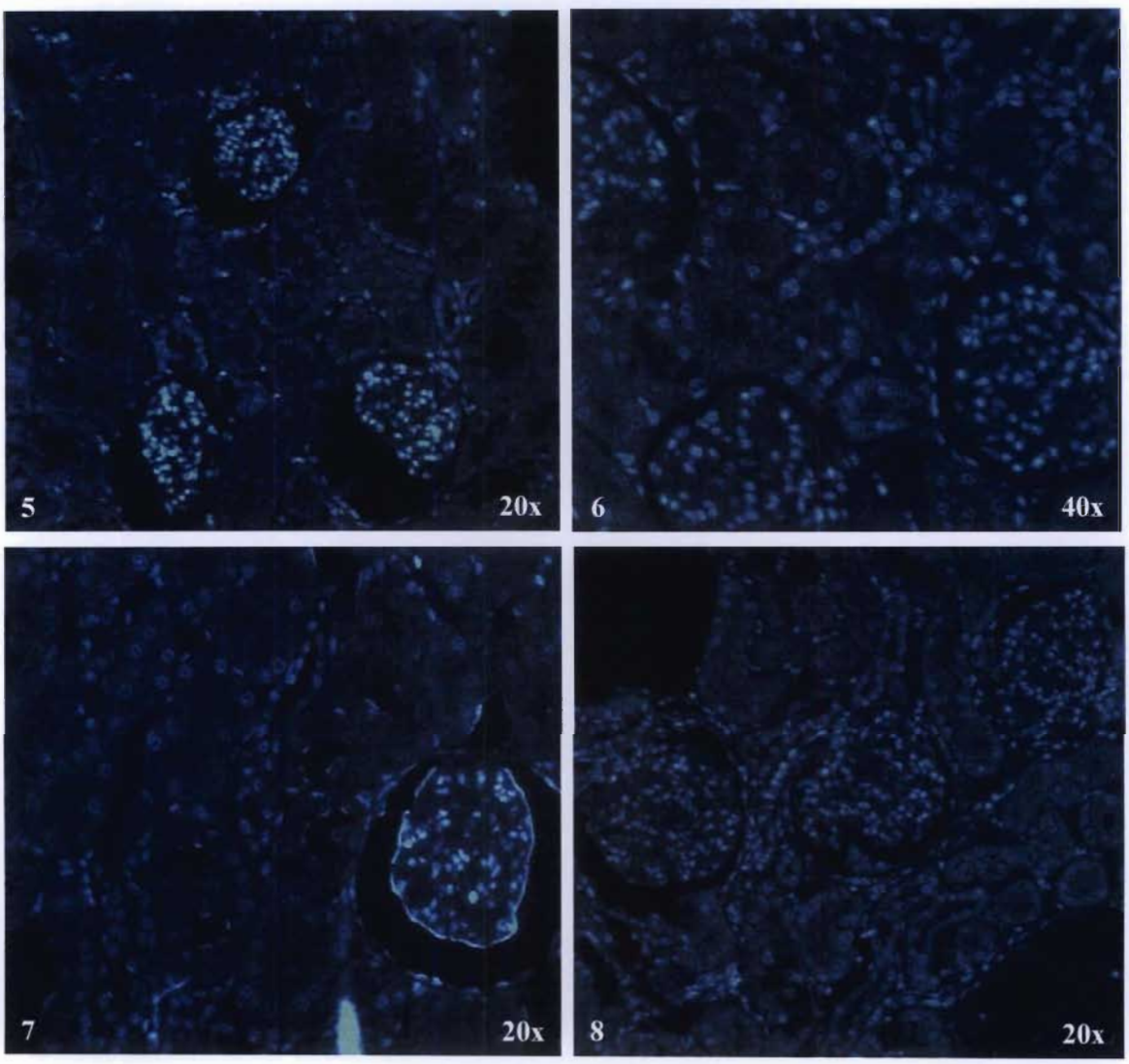

Figure 7.5: Photomicrographs showing kidney sections incubated with Anti-OTA: 5) OTA-only Day 1 (20x); 6) OTA-only Day 7 (40x); 7) OTA and *S. frutescens* Day 1 (20x); 8) OTA and *S. frutescens* Day 7 (20x).

The co-treatment with *S. frutescens* did not decrease OTA detection in the glomerular area (Fig. 7.5). Since OTA preferentially binds to albumin, it seems that *S. frutescens* had little or no effect on inhibition of OTA binding to albumin. Therefore the albumin-bound OTA would recirculate until dissociated. Subsequently, it may be important to displace OTA from albumin, thus increasing OTA elimination.

Other studies have detected OTA in tubular regions of the nephron (Schwerdt *et al.*, 1996; Dahlmann *et al.*, 1998). The organic anion transporter (OAT) family is important in the uptake of anions and may be important in OTA secretion into the tubular regions. However, it is believed that OTA may cause alterations to the OAT, which subsequently delays the blood-to-lumen transport of OTA and thus reduces elimination from the body (Sauvant *et al.*, 1998). In addition, by disrupting the OAT, the elimination of other anionic xenobiotics will also be reduced, which may in turn further increase toxicity in the body. Furthermore, if OTA is unbound and freely available then only can the toxin pass through the OAT. Also, it is believed that excretion of OTA may occur by a similar mechanism as pAH, which relies on α-ketoglutarate (Groves *et al.*, 1998). If the concentration of α-ketoglutarate is decreased then the OATs may not function optimally. When the concentration of α-ketoglutarate in the kidney decreases, then the α-ketoglutarate produced in the blood will be transported to the kidney. Therefore, OTA-induced changes in blood α-ketoglutarate may in turn lead to renal injury. This means that immunotoxicity may play a crucial role in OTA-induced renal cell damage.

Furthermore, the kidneys are the only organ where highly protein-bound drugs are unbound and traverse the tubular cells (De Broe and Roch-Ramel, 1998). Thus, this could also account for the presence of OTA in tubular regions in other studies (Schwerdt *et al.*, 1996; Dahlmann *et al.*, 1998). If the rats had been treated for a longer period of time, OTA may have been detected in the tubules.

The occurrence of OTA in tissues is dependent on the animal species used, the dose administered, the route of toxin exposure, and the health status of the animals (Ringot *et al.*, 2006). When animals are treated by i.p injection, the toxin of interest is rapidly absorbed because of the rich blood supply. Since, in the present study, rats were treated with

OTA by i.p injection, it is possible that a large amount of OTA was bound to albumin. Subsequently, this may have hindered any increase in OTA in the renal tubules.

It has been suggested that OTA decreases renal blood flow and the glomerular filtration rate (Gekle and Silbernagl, 1996) and that the long-term effects of OTA are usually associated with damage to the glomeruli. This may result in an accumulation of the toxin. Thus the presence of OTA in the glomerular region, together with apoptosis in this area, may be responsible for glomerular damage and glomerular or renal disease at large.

7.4 CONCLUSION

Ochratoxin A treatment resulted in the condensation of chromatin in the glomerulus. This was noticed after Day 1 and Day 7, but the staining was more intense by Day 7. This is in concurrence with the fact that renal injury due to OTA increases after extended periods of time. Furthermore, *S. frutescens* did not alleviate the effect on chromatin condensation and the intensity was not changed. Using immunohistochemistry, OTA was localised in the glomerular region. The medicinal plant did not reduce the occurrence of OTA in the glomerulus. Chromatin condensation is an indication of apoptosis and therefore renal cell injury may occur as a result of glomerular disruption.

CHAPTER 8

THE EFFECTS OF OCHRATOXIN A ON PROTEIN EXPRESSION IN RAT TISSUE

8.1 INTRODUCTION

Electrophoresis is the migration of a charged particle under the influence of an electric field. Most biological compounds possess ionisable groups and at any given pH exist in solution as either cations or anions (Wilson and Walker, 2005). Thus, under the influence of an electric field, charged biological compounds, such as proteins, migrate either to the cathode or to the anode. When voltage is applied, molecules with different charges separate as a result of their different electrophoretic mobility. Electrophoretic mobility is the ratio of the velocity of the ion to the field strength (Wilson and Walker, 2005). Frictional force may also retard the movement of a charged molecule. The frictional force is determined by the shape and hydrodynamic size of the molecule, the pore size of the medium in which electrophoresis is taking place and the viscosity of the buffer (Wilson and Walker, 2005). Sodium dodecylsulphate polyacrylamide gel electrophoresis (SDS-PAGE) and Western blot use this principle to separate and transfer proteins from an acrylamide gel onto a polyvinylidene fluoride (PVDF) membrane, respectively.

8.1.1 SDS-PAGE

Sodium dodecyl sulphate polyacrylamide gel electrophoresis (SDS-PAGE) is used for analysing protein mixtures qualitatively and was first described by Laemmli (1970). Initially, proteins are standardised, denatured and then loaded onto an acrylamide stacking gel where the proteins are separated according to size in a resolving gel. Proteins of a high molecular weight will be found towards to the top of the gel and those of a low molecular weight will be found near the bottom. SDS-PAGE is an important application that is used to analyse protein purification and to determine the relative molecular mass of proteins.

8.1.2 Western Blot

Immunochemical techniques make use of antibody technology (Fig. 8.1) and provide powerful tools for toxicological analyses. Such tools include, assessing the effects of a toxicant on intracellular protein localisation, as well as determining the effects of a toxicant on protein levels (Smart and Hodgson, 2008).

Proteins are firstly separated by SDS-PAGE, and then transferred onto a PVDF membrane (Fig. 8.1). The proteins that are transferred onto the membrane are a replica of the pattern of protein separation on the gel. Subsequently, the blot is incubated in a protein solution to prevent non specific binding and thereafter incubated with the relevant primary and secondary antibodies. The secondary antibody is appropriately labelled so that the antigen-antibody complexes can be detected (Wilson and Walker, 2005).

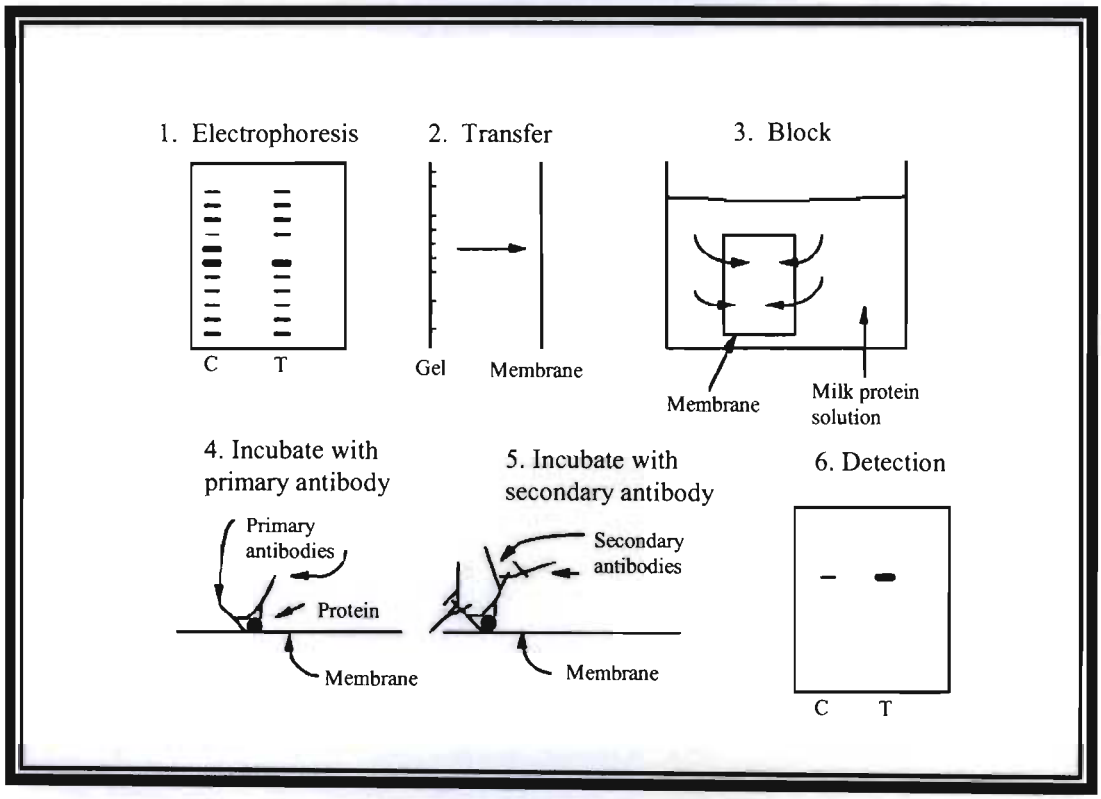

Figure 8.1: Diagrammatic representation of a Western blot procedure (C – control, T – treated) (Smart and Hodgson, 2008).

The aim was to determine the protein expression in the kidney tissue of male Wistar rats after OTA treatment.

8.2 MATERIALS AND METHODS

8.2.1 Materials

Tris, Sodium chloride (NaCl), Sodium dodecyl sulphate (SDS), Tetramethylenediamine (TEMED), Glycerol, Glycine, Potassium chloride (KCl), Tween 20, Dithiothreitol (DTT), Dipotassium ethylenediaminetetraacetic acid (K_2EDTA), Potassium dihydrogen phosphate (KH_2PO_4), Sucrose, Methanol, Formaldehyde, Silver nitrate, Citric acid, Acetic acid, Ammonium hydroxide, Sodium hydroxide (NaOH), PBS tablets and Eppendorfs were purchased from Merck (S.A); Bicinchoninic acid (BCA), Copper sulphate ($Cu(II)SO_4$), B-mercaptoethanol, Bromophenol blue and Rabbit Anti-mouse-HRP secondary antibody were obtained from Capital Laboratory Supplies (S.A.); Ammonium persulphate (APS), Non-fat dry milk and Immun-Star™ Chemiluminescent Detection Kit were obtained from Bio-rad (S.A.); Bovine serum albumin (BSA) was purchased from Roche (S.A.); Anti-OTA was obtained from Abcam and 96 well microtiter plates were purchased from the Scientific Group (S.A.). All other chemicals were purchased from Merck (S.A.)

8.2.2 Methods

8.2.2.1 Protein Isolation

Homogenising buffer (3ml) (Appendix D1) was added to sliced kidney (approximately 0.2g) tissue and the tissue was then homogenised. Thereafter, samples were centrifuged (3 min, 1 000rpm, 4°C), to remove any cellular debris. The pellet was discarded. An aliquot of the supernatant was retained as the crude fraction and another aliquot was subjected to differential centrifugation to yield mitochondrial, nuclear and cytoplasmic fractions. For the nuclear fraction, the supernatant was centrifuged (10 min, 3 500rpm, 4°C) and the pellet (nuclear fraction) obtained was re-suspended in storage buffer (Appendix D2) and stored for further use. The resultant supernatant was re-centrifuged (10 min, 10 000rpm, 4°C), the pellet

was re-suspended in storage buffer and constituted the mitochondrial fraction whilst the supernatant was retained as the cytoplasmic fraction.

8.2.2.2 Protein Quantification: Bicinchoninic Acid (BCA) Assay

Initially a 1mg/ml BSA stock solution was prepared and this solution was diluted accordingly to make standard concentrations (Appendix D3).

Each sample (20µl) was added to a 96 well microtiter plate in duplicate. BCA working solution was prepared by adding BCA (198µl/well) to Cu(II)SO_4 (4µl/well). The working solution (200µl) was dispensed into each well including the standards. Samples were then incubated (30 min, 37°C). Peptide bonds in the protein reduce copper (Cu^{2+}) ions from the copper sulphate (Cu(II)SO_4). The amount of Cu^{2+} that is reduced is proportional to the amount of protein present in the sample. Two molecules of BCA chelate each Cu^{+} ion forming a purple coloured product that strongly absorbs light at a wavelength of 562nm. Thus, the optical density was measured at 562nm on a Quant ELISA plate reader (Analytical Diagnostic products (S.A.)).

Next, a standard curve was drawn to determine protein concentration and samples were then standardised to 1mg/ml (Appendix D3).

8.2.2.3 SDS-PAGE

Initially, a 10% resolving gel (Appendix E1) was prepared and was allowed to set (30-60 min). Thereafter, a 6% stacking gel (Appendix E2) was prepared. A comb was inserted and the stacking gel was poured in, in order to form sample loading wells and was then allowed to set (30 min).

The standardised proteins were diluted in sample buffer (100µl) (Appendix E3) in a 1:1 ratio, and then heated (5 min, 95°C). Sample buffer contains SDS, which denatures and uncoils the polypeptide chains and a thiol reducing agent, mercaptoethanol. Bromophenol blue, a tracker dye, also present in the sample buffer, was used to determine how far the sample moved in the

resolving gel. Glycerol was also incorporated into the sample buffer to add density to the sample, thus ensuring that the sample sunk to the bottom of the well in the stacking gel.

Finally, the denatured sample (25μl) was added to each well, according to each treatment. Running buffer (Appendix E4) was then added to the electrophoresis tank and samples were electrophoresed (1 hr, 150V). On completion of the electrophoretic run, gels were Silver stained (Appendix E5) and thereafter the relative mobility (Rf) was determined. The Rf was calculated by measuring the distance of the molecular weight marker from the top to the bottom dye front. Then, the distance of each band was determined from the top to the position of band, and this was divided by the molecular weight marker distance. A standard curve of Log molecular weight and Rf was used to determine the molecular weight of the proteins.

8.2.2.4 Western Blot

After protein separation by SDS-PAGE, the acrylamide gel and a blotting (PVDF) membrane were sandwiched between fibre pads and filter paper, in a cassette. The cassette was then placed in the electrophoresis tank and completely covered with chilled transfer buffer (pH 8.3) (Appendix E6). A cooling unit was also placed in the tank to ensure that the transfer buffer remained cool during transfer. In addition, a stir bar was also placed in the tank to help maintain an even buffer temperature and ion distribution in the tank. The tank transfer apparatus (tank containing tank buffer and gel sandwich) was placed on a stirrer and the maximum speed was used. Thus, proteins from serum and kidney tissue were electrophoretically transferred onto a PVDF membrane by wet transfer (1 hr, 350mA). After transfer, the gel was Silver stained (Appendix E5) to ensure that the transfer onto the membrane was successful.

Thereafter, the PVDF membrane was immersed in 5% non-fat dry milk (Appendix E7) and placed on an orbital shaker for 1 hr, then incubated overnight (4°C). The purpose of non-fat dry milk is to block all remaining non-specific sites.

Upon removal from the 5 % non-fat dry milk solution, the membrane was then incubated with the primary antibody (Anti-OTA), diluted in a 1:5 000 ratio (50 min, RT). Following this incubation period, the membrane was then washed vigorously with TTBS (Tween-Tris buffered saline) (3 washes, 5 min each) (Appendix E8). Thereafter the membrane was incubated with a rabbit Anti-mouse-HRP secondary antibody (1:10 000) (45 min, RT). An orbital shaker was used for primary and secondary incubation so that the entire membrane was exposed to the antibodies. After secondary antibody incubation, the membrane was again washed with TTBS (3 washes, 5 min each). It is important to note that after each step a clean container was used to avoid carry-over from one step to the next and each rinse was carried out on an orbital shaker.

The Immun-Star™ HRP Chemiluminescent detection kit was utilised and in the presence of hydrogen peroxide, HRP (horse radish peroxidase) catalyses the oxidation of luminol, which acts as the substrate. Luminol and peroxide buffer solutions, provided in the kit, were mixed in a 1:1 ratio and the membrane was then incubated in this solution (3-5 min). The Bio-rad Gel Doc XRS imaging system was used for detection and images were viewed using the Bio-rad Quantity 4.4.1 analysis software.

8.2.3 Statistical Analysis

Band intensity was measured using the Image J analysis software and statistical significance between treatments was determined using One-Way Analysis of Variance (ANOVA) and Tukey Kramer Multiple Comparisons test, on GraphPad Instat v3.06 (GraphPad Software, San Diego, CA). A probability value (p) of less than 0.05 ($p<0.05$) was considered statistically significant.

8.3 RESULTS AND DISCUSSION

Crude, mitochondrial, nuclear and cytoplasmic fractions were each loaded into separate gels. Each fraction consisted of the following treatments: control-Day 1 (Lane 1), control-Day 7 (Lane 2), *S. frutescens*-only-Day 1 (Lane 3), *S. frutescens*-only-Day 7 (Lane 4), OTA-only-Day 1 (Lane 5), OTA-only-Day 7 (Lane 6), OTA and *S. frutescens*-Day 1 (Lane 7), OTA and *S. frutescens*-Day 7 (Lane 8) (Fig. 8.2 and Fig. 8.3).

Comparisons between each fraction revealed a protein, approximately 150kDa, in the mitochondrial and cytoplasmic fractions only. Furthermore, a 63.1kDa protein was detected in the mitochondrial fraction. However, this protein was more prominent in the cytoplasmic fraction. The mitochondrial and cytoplasmic fractions both showed the presence of a 26kDa protein. A 38.9kDa protein was detected in the mitochondrial, nuclear and cytoplasmic fractions. It is possible that proteins of a similar molecular weight were observed since differential centrifugation was used to separate proteins. This may have resulted in some protein residues being either left behind in a previous fraction or carried over into the next fraction.

In the mitochondrial fraction (Fig. 8.2), whilst the 150kDa protein was present in control samples, protein expression was decreased in OTA-only treated rats at Day 1 and 7 and co-treated rats at Day 1 and 7. When compared to the controls OTA-only and combination treatment resulted in a decrease in expression of the 63.1kDa and 26kDa proteins after the Day 1 and 7 regimes. Also, the expression of a 13.8kDa protein, although present in control groups (Lane 1 – Lane 4), was absent in other treatment groups. It has been suggested that OTA treatment results in mitochondrial disruptions, and that this may occur as an early event in toxicity (Aleo *et al.*, 1991; Bouaziz *et al.*, 2008). It is possible that this may be related to the observed decrease in protein expression.

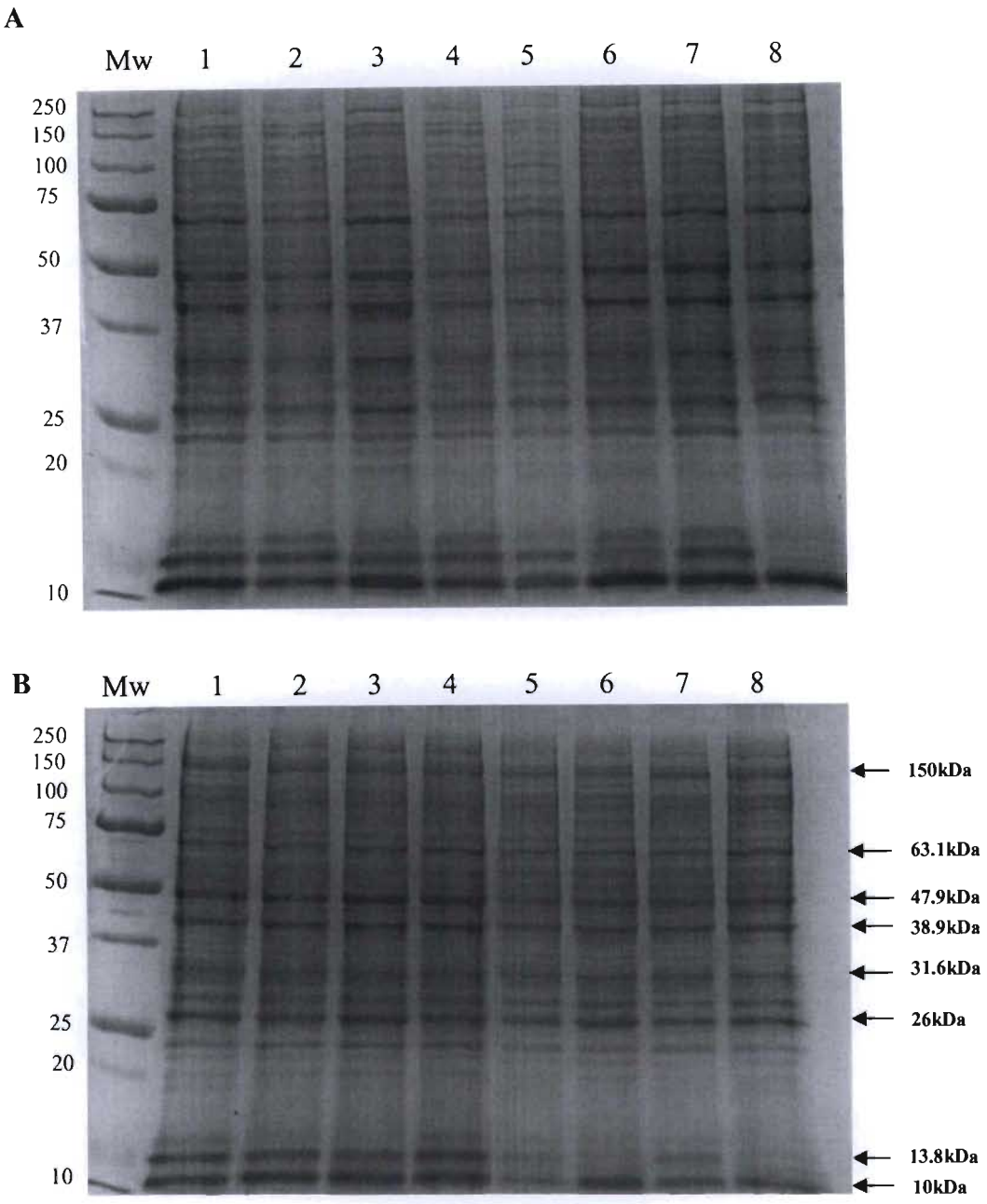

Figure 8.2: SDS-PAGE gels (Silver stained) showing crude (A) and mitochondrial (B) fractions. (Mw) Molecular weight marker; (1) Control Day 1; (2) Control Day 7; (3) *S. frutescens*-only Day 1; (4) *S. frutescens*-only Day 7; (5) OTA-only Day 1; (6) OTA-only Day 7; (7) OTA and *S. frutescens* Day 1; (8) OTA and *S. frutescens* Day 7.

Furthermore, it is possible that protein synthesis may be compromised by OTA by interacting with phenyl-handling proteins at post-transcriptional level, such as phenylalanyl-tRNA-synthase (Schwerdt *et al.*, 1999; Stoev, 1998; Simon *et al.*, 1996; Marin-Kuan *et al.*, 2006). This could alter the production of tyrosine from phenylalanine.

In the cytoplasmic fraction (Fig. 8.3) a decrease in expression of a 12.6kDa and a 10.7kDa protein was detected. The expression of the 63.1kDa and 38.9kDa proteins was prominent in all treatments. Nuclear fractions showed that the expression of a 208.9kDa protein was more prominent in the *S. frutescens* group on Day 1 and combination group rats on Day 7. There was a decrease in expression of a 12.3kDa protein in the nuclear fraction. Furthermore, the 43.7kDa, 38.9kDa and 26.3kDa proteins were highly expressed in all treatments of the nuclear fraction.

In the study by Maaroufi *et al.* (1999), it was observed that a higher concentration of OTA was found in the blood than in the kidney, for all doses tested. Other studies have shown that there was an inhibition of various proteins as a result of OTA toxicity (Schilter *et al.*, 2005). Ochratoxin A may not have caused interruptions in protein synthesis, due to the short time (1 day or 7 days) period in the body and dose given to rats and therefore drastic changes were not observed. Also, since a large portion of OTA is bound to albumin, glomerular filtration is restricted. The albumin-bound OTA therefore returns into circulation. Furthermore, the images presented in Chapter 7 showed that OTA was immunolocalised in the glomerular area and not in the tubules. This demonstrates that the binding of OTA to albumin limits the transfer of OTA from the blood to renal cells. Subsequently, this may result in decreased effects on protein expression in kidney tissue since, only the unbound form may be available for elimination by the kidneys.

Usually, the inhibition of protein synthesis results in the decrease of cell growth or proliferation. Other studies have demonstrated that OTA caused a down regulation of genes that are important for protein synthesis, thereby decreasing protein synthesis (Marin-Kuan *et al.*, 2006). It is possible that OTA may not directly inhibit protein synthesis, but protein inhibition may occur by an indirect mechanism.

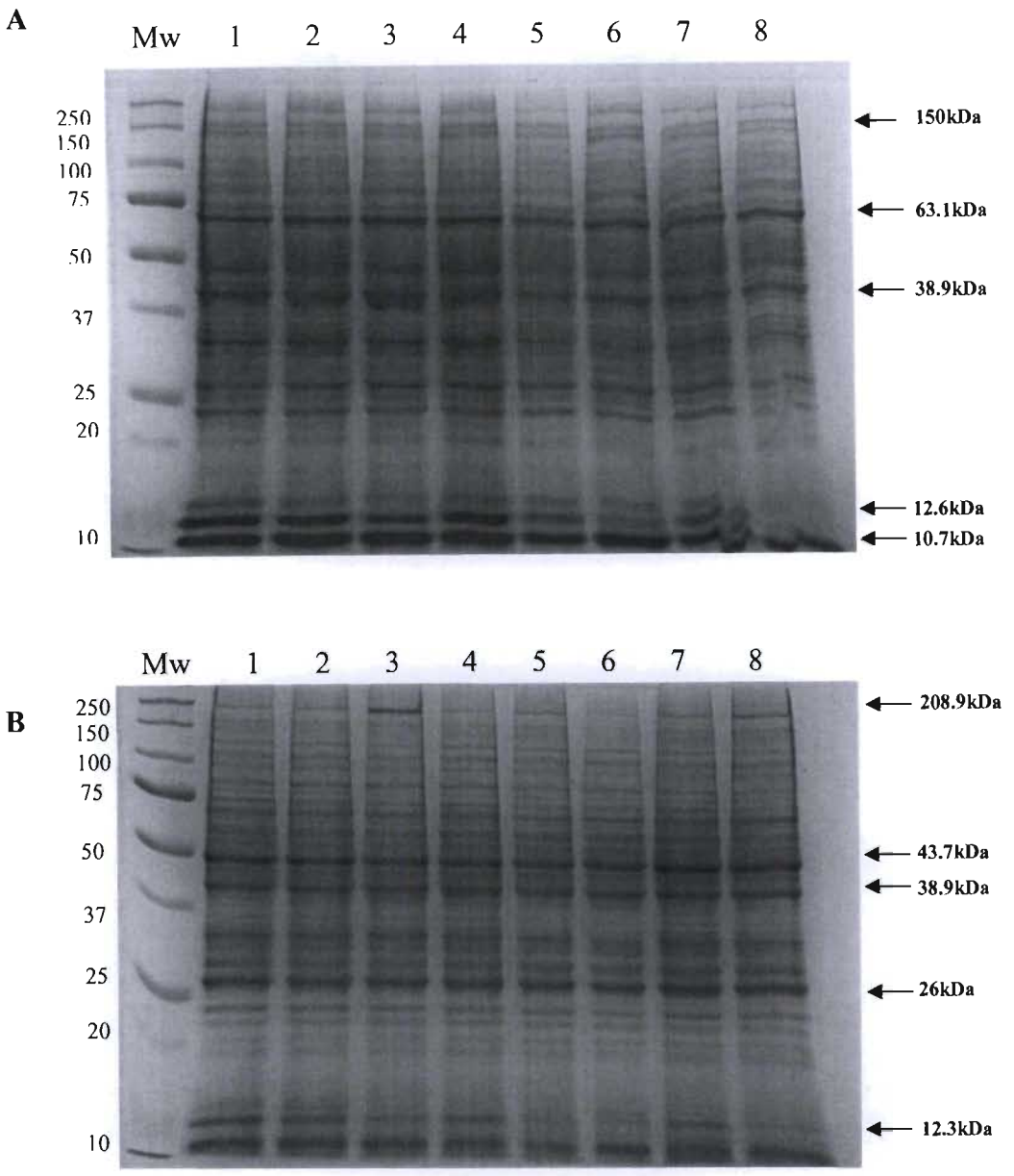

Figure 8.3: SDS-PAGE gels (Silver stained) showing cytoplasmic (A) and nuclear (B) fractions. (Mw) Molecular weight marker; (1) Control Day 1; (2) Control Day 7; (3) *S. frutescens*-only Day 1; (4) *S. frutescens*-only Day 7; (5) OTA-only Day 1; (6) OTA-only Day 7; (7) OTA and *S. frutescens* Day 1; (8) OTA and *S. frutescens* Day 7.

Figure 8.2 and Figure 8.3 also illustrate that there was no difference in protein expression after the *S. frutescens* treatment compared to the controls. Also, protein expression of the combination treatment did not vary from the OTA-only groups. This suggests that *S. frutescens* may not alleviate the observed effects on OTA-induced protein expression.

Previous studies used radiolabeled OTA to determine its distribution in serum and kidney (Stojkovic *et al.*, 1984; Kane *et al.*, 1986). However, this method may have disadvantages, such that not all of the radioactivity detected may be due to OTA, but may also result from degradation products such as phenylalanine or OTA-α (Schwerdt *et al.*, 1996). By using Western blot, the distribution of OTA can be determined with the aid of specific antibodies.

Analysis of the Western blot revealed that OTA bound to albumin and a high molecular weight (120kDa) serum protein (Fig. 8.4 and Fig. 8.5). It was observed that OTA bound to serum proteins even after the Day 1 regime, thus supporting the view that OTA rapidly binds to serum proteins once exposed to them. The binding of OTA to proteins may increase the susceptibility to various diseases.

Ochratoxin A also bound to rat serum-derived proteins even in the co-treatment groups, Group 7 and Group 8 (Fig. 8.4 and Fig. 8.5). Although other studies have shown that OTA could bind to other lower molecular weight proteins (Schwerdt *et al.*, 1999), this was not observed in the present study. Furthermore, the binding of OTA to kidney proteins was not detected in this study.

Schwerdt *et al.* (1999) demonstrated the ability of OTA to bind to various proteins in the kidney tissue. However, in the above study, a method that involved the coupling of OTA to HRP was employed to detect OTA-protein binding. A nitrocellulose membrane was then incubated overnight with the OTA-HRP conjugate. In contrast, the present study used an OTA antibody (Anti-OTA) to test for the presence of OTA bound proteins in rat kidneys *in vivo*. Hence, differences were found regarding the lack of OTA binding in rat kidneys in the present study. Schwerdt *et al.* (1999) also found that OTA bound to serum proteins, 40kDa and 27kDa in molecular weights, which was not found in the present study. However, the present study revealed that OTA may also bind to a high molecular weight (120kDa) serum

protein. Binding to this high molecular weight protein, further ensures that OTA remains in the body for a longer period of time. It is possible that this high molecular weight protein may represent one of the globulins present in plasma.

The combination treatment of OTA and *S. frutescens* also showed the binding of OTA to serum proteins (Fig. 8.4 and Fig. 8.5). In addition, the combination treatment demonstrated that *S. frutescens* did not result in the binding of OTA to other serum proteins. The binding of OTA to serum albumin is an important mechanism by which the toxin may have a longer chronic exposure time. If this binding is inhibited, then OTA can be eliminated from the body more efficiently.

After the analysis of the band intensities, it was revealed that there were significant differences between the band intensities of each treatment. With regard to the 120kDa protein band intensity (Fig. 8.4), it was observed that the band intensity of the 7-day OTA-only group was higher than that of the OTA-only Day 1 regime ($p<0.01$). This means that a higher concentration of OTA was bound to this high molecular weight protein after a long dosage period (OTA-only 7 days). This in agreement with other studies that suggest OTA induces severe toxicity after prolonged exposure (Sauvant *et al.*, 1998; Schwerdt *et al.*, 2007).

Furthermore, a comparison between the OTA-only (Day 1) and the combination treatments (Fig. 8.4), showed that the combination treatment (Day 1) had a significantly higher band intensity for the same period of time ($p<0.001$). This suggests that even when treated with *S. frutescens*, the binding of OTA to the 120kDa serum protein was increased. However, after the 7-day combination regime the band intensity decreased significantly ($p<0.01$). Thus, although *S. frutescens* may not have completely inhibited the binding of OTA to this protein (120kDa), a decrease in band intensity suggests that the amount of protein bound to OTA was decreased.

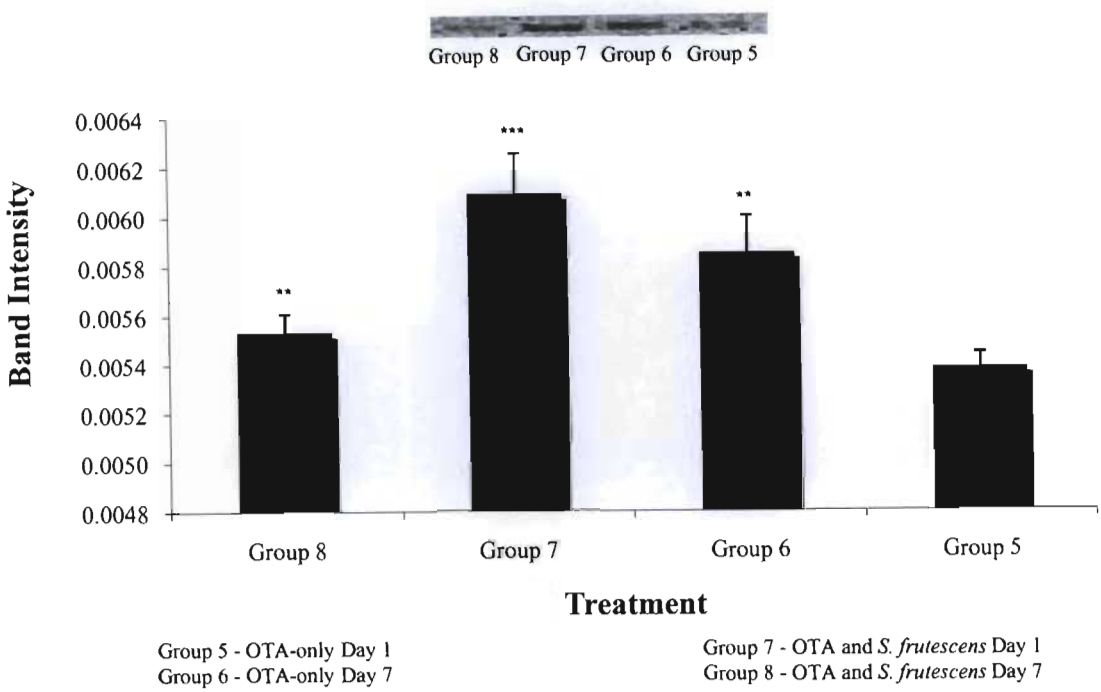

Figure 8.4: Analysis of the band intensities after the detection of Ochratoxin A bound to 120kDa serum protein. Data represent mean ±SEM. **p<0.01, ***p<0.001.

Considering the 65kDa protein, there were no significant differences observed between the band intensities of the OTA-only Day 1 and 7 regimes (Fig. 8.5). In addition, a comparison between the band intensities of the Day 1 OTA-only and combination treatments showed no significant difference (Fig. 8.5). However, there was a significant decrease in the band intensity of the combination treatment after 7 days ($p<0.01$) (Fig. 8.5).

The results displayed in Figure 8.4 and Figure 8.5 indicate that *S. frutescens* may decrease the binding efficiency of OTA to serum proteins. Ochratoxin A is known to preferentially bind to serum albumin (Hagelberg *et al.*, 1989), thus, decreasing this binding may result in the elimination of OTA from the body, since the unbound form may be filtered by the glomerulus. *Sutherlandia frutescens* contains L-ARG and L-CAV. It is possible that OTA may have bound to L-ARG or L-CAV instead of binding to albumin, and thus lower band intensities were noticed after the 7-day combination treatment. Immunoprecipitation is one of the techniques that could be employed to show whether OTA was bound to L-ARG or L-CAV

instead of albumin. It is possible that with the repeated treatment of *S. frutescens*, the binding of OTA to proteins may decrease.

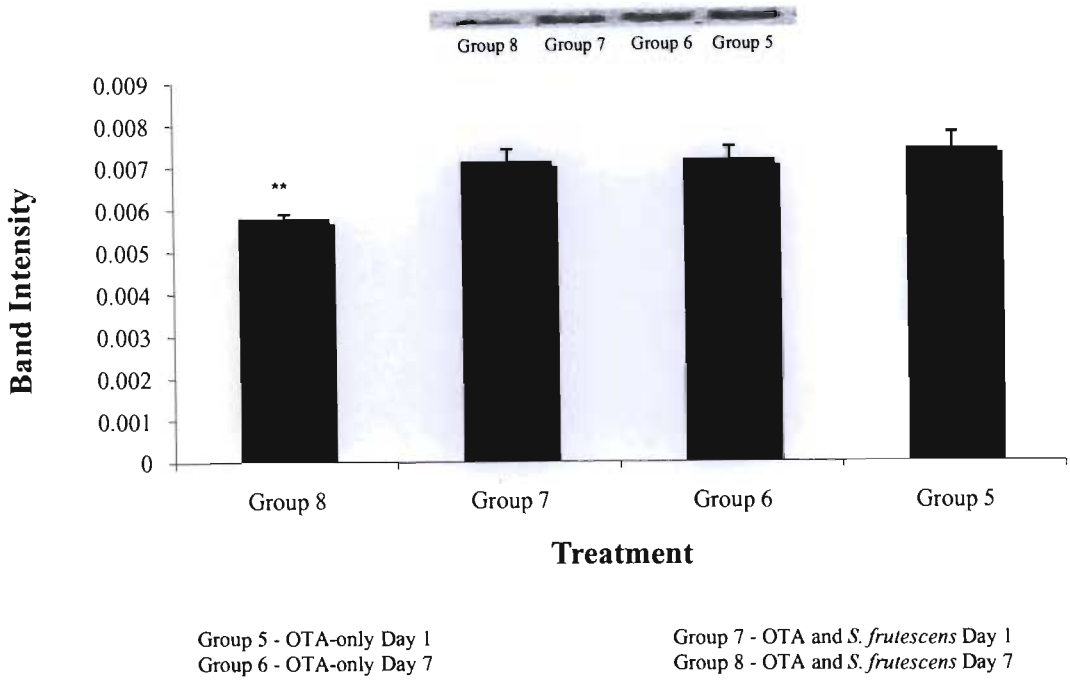

Figure 8.5: Analysis of the band intensities after the detection of Ochratoxin A bound to serum albumin. Data represent mean ±SEM. **p<0.01.

According to Mantle (2008) and Dahlmann *et al.* (1998), OTA can be reabsorbed along various sites of the nephron. Ochratoxin A is an organic anion at physiological pH and it is suggested that organic anion transporters play a significant role in the movement of unbound OTA into the tubules. The differences in transporters may influence OTA accumulation in cells (O'Brien and Dietrich, 2005). Also, high blood and tissue levels of OTA may be observed when there are repeated applications (Zepnik *et al.*, 2003). Thus in the present study, it is probable that the given time period did not allow for OTA accumulation in the target organ, the kidney.

Furthermore, it is necessary to consider that the majority of OTA may have been bound to albumin, following the injection into the peritoneal cavity. Due to the binding of OTA to albumin, the fraction of unbound toxin in the body is low. Therefore, the bound toxin recirculates in the body until dissociation, since only the unbound free toxin would be

available for glomerular filtration. It is the dissociation constant for albumin-OTA complexes that is important for glomerular filtration (Mantle, 2008).

The fact that OTA binds to albumin also means that the amount of free (usable) albumin is decreased. In addition, modifications in albumin may prevent degradation (Nicholson *et al.*, 2000). Thus, the catabolism of albumin may be reduced when bound to OTA. As a result, there would be a decrease in free amino acids, which are the final breakdown products of albumin in cells and plasma. Furthermore, the binding of OTA to albumin may subsequently compromise the immune cells. From the data presented in Chapter 6, it is possible that the increase in lymphocytes with depolarised mitochondria may be due to the albumin-OTA conjugate that was formed.

In accordance with the study by Maaroufi *et al.* (1999), it is possible that a higher concentration of OTA may have been present in blood rather than the kidney.

8.4 CONCLUSION

The results show that, due to OTA treatment, the expression of some proteins was decreased, in particular that of the mitochondria. This effect was not inhibited by the medicinal plant *S. frutescens*. Analysis by Western blot did not detect the binding of OTA to kidney proteins and this may have been attributed to the time period of treatment. However, the results indicate that OTA bound to two rat serum proteins (albumin and 120kDa) in the OTA-only (Day 1 and 7) and the OTA and *S. frutescens* combination treatment groups (Day 1 and 7). The measurement of the 120kDa protein band intensities showed that the combination group produced the highest band intensity (120kDa) after the Day 1 regime. However, the band intensity (120kDa) was reduced after the 7-day combination regime. Regarding serum albumin, there was a significant decrease in band intensity after a 7-day OTA and *S. frutescens* combination treatment. From this study, it is evident that with a repeated dose of *S. frutescens*, the binding of OTA to serum proteins may be reduced.

CHAPTER 9

OVERALL CONCLUSION

The current data highlights mitochondrial dysfunction due to OTA toxicity. This was supported by the drastic changes in PBMC viability as noted by the MTT assay, which is dependent on metabolic activity and the lymphocyte mitochondrial depolarisation after OTA treatment. A significant increase in DNA damage was observed, which may be related to the increase in apoptosis that was noticed after short-term OTA treatment. In the present study kidney mitochondrial protein expression was decreased after OTA treatment. This may be related to the OTA-induced mitochondrial dysfunctions.

Condensed chromatin, indicative of apoptosis, was found in the glomerulus of OTA-treated rats. In addition, OTA was also immunolocalised in the glomerular region, even when treated with a combination of *S. frutescens*. Furthermore, Western blot showed the presence of OTA bound to serum albumin and a 120kDa serum protein. Glomerular filtration does not allow the movement of large proteins into the ultrafiltrate and only the unbound form is filtered and eliminated from the body. Taken together, OTA detection in the glomerulus as well as apoptosis in this area suggests that OTA may cause glomerular damage.

Sutherlandia frutescens proved to have a protective role against OTA-induced alterations in PBMC viability. While *S. frutescens* did not alleviate the OTA-induced increase in lymphocyte mitochondrial depolarisation, a synergistic increase was however observed. This response may have occurred as both OTA and *S. frutescens* affect mitochondrial function. The results also suggest that *S. frutescens* decreased the binding of OTA to serum proteins after repeated treatments. It is possible that OTA may have bound to the positively charged L-ARG or L-CAV, present in *S. frutescens*, instead of albumin, which may have resulted in the observed decreased OTA-albumin binding. If the OTA-protein complexes are decreased, then OTA may be eliminated from the body faster, thus decreasing toxicity.

Finally, the use of *S. frutescens* as a possible antidote for OTA-induced toxicity may prove beneficial after repeated doses. It is evident from the present study that alterations in immune

function may result in renal damage. The immune system may respond earlier to OTA than other organs. And, altered immune functions may result in the increased incidence of disease, which may be linked to the various effects produced by OTA. There are several studies regarding OTA-induced toxicity in the kidney, thus the *in vivo* data here presented on OTA-induced immunotoxicity is pertinent for future research.

REFERENCES

Akaogi, J., Barker, T., Kuroda, Y., Nacionales, D.C., Yamasaki, Y., Stevens, B.R., Reeves, W.H. and Satoh, M. (2006). Role of non-protein amino acid L-canavanine in autoimmunity. Autoimmunity Reviews 5, 429-435

Al-Anati, L. and Petzinger, E. (2006). Immunotoxic activity of ochratoxin A. Journal of Veterinary Pharmacology and Therapeutics 29, 79-90

Aleo, M.D., Wyat, R.D. and Schnellmann, R.G. (1991). Mitochondrial dysfunction is an early event on ochratoxin A but not oosporein toxicity to rat renal proximal tubules. Toxicology and Applied Pharmacology 107, 73-80

Alvarez, L., Gil, A.G., Ezpeleta, O., Garcia-Jalon, J.A. and de Cerain, A.L. (2004). Immunotoxic effects of ochratoxin A in Wistar rats after oral administration. Food and Chemical Toxicology 42, 825-834

Alvarez-Erviti, L., Leache, C., Gonzalez-Penas, E. and de Cerain, A.L. (2005). Alterations induced *in vitro* by ochratoxin A in rat lymphoid cells. Human and Experimental Toxicology 24, 459-466

Arany, I., Megyesi, J.K., Kaneto, H., Tanaka, S. and Safirstein, R.L. (2004). Activation of ERK or inhibition of JNK ameliorates $H(_2)O(_2)$ cytotoxicity in mouse renal proximal tubule cells. Kidney International 65, 1231-1239

Arbillaga, L., Azqueta, A., Ezpeleta, O. and de Cerain, A.L. (2007a). Oxidative DNA damage induced by ochratoxin A in the HK-2 human kidney cell line: evidence of the relationship with cytotoxicity. Mutagenesis 22, 35-42

Arbillaga, L., Azqueta, A., van Delft, J.H.M. and de Cerain, A.L. (2007b). *In vitro* gene expression data supporting a DNA non-reactive genotoxic mechanism for ochratoxin A. Toxicology and Applied Pharmacology, doi:10.1016/j.aap.2007.01.008

Assaf, H., Azouri, H. and Pallardy, M. (2004). Ochratoxin A induces apoptosis in human lymphocytes through down regulation of Bcl-X_L. Toxicological Sciences 79, 335-344

Atroshi, F., Biese, I., Saloniemi, H., Ali-Vehmas, T., Saari, S., Rizzo, A. and Veijalainen, P. (2000). Significance of apoptosis and its relationship to antioxidants after ochratoxin A administration in mice. Journal of Pharmacy and Pharmaceutical Science 3, 281-291

Aydin, G., Ozcelik, N., Cicek, E. and Soyoz, M. (2003). Histopathological changes in liver and renal tissues induced by ochratoxin A and melatonin in rats. Human and Experimental Toxicology 22, 383-391

Barisic, K., Rumora, L., Petrik, J., Cepelak, I. and Zanic-Grubisic, T. (2005). Ochratoxin A induces apoptosis in LLC-PK1 cells via JNK and p38 MAPK activation. Croatia Chemica Acta 78, 385-392

BD Biosciences (2000). Introduction to flow cytometry: a learning guide. Manual, 11-11032-01, 1-52

BD Biosciences (2003). BD™ Mitoscreen: Flow cytometry mitochondrial membrane potential detection kit. Instruction Manual 551302, 4-15

Becker, W.M., Kleinsmith, L.J. and Hardin, J. (2003). The World of the cell. 5th ed. San Francisco: Benjamin Cummings 5-6, 284

Bence, A.K., Worthen, D.R., Adams, V.R. and Crooks, P.A. (2002). The antiproliferative and immunotoxic effects of L-canavanine and L-canaline. Anti-cancer Drugs 13, 313-320

Bence, A.K. and Crooks, P.A. (2003). The mechanism of L-canavanine cytotoxicity: arginyl-tRNA synthetase as a novel target for anticancer drug discovery. Journal of Enzyme Inhibition and Medicinal Chemistry 18, 383-394

Berger, F.G., Kramer, D.L. and Porter, C.W. (2007). Polyamine metabolism and tumorigenesis in the $Apc^{Min/+}$ mouse. Biochemical Society Transactions 35, 336-339

Bernhard, D., Schwaiger, W., Crazzolara, R., Tinhofer, I., Kofler, R. and Csordas, A. (2003). Enhanced MTT-reducing activity under growth inhibition by resveratrol in CEM-C7H2 lymphocytic leukaemia cells. Cancer Letters 195, 193-199

Berridge, M.V. and Tan, A.S. (1993). Characterisation of the cellular reduction of 3-(4,5-dimethylthiazol-2-yl]-2,5-diphenyltetrazolium bromide (MTT): subcellular localisation, substrate dependence and involvement of the mitochondrial electron transport in MTT reduction. Archives of Biochemistry and Biophysics 303, 474-482

Berridge, M.V., Tan, A.S., McCoy, K. and Wang, R. (1996). The biochemical and cellular basis of cell proliferation assays that use tetrazolium salts. Biochemica 4, 14-19

Blank, R., and Wolffram, S. (2004). Alkalinisation of urinary pH accelerates renal excretion of ochratoxin A in pigs. The Journal of Nutrition 134, 2355-2358

Boesch-Saadatmandi, C., Loboda, A., Jozkowicz, A., Huebbe, P., Blank, R., Wolffram, S., Dulak, J. and Rimbach, G. (2008). Food and Chemical Toxicology 46, 2665-2671

Bondy, Y. G., Suzuki, C., Barker, M., Armstrong, C., Fernie, S., Hierlihy, L., Rowsell, P. and Mueller, R. (1995). Toxicity of Fumonisin B1 administered intraperitoneally to male Sprague-Dawley rats. Food and Chemical Toxicology 33, 653-665

Bouaziz, C., el dein Sharafi, O., El Golli, E., Abid-Essefi, S., Brenner, C., Lemaire, C. and Bacha. H. (2008). Different apoptotic pathways induced by zearalenone T-2 toxin and ochratoxin A in humans. Toxicology 254, 19-28

Castegnaro, M., Mohr, U., Pfohl-leszkowicz, A., Esteve, J., Steinmann, J., Tillmann, T., Michelon, J. and Bartsch, H. (1998). Sex and strain-specific induction of renal tumors by ochratoxin A in rats correlates with DNA adduction. International Journal of Cancer 77, 70-75

Chadwick, A. W., Roux, S., de Venter, M., Louw, J. and Oelofsen, W. (2007). Anti-diabetic effects of *Sutherlandia frutescens* in Wistar rats fed a diabetogenic diet. Journal of Ethnopharmacology 109, 121-1270

Chinkwo, A.K. (2005). *Sutherlandia frutescens* extracts can induce apoptosis in cultured carcinoma cells. Journal of Ethnopharmacology 98, 163-170

Creppy, E.E., Kane, A., Dirheimer, G., Lafarge-Frayssinet, C., Mousset, S. and Frayssinet, C. (1985). Genotoxicity of ochratoxin A in mice: DNA single-strand break evaluation in spleen, liver and kidney. Toxicology Letters 28, 29-35

Coria-Avila, G.A., Gavila, A.M., Mernard, S., Ismail, N. and Pfaus, J.G. (2007). Cecum location in rats and the implication for intraperitoneal injections. Lab Animal 36, 25-30

Cribb, A.E., Peyrou, M., Muruganandan, S. and Scheider, L. (2005). The endoplasmic reticulum in xenobiotic toxicity. Drug Metabolism Reviews 37, 405-442

Criss, W.E. (2003). A review of polyamines and cancer. Turkish Journal of Medical Science 33, 195-205

Dahlmann, A., Dantzler, W.H., Silbernagl, S. and Gekle, M. (1998). Detailed Mapping of ochratoxin A reabsorption along the rat nephron in vivo: the nephrotoxin can be reabsorbed in all nephron segments by different mechanisms. Journal of Pharmacology and Experimental Therapeutics 286, 157-162

Dais, P., Stefanaki, I., Fragaki, G. and Mikros, E. (2005). Conformational analysis of ochratoxin A by NMR spectroscopy and computational molecular modelling. Journal of Physical Chemistry B 109, 16926-16936

Dash, P.R., McCornick, J., Thomas, M.J.C.B., Cartwright, J.J.E. and Whitley, G.S. (2007). Fas ligand-induced apoptosis is regulated by nitric oxide through the inhibition of fas receptor clustering and nitrosylation of protein kinase C. Experimental Cell Research 313, 3421-3431

Davis, A., Christiansen, M., Horowitz, J.F., Klein, S., Hellerstein, M.K. and Ostlund, R.E. (2000). Effect of pinitol treatment on insulin action in subjects with insulin resistance. Diabetes Care 23, 1000-1005

De Broe, M.E. and Roch-Ramel, F. (1998). Renal handling of drugs and xenobiotics. In: De Broe, M.E., Porter, G.A., Bennett, W.M. and Verpooten, G.A. (eds) Clinical Nephrotoxins: Renal Injury from Drugs and Chemicals. Dordrecht: Kluwer Academic Publishers 13-30

Desagher, S. and Martinou, J. (2000). Mitochondria as the central control point of apoptosis. Trends in Cell Biology 10, 369-377

Disease control priorities project (2008). Controlling kidney disease: disease control and early detection. Fact Sheet November, 1-3

Domijan, A., Peraica, M., Ferencic, Z., Cuzic, S., Fuchs, R., Lucic, A. and Radic, B. (2004). Ochratoxin A-induced apoptosis in rat kidney tissue. Archives of Industrial Hygiene and Toxicology 55, 243-248

Domijan, A., Rudeš, K. and Peraica, M. (2005). The effect of ochratoxin A on the concentration of protein carbonyls in rats. Archives of Industrial Hygiene and Toxicology 56, 311-315

Dubmann, H., Rehm, M., Kogel, D. and Prehn, J.H.M. (2003). Outer mitochondrial membrane permeabilization during apoptosis triggers caspase-independent mitochondrial and caspase-dependent plasma membrane depolarisation: a single cell analysis. Journal of Cell Science 116, 525-536

Fagian, M.M., Pereira-da-Silva, L., Martins, I.S. and Vercesi, A.E. (1990). Membrane protein thiol cross-linking associated with the permeabilisation of the inner mitochondrial membrane by Ca^{2+} plus prooxidants. Journal of Biological Chemistry 265, 19955-19960

Fernandes, A.C., Cromarty, A.D., Albrecht, C. and van Rensburg, J.E.C. (2004). The antioxidant potential of *Sutherlandia frutescens*. Journal of Ethnopharmacology 95, 1-5

Gautier, J.C., Richoz, J., Welti, D.H., Markovic, J., Gremaud, E., Guengerich, P.F. and Turesky, R.J. (2001a). Metabolism of ochratoxin A: absence of formation of genotoxic derivatives by human and rat enzymes. Chemical Research in Toxicology 14, 34-45

Gautier, J.C., Holzhaeuser, D., Markovic, J., Gremaud, E., Schilter, B. and Turesky, R.J. (2001b). Oxidative damage and stress response from ochratoxin A exposure in rats. Free Radical Biology and Medicine 30, 1089-1098

Gekle, M. and Silbernagl, S. (1994). The role of the proximal tubule in ochratoxin A nephrotoxicity in vivo: toxicokinetic and toxicodynamic aspects. Renal Physiology and Biochemistry 17, 40-49

Gekle, M., Pollock, C.A. and Silbernagl, S. (1995). Time and concentration-dependent biphasic effect of ochratoxin A on growth of tubular cells in primary culture. Journal of Pharmacology and Experimental Therapeutics 275, 397-404

Gekle, M. and Silbernagl, S. (1996). Renal toxicodynamics of ochratoxin A. Kidney and Pressure Research 19, 225-235

Gekle, M., Schwerdt, G., Freudinger, R., Mildenberger, S., Wilflingseder, D., Pollack, V., Dander, M. and Schramek, H. (2000). Ochratoxin A induces JNK activation and apoptosis in MDCK-C7 cells at nanomolar concentrations. Journal of Pharmacology and Experimental Therapeutics 293, 837-844

Gillman, I.G., Yezek, J.M. and Manderville, R.A. (1998). Ochratoxin A acts as a photoactivatable DNA cleaving agent. Chemical Communications. 647-648 doi: 1039/a708275d

Gillman, I.G., Clark, T.N. and Manderville, R.A. (1999). Oxidation of ochratoxin A by an Fe-porphyrin system: model for enzymatic cleavage. Chemical Research in Toxicology 12, 1066-1076

Grajewski, J., Moraczewska, J., Fogt, K. and Twaruzek, M. (2008). Capacity of blood albumins to bind to ochratoxin A and roridin A. Medycyna Weterynaryjna 64, 650-653

Green, M.H., Brooks, T.L., Mendelson, J. and Howell, S.B. (1980). Anti-tumour activity of L-canavanine against L1210 murine leukemia. Cancer Research 40, 4180-4182

Groves, C.E., Morale, M. and Wright, S.H. (1998). Peritubular transport of ochratoxin A in rat renal proximal tubules. Journal of Pharmacology and Experimental Therapeutics 284, 943-948

Guo, Y., Srinivasula, S.M., Druilhe, A. and Fernandes-Alnemri, T. (2002). Caspase-2 induces apoptosis by releasing proapoptotic proteins from mitochondria. Journal of Biological Chemistry 277, 13430-13437

Hagelberg, S., Hult, K. and Fuchs, R. (1989). Toxicokinetics of OTA in several species and its plasma binding properties. Journal of Applied Toxicology 9, 91-96

Hare, J.D. (1969). Nuclear alterations in mammalian cells induced by L-canavanine. Cellular Physiology 75, 129-131

Hassen, W., Ayed-Boussema, I., Bouslimi, A. and Bacha, H. (2007). Heat shock proteins (Hsp 70) response is not systematic to cell stress: case of the mycotoxin ochratoxin A. Toxicology 242, 63-70

Heiskanen, K.M., Bhat, M.B., Wang, H.W., Ma, J. and Nieminien, A.L. (1999). Mitochondrial depolarisation accompanies cytochrome c release during apoptosis in PC6 cells. The Journal of Biological Chemistry 274, 5654-5658

Hengartner, M.O. (2000). The biochemistry of apoptosis. Nature 407, 770-776

Herman, B. (1998). Fluorescence Microscopy. 2nd ed. Oxford: Bios Scientific Publishers 15-37

Hladky, S.B. and Rink, T.J. (1986). Body Fluid and Kidney Physiology. London: Edward Arnold Publishers 48-55

Horvath, A., Upham, B.L., Ganev, V. and Trosko, J.E. (2002). Determination of the epigenetic effects of ochratoxin A in a human kidney and a rat liver epithelial cell line. Toxicon 40, 273-282

Hotchkiss, R.S. and Nicholson, D.W. (2006). Apoptosis and caspases regulate death and inflammation in sepsis. Nature Reviews Immunology 6, 813-822

International Agency for Research on Cancer (1993). International Agency for Research on Cancer (IARC), Ochratoxin A, Monographs on the evaluation of carcinogenic risks to humans. Some naturally occurring substances: food items and constituents, hetrocylic aromatic amines and mycotoxins 56, 489-521

Il'ichev, Y.V., Perry, J.L. and Simon, J.D. (2002). Interaction of ochratoxin A with human serum albumin. Preferential binding of the dianion and pH effect. Journal of Physical Chemistry B 106, 452-459

Iyer, A.K.V., Azad, N., Wang, L. and Rojanaskul, Y. (2008). Role of S-nitrosylation in apoptosis resistance and carcinogenesis. Nitric Oxide 19, 146-151

Jang, M.H., Jun, D.Y., Rue, S.W., Han, K.H., Park, W. and Kim, Y.H. (2002). Arginase antimetabolite L-canavanine induces apoptotic cell death in human Jurkat cells via caspase-3 activation regulated by Bcl-2 or Bcl-xL. Biochemical and Biophysical Research Communications 295, 283-288

Jung, K.Y. and Endou, H. (1989). Nephrotoxicity assessment by measuring cellular ATP content. II. Intranephron site to ochratoxin A nephrotoxicity. Toxicological Application and Pharmacology 100, 383-390

Kamp, H.G., Eisenbrand, G., Schlatter, J., Wurth, K. and Janzowski, C. (2005). Ochratoxin A: induction of (oxidative) DNA damage, cytotoxicity and apoptosis in mammalian cell lines and primary cells. Toxicology 206, 413-425

Kane, A., Creppy, E.E., Roth, A., Roschenthaler, R. and Dirheimer, G. (1986). Distribution of the [^{3}H]-label from low doses of radioactive ochratoxin A ingested by rats, and evidence for DNA single strand breaks caused in liver and kidneys. Archives of Toxicology 58, 219-224

Kikuchi, T., Akihisa, T., Tokuda, H., Ukiya, M., Watanabe, K. and Nishino, H. (2007). Cancer chemopreventive effects of cycloartane-type and related triterpenoids in *in vitro and in vivo* models. Journal of Natural Products 70, 918-922

Köller, G., Wichmann, G., Rolle-Kampczyk, U., Popp, P. and Herbarth, O. (2006). Comparison of ELISA and capillary electrophoresis with laser induced fluorescence detection in the analysis of ochratoxin A in low volumes of human blood serum. Journal of Chromatography B 840, 94-98

Kroemer, G., Zamzami, N. and Susin, S.A. (1997). Mitochondrial control of apoptosis. Immunology Today 18, 44-51

Kroemer, G., Galluzzi, L. and Brenner, C. (2007). Mitochondrial permeabilisation in cell death. Physiological Reviews 87, 99-163

Kumagi, S. (1985). Ochratoxin A: plasma concentration and excretion into bile and urine in albumin-deficient rats. Food and Chemical Toxicology 23, 941-943

Laemmli, U.K. (1970). Cleavage of structural proteins during the assembly of the head of bacteriophage T4. Nature 227, 680-685

Li, S., Marquardt, R.R., Frohlich, A.A., Vitti, T.G. and Crow, G. (1997). Pharmacokinetics of ochratoxin A and its metabolites in rats. Toxicology and Applied Pharmacology 145, 82-90

Luster, M.I., Germolec, D.R., Burleson, G.R., Jameson, C.W., Ackermann, M.F., Lamm, K.R. and Hayes, T.H. (1987). Selective immunosuppression in mice of natural killer cell activity by OTA. Cancer Research 47, 2259-2263

Maaroufi, K., Zakhama, A., Baudrimont, I., Achour, A., Abid, S., Ellouz, F., Dhouib, S., Creppy, E.E. and Bacha, H. (1999). Karyomegaly of tubular cells as early stage marker of the nephrotoxicity induced by ochratoxin A. Human and Experimental Toxicology 18, 410-415

Madsen, K.M. and Tisher, C.C. (2004). In: Brenner, M. (ed) Brenner and Rector's The Kidney. Philadelphia: W.B Saunders Company. 7th ed. 1v. 3-16, 19-20, 34-48

Mally, A. and Dekant, W. (2005). DNA adduct formation by ochratoxin A: review of the available evidence. Food Additives and Contaminants 1, 65–74

Mally, A., Pepe, G., Bavoori, S., Fiore, M., Gupta, C.R., Dekant, W. and Mosesso, P. (2005). Ochratoxin A causes DNA damage and cytogenetic effects but no DNA adducts in rats. Chemical Research in Toxicology 18, 1253-1261

Mally, A., Hard, G.C. and Dekant, W. (2007). Ochratoxin A as a potential etiologic factor in endemic nephropathy: lessons from toxicity studies in rats. Food and Chemical Toxicology 45, 2254-2260

Manolova, Y., Manolov, G., Parvanova, L., Petkova-Bocharova, T., Castegnaro, M. and Chernozemsky, I.N. (1990). Induction of particular X-trisomy in cultured human lymphocytes treated with OTA, a mycotoxin implicated in Balkan endemic nephropathy. Mutation Research 231, 143-149

Mantle, P.G. (2008). Interpretation of the pharmokinetics of ochratoxin A in blood plasma of rats, during and after acute or chronic ingestion. Food and Chemical Toxicology 46, 1808-1816

Marin-Kuan, M., Nestler, S., Verguet, C., Bezencon, C., Piguet, D., Mansourian, R., Holzwarth, J., Grigorov, M., Delatour, T., Mantle, P., Cavin, C. and Schilter, B. (2006). A toxicogenomics approach to identify new plausible epigenetic mechanisms of ochratoxin A carcinogenicity in rats. Toxicological Sciences 89, 120-134

Marin-Kuan, M., Nestler, S., Verguet, C., Bezencon, C., Piguet, D., Delatour, T., Mantle, P., Cavin, C. and Schilter, B. (2007). MAPK-ERK activation in kidney of male rats chronically fed ochratoxin A at a dose causing a significant incidence of renal carcinoma. Toxicology and Applied Pharmacology 224, 174-181

Marin-Kuan, M., Cavin, C., Delatour, T. and Schilter, B. (2008). Ochratoxin A involves a complex network of epigenetic mechanisms. Toxicon 52, 195-202

Marquardt, R.R. and Frohlich, A.A. (1992). A Review of Ochratoxicosis. Journal of Animal Science 70, 3968-3988

Mates, J.M., Perez-Gomez, C., de Castro, I.N., Asenjo, M. and Marquez, J. (2002). Glutamine and its relationship with intracellular redox status, oxidative stress and cell death/proliferation. The International Journal of Biochemistry and Cell Biology 34, 439-458

Mayer, B. and Oberbauer, R. (2003). Mitochondrial regulation of apoptosis. News in Physiological Sciences 18, 89-94

McKelvey-Martin, V.J., Green, M.H.L., Schmezer, P., Pool-Zobel, B.L., De Meo, M.P. and Collins, A. (1993). The single cell gel electrophoresis assay (comet assay): a European review. Mutation Research 288, 47-63

Mills, E., Cooper, C., Seely, D. and Kanfer, I. (2005). African herbal medicines in the treatment of HIV: Hypoxis and Sutherlandia. An overview of evidence and pharmacology. Nutrition Journal doi:10.1186/1475-2891-4-19

Ming-Fang Hseih, M.D., Hsiao-Ying Chiu, M.D., Dan-Tzu Lin-Tan, R.N. and Ja-Liang Lin, M.D. (2004). Does human ochratoxin A aggravate proteinuria in patients with chronic renal disease? Renal Failure 26, 311-316

Mosmann, T. (1983). Rapid calorimetric assay for cellular growth and survival: application to proliferation and cytotoxicity assays. Journal of Immunological Methods 65, 55-63

Muller, G., Kielstein, P., Rosner, H., Berndt, A., Heller, M. and Kohler, H. (1999). Studies of the influence of ochratoxin A on immune and defence reactions in weaners. Mycoses 42, 495-505

Newsholme, E.A., Crabtree, B. and Ardawi, M.S.M. (1985). Glutamine metabolism in lymphocytes: it's biochemical, physiological and clinical importance. Quarterly Journal of Experimental Physiology 70, 473-489

Newsholme, P., Lima, N.M.R., Procopio, J., Pithon-Curi, T.C., Doi, S.Q., Bazotte, R.B. and Curi, R. (2003). Glutamine and glutamate as vital metabolites. Brazilian Journal of Medical and Biological Research 36, 153-163

Nicholson, J.P., Wolmarans, M.R. and Park, G.R. (2000). The role of albumin in critical illness. British Journal of Anaesthesia 85, 599-610

O'Brien, E., Heussener, A.H. and Dietrich, D.R. (2001). Species-sex and cell type-specific effects of ochratoxin A and B. Toxicological Sciences 63, 256-264

O'Brien, E. and Dietrich, D.R. (2005). Ochratoxin A: the continuing enigma. Critical Reviews in Toxicology 35, 33-60

Obrecht-Pflumio, S., Grosse, Y., Pfohl-Leszkowicz, A. and Dirheimer, G. (1996). Protection by indomethacin and aspirin against genotoxicity of ochratoxin A, particularly in the urinary bladder and kidney. Archives of Toxicology 70, 244-248

Obrecht-Pflumio, S. and Dirheimer, G. (2000). *In vitro* DNA and dGMP adducts formation caused by ochratoxin A. Chemico-Biological Interactions 127, 29-44

Odhav, B., Adam, J. and Bhoola, K.D., (2008). Modulating effects of Fumonisin B_1 and Ochratoxin A on leukocytes and messenger cytokines of the human immune system. International Immunopharmacology 8, 799-809

Ojewole, J.O.A. (2008). Anticonvulsant property of *Sutherlandia frutescens* R.BR. (variety Incana E. MEY.) [Fabaceae] shoot aqueous extract. Brain Research Bulletin 75, 126-132

Omar, R.F., Hasinoff, B.B., Mejilla, F. and Rahimtula, A.D. (1990). Mechanism of ochratoxin A stimulated lipid peroxidation. Biochemical Pharmacology 40, 1183-1191

Ormerod, M.G. (2000). Flow Cytometry: A Practical Approach. 3rd ed. Oxford: Oxford University Press 1-27, 240, 243

Ostling, O. and Johanson, K.J. (1984). Microelectrophoretic study of radiation-induced DNA damages in individual mammalian cells. Biochemical and Biophysical Research Communications 123, 291-298

Petit, X.P., Susin, S., Zamzani, N., Mignotte, B. and Kroemer, G. (1996). Mitochondria and programmed cell death: back to the future. FEBS letters 396, 7-13

Petrik, J., Zanic-Grubisic, T., Barisic, K., Pepeljnjak, S., Radic, B., Ferencic, Z. and Cepelak, I. (2003). Apoptosis and oxidative stress induced by ochratoxin A in rat kidney. Archives of Toxicology 77, 685-693

Petzinger, E. and Ziegler, K. (2000). Ochratoxin A from a toxicological perspective. Journal of Veterinary Pharmacology and Therapeutics 23, 91-98

Pfaller, W. and Gstraunthaler, G. (1998). Nephrotoxicty testing *in vitro*: what we know and what we need to know. Environmental Health Perspectives 106, 559-569

Prior, M.G. and Sisodia, C.S. (1982). The effects of ochratoxin A on the immune response of swiss mice. Canadian Journal of Comparative Medicine 46, 91-96

Proskuryakov, S.Y., Konoplyannikov, A.G. and Gabaib, V.L. (2003). Necrosis: a specific form of programmed cell death. Experimental Cell Research 283, 1-16

Rahman, M. (2006). Introduction to flow cytometry. AbD Serotec Lit.Flow.Mar.2006.1, 1-33

Ramos-Vara, J.A. (2005). Technical aspects of immunohistochemistry. Veterinary Pathology 42, 405-426

Rastogi, R.P., Sinha, R. and Sinha, R.P. (2009). Apoptosis: molecular mechanisms and pathogenicity. EXCLI Journal 8, 155-181

Reid, K.A., Maes, J., Maes, A., van Staden, J., De Kimpe, N., Mulholland, D.A. and Verschaeve, L. (2006). Evaluation of the mutagenic and antimutagenic effects of South African plants. Journal of Ethnopharmacology 106, 44–50

Riganti, C., Aldieri, E., Bergandi, L., Miraglia, E., Costamagna, C., Bosia, A. and Ghio, D. (2003). Nitroarginine methyl ester and canavanine lower intracellular reduced glutathione. Free Radical Biology and Medicine 35, 1210-1216

Ringot, D., Chango, A., Schneider, Y. and Larondelle, Y. (2006). Toxicokinetics and toxicodynamics of ochratoxin A an update. Chemico-Biological Interactions 159, 18-46

Rojas, E., Lopez, M.C. and Valverde, M. (1999). Single cell gel electrophoresis assay: methodology and applications. Journal of Chromatography 722, 225-254

Russel, F.G.M., Masereeuw, R. and van Aubel, R.AM.H. (2002). Molecular aspects of renal anionic drug transport. Annual Reviews of Physiology 64, 563-594

Sauvant, C., Silbernagl, S. and Gekle, M. (1998). Exposure to ochratoxin A impairs organic anion transport in proximal-tubule-derived opossum kidney cells. Pharmacology and Experimental Therapeutics 287, 13-20

Sauvant, C., Holzinger, H. and Gekle, M. (2005). Proximal tubular toxicity of ochratoxin A is amplified by simultaneous inhibition of the extracellular signal-regulated kinases1/2. Journal of Pharmacology and Experimental Therapeutics 313, 234-241

Schaaf, G.J., Nijmeijer, S.M., Maas, R.F.M., Roestenberg, P., de Groene, E.M. and Fink-Gremmels, J. (2002). The role of oxidative stress in the ochratoxin A-mediated toxicity in proximal tubular cells. Biochimica et Biophysica Acta 1588, 149-158

Schilter, B., Marin-Kuan, M., Delatour, T., Nestler, S., Mantle, P. and Cavin, C. (2005). Ochratoxin A: potential epigenetic mechanisms of toxicity. Food Additives and Contaminants 1, 88-93

Schlatter, C., Studer-Rohr, J. and Rasonyi, T. (1996). Carcinogenicity and kinetic aspects of ochratoxin A. Food Additives and Contaminants 13, 43-44

Schnellmann, R.G. (2003). Toxic Responses of the kidney. In: Klaassen, C.D. and Watkins, J.B. (eds) Casarett and Doull's Essentials of Toxicology. New York: McGraw-Hill Companies, Inc. 208-219

Schwerdt, G., Bauer, K., Gekle, M. and Silbernagl, S. (1996). Accumulation of ochratoxin A in rat kidney *in vivo* and in cultivated rat epithelial cells *in vitro*. Toxicology 114, 177-185

Schwerdt, G., Freudinger, R., Silbernagl, S. and Gekle, M. (1999). Ochratoxin A binding in rat organs and plasma and in different cell lines of the kidney. Toxicology 135, 1-10

Schwerdt, G., Freudinger, R., Schuster, C., Silbernagl, S. and Gekle, M. (2004). Inhibition of mitochondria and extracellular acidification enhance ochratoxin A-induced apoptosis in renal collecting duct-derived MDCK-C7 cells. Cellular Physiology and Biochemistry 14, 47-56

Schwerdt, G., Holzinger, H., Sauvant, C., Konigs, M., Humpf, H. and Gekle, M. (2007). Long-term effects of ochratoxin A on fibrosis and cell death in human proximal tubule or fibroblast cells in primary culture. Toxicology 232, 57-67

Seegers, J.C., Bohmer, L.H., Kruger, M.C., Lottering, M.L. and de Kock, M. (1994a). A comparative study of ochratoxin A-induced apoptosis in hamster kidney and HeLa cells. Toxicology and Applied Pharmacology 129, 1-11

Seegers, J.C., Lottering, M.L. and Galinkski, P.J. (1994b). The mycotoxin ochratoxin A causes apoptosis-associated DNA degradation in human lymphocytes. Medical Science Research 22, 417-419

Seier, J.V., Mdhuli, M., Dhansay, M.A., Loza, J. and Laubscher, R. (2002). A toxicity study of *Sutherlandia* leaf powder (*Sutherlandia microphylla*) consumption. Medical Research Council of South Africa: Final Report April 2002

Selzner, M., Bielawska, A., Morse, M.A., Rudiger, H.A., Sindram, D., Hannun, Y.A. and Clavien, P. (2001). Induction of apoptotic cell death and prevention of tumour growth by ceramide analogues in metastatic human colon cancer. Cancer Research 61, 1233-1240

Sia, C. (2004). Spotlight on ethnomedicine: usability of *Sutherlandia frutescens* in the treatment of diabetes. The Review of Diabetic Studies 1, 145-149

Sigma-Aldrich Product Booklet (2003). Histopaque®-1077. Procedure No. 1077, 1-2

Simarro Doorten, A.Y., Bull, S., van de Doelen, M.A.M. and Fink-Gremmels, J. (2004). Metabolism-mediated cytotoxicity of ochratoxin A. Toxicology in Vitro 18, 271-277

Simon, P., Godin, M. and Fillastre, J.P. (1996). Ochratoxin A: a new environmental factor which is toxic for the kidney. Nephrology Dialysis and Transplantation 11, 2389-2391

Singh, N.P., McCoy, T.M., Tice, R.T. and Schneider, E.L. (1988). A simple technique for quantification of low levels of DNA damage in individual cells. Experimental Cell Research 175, 184-191

Skulachev, V.P. (1996). Why are mitochondria involved in apoptosis? Permeability transition pores and apoptosis as selective mechanisms to eliminate superoxide-producing mitochondria and cell. FEBS Letters 397, 7-10

Smart, R.C. and Hodgson, E. (2008). Molecular and Biochemical Toxicology. 4th ed. Hoboken, New Jersey: John Wiley and Sons, Inc. 119-120, 295-296, 310, 555, 587, 693-702

Stander, B.A., Marais, S., Steynberg, T.J., Theron, D., Joubert, F., Albrecht, C. and Joubert, A.M. (2007). Influence of *Sutherlandia frutescens* extracts on cell morphology and gene expression in MCF-7 cells. Journal of Ethnopharmacology 112, 312-318

Stoev, S.D. (1998). The role of ochratoxin A as a possible cause of BEN and its risk evaluation. Veterinary and Human Toxicology 40, 352-360

Stojkovic, R., Hult, K., Gamulin, S. and Plestina, R. (1984). High affinity binding of ochratoxin A to plasma constituents. Biochemistry International 9, 33-38

Tai, J., Cheung, S., Chan, E. and Hasman, D. (2004). *In vitro* culture studies of *Sutherlandia frutescens* on human tumour cell lines. Journal of Ethnopharmacology 9, 9-19

Thomas, D.A., Rosenthal, G.A., Gold, D.V. and Dickey, K. (1980). Growth inhibition of a rat colon tumour by L-canavanine in the rat. Cancer Research 46, 2898-2903

Tice, R.R., Agurell, E., Anderson, D., Burlinson, B., Hartmann, A., Kobayashi, H., Miyamae, Y., Rojas, E., Ryu, J.C. and Sasaki, Y.F. (2000). Single cell gel/comet assay: guidelines for in vitro and in vivo genetic toxicology testing. Environmental and Molecular Mutagenesis 35, 206-221

Trevigen (2007). TACS™ Annexin V Kits: apoptosis detection by flow cytometry and in situ labelling. Instruction Manual E5/3/07v1, 1-11

van Wyk, B.E. and Albrecht, C. (2008). A review of the taxonomy, ethnobotany, chemistry and pharmacology of *Sutherlandia frutescens*. Journal of Ethnopharmacology 119, 620-629

Vermes, I., Haanen, C., Steffens-Nakken, H. and Reutelingsperger, C. (1995). A novel assay for apoptosis. Flow cytometric detection of phosphatidylserine expression on early apoptotic cells using fluorescin labelled Annexin V. Journal of Immunological Methods 184, 39-51

Webber, F., Freudinger, R., Schwerdt, G. and Gekle, M. (2005). A rapid screening method to test apoptotic synergisms of OTA with other nephrotoxic substances. Toxicology *In Vitro* 19, 135–143

Wei, Y.H., Lu, C.Y., Lin, T.N. and Wei, R.D. (1985). Effect of ochratoxin A on rat liver mitochondrial respiration and oxidative phosphorylation. Toxicology 36, 119-130

Willingham, M.C. (1999). Cytochemical methods for the detection of apoptosis. Journal of Histochemistry and Cytochemistry 47, 1101-1109

Wilson, K. and Walker, J. (2005). Principles and Techniques of Biochemistry and Molecular Biology. 6th ed. Cambridge: Cambridge University Press 143-144, 322-323, 449-459, 461, 469-472

Worthen, D.R., Chien, L., Tsuboi, C.P., Mu, X.Y., Bartik, M.M. and Crooks, P.A. (1998). L-canavanine modulates cellular growth, chemosensitivity and P-glycoprotein substrate accumulation in cultured human tumor cell lines. Cancer Letters 132, 229-239

Yerlikaya, A. (2004). Polyamines and S-adenosylmethionine decarboxylase. Turkish Journal of Biochemistry 29, 208-214

Zamzami, N., Marchetti, P., Castedo, M., Zanin, C., Vayssiere, J.L., Petit, P.X. and Kroemer, G. (1995). Reduction in mitochondrial potential constitutes an early irreversible step of programmed lymphocyte death in vivo. Journal of Experimental Medicine 181, 1661-1672

Zanic-Grubisic, T., Zrinski, R., Cepelak, I., Petrik, J., Radic, B. and Pepeljnjak, S. (2000). Studies of ochratoxin A-induced inhibition of phenylalanine hydroxylase and its reversal by phenylalanine. Toxicology and Applied Pharmacology 167, 132-139

Zeljezic, D., Domijan, A.M. and Peraica, M. (2006). DNA damage by ochratoxin A in rat kidney assessed by the alkaline comet assay. Brazilian Journal of Medical and Biological Research 39, 1563-1568

Zepnik, H., Pahler, A., Schauer, U. and Dekant, W. (2001). Ochratoxin A-induced tumour formation: is there a role for toxic metabolites. Toxicological Sciences 59, 59-67

Zepnik, H., Volkel, W. and Dekant, W. (2003). Toxicokinetics of the mycotoxin ochratoxin A in F 344 rats after oral administration. Toxicology and Applied Science 192, 36-44

Zhang, Q., Zhao, X.H. and Wang, Z.J. (2008). Flavones and flavonoids exert cytotoxic effects on a human oesophageal adenocarcinoma cell line (OE33) by causing G2/M arrest and inducing apoptosis. Food and Chemical Toxicology 46, 2042-2053

APPENDIX

Appendix A

1. Preparation of Ochratoxin A

5mg/ml stock solution was made. From this stock, 100µl was used for 1kg rats = 0.5mg. So, for 300g rats 30µl this is = 0.15mg.

Therefore 15 doses = 30µl x 15 = 450µl

To make 3ml, 450µl of toxin was added to 2 550µl of vehicle.

Vehicle was 70% H_2O and 30% EtOH.

Therefore:

2 550 × 70% = 1 785µl dH_20

2 550 × 30% = 765µl EtOH

2. Preparation of *Sutherlandia frutescens* stock solution

Ten 300mg (total mass = 3g) *Sutherlandia frutescens* tablets were crushed with a pestle and mortar and subjected to polar solvent extraction of active ingredients in 13.5ml vehicle (EtOH:dH_2O;70:30) (4 hr, RT). Following extraction, particular matter was pelleted by centrifugation (5 min, 400xg, RT).

The stock *S. frutescens* solution = ~300mg/13.5ml = 222.2mg/ml

The stock was further diluted 10-fold = 22.22mg/ml

The treatment dose of 1mg *S. frutescens* (Sf)/kg rat body weight (bw) was required therefore:

$$\frac{22.22}{1} = \frac{1.0\text{mg}}{x}$$

$$x(22.22\text{mg}) = \frac{1.0\text{mg}}{\text{ml}}$$

$$x = \frac{1.0\text{mg}}{22.22\text{mg}}$$

Therefore 0.05ml (50µl) SF /kg bw

Average rat body weight = 0.3kg (300g). Therefore 50µl x 0.3kg = 15µl Sf/300g bw. As 15µl was an insufficient volume to inject directly into the rat, this dose was further increased to 200µl (Sf mass/bw ratio remains the same). 50µl of 10-fold diluted Sutherlandia stock (with 150µl vehicle) was injected into each rat at Day 1 and Day 7 dosing.

Appendix B

Calculations for SCGE

1. LMPA

1% LMPA – 1g of LMPA was dissolved in 100ml PBS

0.5% LMPA – 0.5g of LMPA was dissolved in 100ml PBS

2. 250ml Lysing Solution

- **2.5M NaCl – Molecular weight 58.44g/mol**

$$c = \frac{n}{v}$$

$$2.5 = \frac{n}{0.25}$$

$$n = 0.625$$

$$n = \frac{\text{mass}}{\text{Molecular weight}}$$

mass = n×M = 0.625 × 58.44 = 36.53g for 250ml

- **100mM EDTA – Molecular weight 292.94g/mol**

$$c = \frac{n}{v}$$

$$0.1 = \frac{n}{0.25}$$

$$n = 0.025$$

$$n = \frac{\text{mass}}{\text{Molecular weight}}$$

mass = n×M = 0.025 × 292.94 = 7.32g for 250ml

- **1% 1M Tris** (6.06g in 50ml dH2O, pH 10)
- **1% Triton X-100**
- **10% DMSO**

NaCl (36.53g), EDTA (7.32g), 1M Tris (2.5ml), Triton X-100 (2.5ml) and DMSO (25ml) were added to dH_2O, to make a total volume of 250ml lysing solution.

3. 1 litre Electrophoresis buffer (pH 13)

- **300mM NaOH – Molecular weight = 40g/mol**

$$c = \frac{n}{v}$$

$$0.3 = \frac{n}{1}$$

$$n = 0.3$$

$$n = \frac{\text{mass}}{\text{Molecular weight}}$$

$$\text{mass} = n \times M = 0.3 \times 40 = 12\text{g}$$

- **1mM Na_2EDTA – Molecular weight = 372g/mol**

$$c = \frac{n}{v}$$

$$0.001 = \frac{n}{1}$$

$$n = 0.001$$

$$n = \frac{\text{mass}}{\text{Molecular weight}}$$

$$\text{mass} = n \times M = 0.001 \times 372 = 0.372\text{g}$$

Thus NaOH (12g) and Na_2EDTA (0.37g) were dissolved in 800ml of dH_2O, the pH was checked (pH 13) and volume was then adjusted to 1 000ml with dH_2O.

4. 0.4M Tris (pH 7.4) to wash slides – Molecular weight = 121.14

$$c = \frac{n}{v}$$

$$0.4 = \frac{n}{1}$$

$$n = 0.4$$

$$n = \frac{\text{mass}}{\text{Molecular weight}}$$

$$\text{mass} = n \times M = 0.4 \times 121.14 = 48.46\text{g}$$

Tris (48.46g) was added to 800ml of dH_2O, pH was adjusted and volume was topped up to 1 000ml with dH_2O

Appendix C

Immunohistochemistry

1. Sodium citrate buffer (pH 6.0) for Antigen retrieval

Tri-sodium citrate (2.94g) was dissolved in 800ml of distilled water. The pH was adjusted to 6.0, and then brought to a final volume of 1 000ml and 0.5ml of Tween 20 was added.

2. 2% BSA

2g of BSA was dissolved in 100ml of PBS

3. 1% Bovine serum albumin (BSA)

1g of BSA was dissolved in 100ml of PBS

4. Dilutions for primary antibody optimisation

1/50 - 2µl of primary antibody diluted in 98µl of 1% BSA

1/100 - 2µl of primary antibody was diluted in 198µl of 1% BSA

1/200 - 2µl of primary antibody was diluted in 398µl of 1% BSA

1/500 - 2µl of primary antibody was diluted in 998µl of 1% BSA

5. Dilution of secondary antibody

1/500 - 2µl of secondary antibody (Goat anti-mouse IgG) in 998µl of 1% BSA

Appendix D

Protein Isolation and Standardisation

1. **Isolation/Homogenising Buffer (100ml)**

- **50mM Tris – Molecular weight = 121.14g/mol**

$$c = \frac{n}{v}$$

$$0.05 = \frac{n}{0.1}$$

$$n = 0.005$$

$$n = \frac{\text{mass}}{\text{Molecular weight}}$$

$$\text{mass} = n \times M = 0.005 \times 121.14 = 0.61\text{g}$$

- **1mM K_2EDTA – Molecular weight = 404.47g/mol**

$$c = \frac{n}{v}$$

$$0.001 = \frac{n}{0.1}$$

$$n = 0.000\ 1$$

$$n = \frac{\text{mass}}{\text{Molecular weight}}$$

$$\text{mass} = n \times M = 0.000\ 1 \times 404.47 = 0.040\text{g}$$

- **1mM DTT**

Taken from 1M DTT stock solution

$$C_1V_1 = C_2V_2$$

$$1\text{M} \times V_1 = 0.001 \times 100\text{ml} = 0.1\text{ml}$$

Thus Tris (0.61g), K_2EDTA (0.04g), DTT (0.1ml) and a protease cocktail, was added to 60ml dH_2O. The pH was adjusted to 7.4 and was then brought to a volume of 100ml in dH_2O.

2. **Storage Buffer (pH 7.4) (50ml)**

- **0.1M KH_2PO_4 – Molecular weight = 136g/mol**

$$c = \frac{n}{v}$$

$$0.1 = \frac{n}{0.05}$$

$$n = 0.005$$

$$n = \frac{\text{mass}}{\text{Molecular weight}}$$

$$\text{mass} = n \times M = 0.005 \times 136 = 0.68\text{g}$$

- **0.5mM K_2EDTA – Molecular weight = 404.4g/mol**

$$c = \frac{n}{v}$$

$$0.000\,5 = \frac{n}{0.05}$$

$$n = 0.000\,025$$

$$n = \frac{\text{mass}}{\text{Molecular weight}}$$

$$\text{mass} = n \times M = 0.000\,025 \times 404.4 = 0.010\,1\text{g}$$

- **1mM DTT**

Taken from 1M DTT stock solution

$$C_1V_1 = C_2V_2$$

$$1\text{M} \times V_1 = 0.001 \times 50\text{ml} = 0.005\text{ml}$$

- **0.25M Sucrose – Molecular weight = 342.3g/mol**

$$c = \frac{n}{v}$$

$$0.25 = \frac{n}{0.05}$$

$$n = 0.012\,5$$

$$n = \frac{\text{mass}}{\text{Molecular weight}}$$

$$\text{mass} = n \times M = 0.012\,5 \times 342.3 = 4.28\text{g}$$

KH_2PO_4 (0.68g), K_2EDTA (0.01g), DTT (0.005 ml) and Sucrose (4.28g) was added together in 30ml dH_20; adjusted to pH 7.4, and then brought to a volume of 50ml with dH_2O.

3. BSA Standards

Table D1: BSA standards for protein standardisation

Concentration (mg/ml)	**0**	**0.2**	**0.4**	**0.6**	**0.8**	**1.0**
Buffer (µl)	100	80	60	40	20	0
BSA (µl)	0	20	40	60	80	100

A standard curve was drawn to determine protein concentration. The linear equation ($y = mx + c$) obtained from the standard curve was used to determine protein concentration, by solving for x. Samples were standardized to 1mg/ml, using the equation $C_1V_1 = C_2V_2$.

Appendix E

SDS PAGE

1. 10% resolving gel

dH_2O (4 100µl), Acrylamide bis (3 300µl), 1.5M Tris (2 500µl), 10% SDS (100µl), 10% APS (50µl) and TEMED (5µl) were added together.

- **1.5M Tris (pH 8.8) for 10% resolving gel**

27.23g of Tris was dissolved in 100ml dH_2O, corrected to pH 8.8, and then adjusted volume to 150ml.

2. 6% Stacking gel

dH_2O (54 000µl), Acrylamide bis (2 000µl), 0.5M Tris (2 500µl), 10% SDS (100µl), 10% APS (50µl) and TEMED (10µl) were added together.

- **0.5M Tris (pH 6.8) for 6% Stacking gel**

Tris (6g) was dissolved in 80ml dH_2O, corrected to pH 6.8, then adjusted volume to 100ml.

- **10% Ammonium persulphate (APS)**

Dissolved 25mg APS in 250µl dH_2O

3. Sample buffer (Final volume – 9.5ml)

dH_2O (3.55ml), 0.5M Tris-HCl pH 6.8 (1.25ml), Glycerol (2.5ml), 10% (w/v) SDS (2.0 ml), 0.5% (w/v) bromophenol blue (0.2ml).

50µl mercaptoethanol was added to 950µl sample reducing buffer, which was then mixed with isolated proteins (1:1).

4. Electrode Running buffer (pH 8.3)

Tris base (30.3g), Glycine (144g) and SDS (10g) were dissolved in 1 000ml of dH_2O, which was a 10x buffer. To obtain a 1x electrode running buffer, 50ml of the 10x buffer was diluted in 450ml dH_2O.

5. Silver Stain

Gels were soaked in a 7% acetic acid solution for 7 min. Gels were then soaked twice in 50% methanol (20 min each). Thereafter, solution A, silver nitrate, was made by adding 0.8g of silver nitrate to 4ml of water. After soaking gels in methanol, gels were rinsed twice in water (10 min each). 5 min before the end of the final water rinse solution B was made. Solution B consisted of 21ml of water, 250µl of 30% sodium hydroxide (NaOH) and 1.4ml of ammonium hydroxide. In order to make the staining solution, solution A was added to solution B in a drop-wise manner, whilst stirring, thereafter, 76ml of water was added. Gels were then soaked in the staining solution for about 4-5 min. Thereafter, gels were rinsed in two changes of water (5 min each). The developing solution was made using 200ml of water, 1ml of 1% citric acid and 100µl of 37% formaldehyde. After rinsing, gels were soaked in developing solution between 1-4 min. Finally, 7% acetic acid was added to the gels to stop development; this was followed by three changes of water.

Western Blot

6. Transfer buffer

Mix together 25mM Tris (3.03g), 192mM Glycine (14.4g) and 20% v/v methanol (200ml) in 500ml of dH_2O (pH 8.3). Bring volume up to 1l with dH_2O and chill until ready to use.

7. 5% non-fat dry milk to block the membrane

3g non-fat dry milk was dissolved in 60ml of TTBS

8. **TBS:** NaCl (8g), KCl (0.2g) and Tris (3g) were added together in 800ml dH_2O, adjusted to pH 7.5 and brought to a volume of 1l with dH_2O.
   - **TTBS** – add 0.5ml Tween 20 to 1litre TBS